ADJACENT LONG NON-CODING RNA PVT1 AND MYC CO-OPERATE IN BREAST CANCER WITH GAIN OF 8q24

A DISSERTATION
SUBMITTED TO THE FACULTY OF THE GRADUATE SCHOOL
OF THE UNIVERSITY OF MINNESOTA
BY

YUEN-YI TSENG

IN PARTIAL FULFILLMENT OF THE REQUIREMENTS
FOR THE DEGREE OF
DOCTOR OF PHILOSOPHY

ANINDYA BAGCHI
ADVISOR

Augest 2013

Acknowledgements

"Do great science" is the first thing I learned from my advisor, Dr. Anindya Bagchi and would like to express the deepest appreciation to Anindya for encouraging me to pursue science. Anindya is a great dream builder and his unique way inspirits me to challeng the most important questions in science. Anindya is not only my adviser, but also, sometimes acts as a father or a big brother under different circumstances. I could not thank Anindya enough.

I would like to thank the collaborator of this thesis project, Dr. Kaylee Schwertfeger. Without her guidance and persistent help this dissertation would not have been possible. Her good advice, support and patience have been invaluable for my thesis research, for which I am extremely grateful.

I would also like to thank my current dissertation committee members including the chair, Dr. David Largaespada, Dr. Kaylee Schwertfeger, Dr. Douglas Yee, Dr. Tim Starr, and Dr. Michael O'Conner as well as my previous committee members including Dr. Jonathan Slack and Dr. Jocelyn Shaw. Thank you for your suggestions and criticisms to help me develop the better thesis work.

Routinely meeting with Dr. York Marahrens and Dr. Naoko Shima provided the chance to present my work. Your insights and perspectives were especially valuable.

There are several undergraduate students who were working with me to complete this work. I would like to thank Jacki Essig, Bhuvani Dakshina, and Brain Reuland. Also, I would like to express a special thank you to Thomas Beadnell from Dr. Kaylee Schwertfeger's lab. I would not be here without your help. I wish you all the best for pursuing your career goals.

I am very fortune to meet many good friends at University of Minnesota. Robyn Leary has been my best lab mate during every stage of my exciting Ph.D. journey. Jacki Essig and Paula Croonquist always gave me fair suggestions to relieve the stress. Jessica Fiege, Theresa Edelman, Holly Stessman, Kristin Anderson, and Sarah Bloch have shared their research experiences and wisdoms. I would thank all of you for bringing me a great time and being my English teachers. Macros Kuroki and Sheila Nguyen have been wonderful friends and life mentors, providing me with an endless friendship.

I am most grateful to my boyfriend, Adam Vogel, and his family, Lois Vogel, James Vogel, and Elly Vogel. Your patience, encouragement and support fill my personal life with all the wonderful color. To me, you are my second family.

Finally, I greatly appreciate my family's support and encouragement in the five years, although you are far away from here. My mom (Cheng-Ming), aunt (Cheng-Hui)

and dad (Cheng-Ping) are very generous to host my visiting. I would like to thank my brother and twin sister to take care of our parents when I am not there. In addition, cheers from my uncles, aunts, and cousins help me overcome a lot of difficult situations.

It would not have been possible to write this dissertation without the help and support of you. Because of you, pursuing my Ph. D. has been a joyous path.

Dedication

This dissertation is dedicated to my mother Cheng-Ming Chin with love.

*"將此博士**畢**業**論**文獻給**我親愛**的娘—覃正明"*

Abstract

Copy number gain of 8q24 is a common structural abnormality in human cancers. Although *MYC* is usually assumed to be responsible for 8q24 gain cancer, the role of the other genes in the 8q24 region remains mostly unknown. We derived chromosome engineered mice with an extra copy of *Myc-Gsdmc* region which is syntenic to the common region gained in human 8q24-associated cancer. These mice show aberrant differentiation and loss of proliferation arrest of mammary epithelial cells, excessive branching of mammary ducts, and increased sensitization to mammary tumors. In contrast, mice carrying a duplication of either *Myc* or *Pvt1-Gsdmc* were found to be insufficient for neoplasia. We show that the long non-coding RNA *Pvt1* and adjacent *Myc* can co-operate in tumorigenesis. Furthermore, *PVT1* can regulate MYC protein stability in human breast cancer cells. Our study reveals a novel mechanism of MYC regulation by a long non-coding RNA in cancer cells and could provide therapeutic targets.

Table of Contents

List of Tables vii
List of Figures viii
Introduction and Literature Review 1
Genomic mutations in cancers 2
Chromosome 8q24 region is associated with human cancers 3
The role of 8q24 gains in cancer development is unclear 4
PVT1 locus is co-amplified with MYC 5
Breast cancer with 8q24 gain is associated with poor prognosis 6
Chromosome engineered mouse models mimic human genetic diseases 7
Her2 amplification is a common co-mutation with 8q24 gain in breast cancer 8
Summary 9
Materials and Methods 11
Chromosome Engineering 11
Mouse Strains and Tumor Analysis 11
Mammary Gland Isolation, Whole Mounts, and Measurement of Mammary Ductal Branching 13
Histological Analysis and Tissue Immunofluorescence Staining 13
Cell Culture and Reagents 15
RNA Isolation, Reverse-Transcription, and RT-qPCR Analysis 15
Western Analysis 16
siRNA Transfections and 3D Culture 18
Determination of Protein Stability 19
Ki67 Proliferation Assay 19
Statistical Analysis 20
Results 21
Generation of Mouse Strains with ~2 Mb Rearrangements Corresponding to Human 8q24.21 21
Single Copy Gain of *Myc-Gsdmc* Affects Mammary Structure, Proliferation and Differentiation 31
Generation of *Myc*$^{dp/+}$ and *Pvt1-Gsdmc*$^{dp/+}$ mice 38
Gain of Myc or Pvt1-Gsdmc Alone is Insufficient to Produce Aberrant Phenotype in Mammary Epithelium 42

Single Copy Gain of *Myc-Gsdmc* is an Oncogenic Aberration which Promotes Mouse Mammary Tumors 51
Non-coding RNA PVT1 Controls Cellular Proliferation in Mammary Tumors 65
PVT1 Regulates MYC Stability in Human Breast Cancer 74
Discussion 82
Bibliography 88
Appendix A 106
Appendix B 107

List of Tables

Table 1. Gene targeting of mouse genome at the *Myc*^{L}, *Myc*^{R} and *Gsdmc*^{R} loci..... 12
Table 2. Oligonucleotide sequences..... 17
Table 3. Genetic elements shared between human and mouse in the *MYC*-*GSDMC* interval..... 24

List of Figures

Figure 1 A. The sytenic region of Hu 8q24.21 is at Mus chromosome 15. 22
Figure 1 B. Genes and other structural features conserved between human and mouse in the *Myc-Gsdmc* interval. 23
Figure 1 C. First gene targeting at D15Mit103 locus. 26
Figure 1 D. Second gene targeting at D15Mit27 locus. 27
Figure 1 E. Cre-mediated recombination. 28
Figure 1 F. FISH analysis of *Myc-Gsdmc*$^{df/dp}$ ES cells. 29
Figure 1 G. Germline transmission of engineered allele. 30

Figure 2 A. Mammary epithelial cells isolated from *Myc-Gsdmc*$^{dp/+}$ mice promote proliferation in 3D Matrigel cultures. 32
Figure 2 B . Excessive lateral branching in *Myc-Gsdmc*$^{dp/+}$ mammary glands. 34
Figure 2 C. Precocious alveolar-like phenotype in *Myc-Gsdmc*$^{dp/+}$ mammary ducts. 36
Figure 2 D. Loss of proliferation arrest in *Myc-Gsdmc*$^{dp/+}$ mammary glands. 37
Figure 2 E. Aberrant differentiation of mammary epithelial cells in *Myc-Gsdmc*$^{dp/+}$ mice. 39
Figure 2 F. Excessive proliferation of myoepithelia cells and luminal cells in *Myc-Gsdmc*$^{dp/+}$ mammary ducts. 40
Figure 2 G. Reduced expansion of ERα^{+} cells in *Myc-Gsdmc*$^{dp/+}$ mammary ducts. 41

Figure 3 A. Chromosome engineered mouse for a single copy gain of *Myc* or *Pvt1-Gsdmc*. 43
Figure 3 B. Engineering *Myc*$^{df/dp}$ allele in mouse ES cells. 44
Figure 3 C. Engineering *Pvt1-Gsdmc*$^{df/dp}$ allele in mouse ES cells. 46
Figure 3 D. *Myc*$^{dp/+}$ and *Pvt1-Gsdmc*$^{dp/+}$ mice do not display mammary gland hyperplasia. 48
Figure 3 E. Neither *Myc* nor *Pvt1* alone are sufficient to inhibit proliferation arrest. 50
Figure 3 F. *Myc-Gsdmc*$^{df/dp}$ mammary ducts are as normal as wt. 52
Figure 3 G. *Myc-Gsdmc*$^{df/dp}$ mammary epithelial cells (MECs) are quiescent. 53

Figure 4 A. Quantitative RT-PCR analysis to assess the relative expression of Myc, Pvt1, and Gsdmc mRNA in mammary glands. 54
Figure 4 B. Western analysis of total protein lysates from mammary glands of indicated genotypes. 55
Figure 4 C. Increased apoptosis in mammary ducts of *Myc-Gsdmc*$^{dp/+}$ mice. 57
Figure 4 D. IF staining for γ-H2AX foci. 59
Figure 4 E. Generation of mouse with double mutations by crossing the duplication and MMTVneu lines. 60
Figure 4 F. *Myc-Gsdmc*$^{dp/+}$, MMTVneu/+ MECs exhibit increased number of abnormal acinar structure than MMTVneu/+ MECs in 3-D culture. 62
Figure 4 G. Transwell migration assay shows the MMTVneu/+, *Myc-Gsdmc*$^{dp/+}$ mammary epithelial cells has a higher migratory ability to EGF compared to the MMTVneu cells. 63
Figure 4 H. Early onset of hyperplastic alveolar nodules (HAN) like structures in MMTVneu/+, *Myc-Gsdmc*$^{dp/+}$ mammary glands. 64

Figure 4 I. Kaplan–Meier analysis of mammary tumor free among the different genotypes. 66
Figure 4 J. Representative histopathology of mammary tumors from *Myc-Gsdmc*$^{dp/+}$,MMTV-neu/+ mice..... 67

Figure 5 A. Schematic of proliferation assay for *Myc-Gsdmc*$^{dp/+}$, MMTV-neu/+ mammary tumor derived cells obtained from two mice, YYT549 and YYT409..... 69
Figure 5 B. Ki-67 proliferation indexes from siRNA mediated silencing of Myc, Pvt1, and Myc+Pvt1 in primary mammary tumor cells..... 70
Figure 5 C. Quantitative RT-PCR analysis to assess the relative expression of Myc, Pvt1, and Gsdmc mRNA in primary mammary tumor cells after siRNA mediated silencing..... 72
Figure 5 D. Ki-67 proliferation indexes from siRNA mediated silencing of MYC, PVT1, and MYC+PVT1 in human breast cancer cells. 73
Figure 5 E. Quantitative RT-PCR analysis to assess the relative expression of MYC, PVT1, and GSDMC mRNA in human breast cancer cells after siRNA mediated silencing. 75

Figure 6 A. Quantitative RT-PCR analysis to assess the relative expression of MYC, PVT1, and GSDMC mRNA in human breast cancer cells..... 76
Figure 6 B. SK-BR-3 and MDA-MB-231 cells express higher level of MYC protein compared to MCF10A. 77
Figure 6 C. Western analysis for MYC protein in the total lysates obtained from SK-BR-3 and MDA-MB-231 cell lines transfected with different si-RNAs..... 79
Figure 6 D. PVT1 regulates MYC stability in SK-BR-3 breast cancer cells..... 80

Introduction and Literature Review

Chromosomal aberration is a signature of cancer (Hanahan and Weinberg, 2000; Mitelman, 2005; Storchova and Pellman, 2004). Several chromosomal regions with increased/decreased copy numbers have been frequently identified across diverse human cancers by current genome scanning platforms, such as high resolution array-Comparative Genomic Hybridization (aCGH) and Single Nucleotide Polymorphism (SNP) array (Aguirre et al., 2004; Carrasco et al., 2006; Tonon et al., 2005; Zhao et al., 2005). In addition, cancer clinical outcomes (Engler et al., 2012; Kim et al., 2012) and therapeutic treatment has been successfully predicted by large-scale DNA copy number variations (CNVs). A notable genomic event is chromosome 8q24 gain, which is frequently observed in many cancer types, including breast cancer (Horlings et al., 2010). In breast cancer, 8q24 gain is observed in over 20% of primary tumors and cell lines. Importantly, 8q24 gain is reinforced by its association with poor prognosis. While the well-established oncogene, *MYC*, maps to this region and likely contributes to the pathology of cancers, the long non-coding RNA, *PVT1*, also maps to this region and has been implicated in carcinogenesis in which it is co-amplified with *MYC* (Guan et al., 2007; Huppi et al., 2012; TCGA, 2011, 2012a, b). However, an *in vivo* functional role of 8q24 gain in cancer development remains a daunting challenge for lack of suitable animal models. Thus, in this study, we developed new chromosome engineered mouse models to accurately mimic human chromosome 8q24 gain in cancer and determine how this gain contributes to the initiation and progression of breast cancer.

Genomic mutations in cancers

Cancer is a genetic disease. For decades, scientists have identified many genomic mutations that influence key cellular pathways involved in carcinogenesis. These discoveries provide a solid foundation for understanding molecular mechanisms of tumor formation and developing better therapeutic strategies of cancer treatments. However, most research has focused on mutations, affecting the DNA sequence of genes. Little is known about the role of large-scale mutations in chromosomal structure, such as deletions and gains involving large spans of DNA. These structural mutations are a common occurrence in all forms of cancer (Beroukhim et al., 2010; Degenhardt et al., 2008; Santarius et al., 2010). As such, an important aspect of functional genomic analyses in cancer is to faithfully recapitulate these structural mutations. Current mouse models have greatly improved our understanding of cancer, but the fact that the majority of mouse models are representative of sequence mutations leaves a gap in our understanding of the complexity of chromosomal aberrations. For example, a large-scale deletion or duplication region may alter the dosage of several tumor suppressor genes or oncogenes to collaboratively contribute the pathology of cancer. In such events, mouse models of single gene alteration are not suitable to address these structural mutations in cancer. Therefore, there is a need to generate mouse models that can mimic these penetrant mutations. Our goal is to closely mimic a chromosomal abnormality, gain of human 8q24 region, that has frequently been observed in the patients' tumor by using mouse models, and to be able to understand the significance of 8q24 gain in the growth and development of the tumor.

Chromosome 8q24 region is associated with human cancers

A gene desert located on human chromosome region 8q24.21 is particularly intriguing because of the complexity of the sequence variants and structural aberrations associated with 8q24 region in different cancer genomes. For example, genome wide association studies (GWAS) have identified several 8q24 single nucleotide polymorphisms (SNPs) linked to the development of breast cancer (Easton and Eeles, 2008; Turnbull et al., 2010), prostate cancer (Gudmundsson et al., 2007; Turnbull et al., 2010; Yeager et al., 2007), ovarian cancer (Ghoussaini et al., 2008; Goode et al., 2010; Yeager et al., 2007), colon cancer (Yeager et al., 2007), esophageal cancer (Gudmundsson et al., 2007; Lochhead et al., 2011; Yeager et al., 2007), bladder cancer (Ghoussaini et al., 2008; Kiemeney et al., 2008), chronic lymphocytic leukemia (Crowther-Swanepoel et al., 2010) and Hodgkin's lymphoma (Enciso-Mora et al., 2010). Furthermore, the 8q24 region is one of the most common sites for human papilloma virus (HPV) integration in genital neoplasia (Ferber et al., 2003; Kraus et al., 2008; Peter et al., 2006). In addition, the chromosomal 8q24-based translocation is a hallmark lesion in Burkitt's lymphoma, large B-cell lymphoma, and T-cell leukemia (Erikson et al., 1983; Graham and Adams, 1986; Shtivelman et al., 1989; Webb et al., 1984). More importantly, gain of 8q24, such as duplication and amplification of 8q24 region, is also observed in numerous cancers, including 20% of breast cancer, 60% of ovarian, 25-40% of cervical cancers, 15-40% of prostate cancer, 42% of gastric cancers, 10-25% of melanoma, 7% of head and neck cancers, and 20% of lymphoma and leukemia. (Borg et al., 1992; Boyd et al., 2012; Guan et al., 2007; Hartmann et al., 2008; Haverty et al., 2009; Kim et al., 2006; Kraehn et al., 2001; Mangano et al., 1998; Treszl et al., 2004; van

Duin et al., 2007). Therefore, to fully understand the role of 8q24 in cancer development, it is important to investigate how this region contributes to cellular transformation.

The role of 8q24 gains in cancer development is unclear

A segment of 8q24 region linked to susceptibility for cancers is about 2.7 Mb (8q24.21, 128.0 Mb ~ 130.7 Mb) (Huppi et al., 2012). One gene found at this 8q24.21 region, *c-MYC* (*MYC*) proto-oncogene, stands out as a key player in malignant transformation. For instance, in most of Burkitt's lymphoma cases, the reciprocal chromosomal translocation is between the immunoglobulin (Ig) heavy chain and *MYC*. Deregulated MYC expression as a result of this fusion has been validated as an initiating step of Burkitt's lymphoma development (Adams et al., 1985; Zhu et al., 2005). In addition, MYC activation that is triggered by the insertion of HPV DNA sequences has been reported to contribute cervical oncogenesis (Gurel et al., 2008; Peter et al., 2006). In the case of cancers with 8q24 gain, it was originally thought that increased copies of 8q24 region simply lead to deregulated expression of MYC. However, inconsistent correlations between copy number variation (CNV) studies and gene expression analyses (Gurel et al., 2008; Haverty et al., 2009) have raised the possibility that MYC is not the only factor. The question is, could other co-amplified genes on the 8q24 region be responsible for cancer development? Or, is MYC itself sufficient to drive pathogenesis of cancer? Comprehending the fact that increased 8q24 copy number is not equal to MYC overexpression is critical for finding a better therapeutic strategy to treat cancer patients with 8q24 gain.

PVT1 locus is co-amplified with MYC

With a study of high-resolution SNP array analysis, the hot zone of 8q24 copy number gains is around 2.1 Mb (8q24.21, 128.6 Mb ~ 130.7 Mb) including *MYC*, plasmacytoma variant translocation (*PVT1*), and CCDC26 (Haverty et al., 2009; Hirano et al., 2008; Huppi et al., 2012; TCGA, 2011, 2012a, b). Though an obvious candidate, the fact that copy-number increases of 8q24 frequently include *MYC* and the adjacent gene-desert, which may subsume additional genetic elements that contribute to induction of cancer is under-investigated. Adjacent to *MYC* is *PVT1*, a long non-coding (lnc) RNA locus originally identified as a cluster of breakpoints for viral integration and translocation in T- and B-cell lymphomas (Erikson et al., 1983; Webb et al., 1984). The *PVT1* locus spans more than 300 kb that encompasses six microRNA-encoding sequences, miR-1204 ~ miR-1208 and is conserved in the human and mouse genomes (Beck-Engeser et al., 2008; Huppi et al., 2008). Despite being a mutational hotspot, the role of PVT1 in cancer is poorly understood. A recent cell culture-based study has suggested anti-apoptotic and pro-survival roles for PVT1 (Guan et al., 2007). One of the miRNAs encoded by the *PVT1* locus, miR-1204, has been reported to be enriched in 8q24 gain-specific cancer cell lines (Beck-Engeser et al., 2008; Huppi et al., 2008), although another study has implicated miR-1204 with tumor suppressive activity (Barsotti et al., 2012). The lack of an *in vivo* system that links *MYC* with additional elements in the 8q24 region has been a major impediment in understanding the role of genetic elements in this region to the pathophysiology of cancer.

Breast cancer with 8q24 gain is associated with poor prognosis

Breast cancer is second leading cause of cancer death in women. According to American Cancer Society's statistics, one of every eight women in United State will develop invasive breast cancer during their lifetime. These statistics highlight the burden that breast cancer poses on the national healthcare system in particular and society in general. Recent advances in our understanding of breast cancer have resulted in improvement in the treatment and management of the disease; nevertheless, the development of more effective and targeted therapies for breast cancer patients remains a goal in the cancer community. Therefore, developing *in vivo* models that finely mimic the genetic alterations of breast cancer can not only explore basic pathophysiological mechanisms but also evaluate new therapeutic approaches.

DNA copy-number gains, such as duplication and amplification, are common mutations found in epithelial cancers, including breast cancer. Around 20% breast cancers show increased copies of 8q24 region (Berns et al., 1992a; Letessier et al., 2006) and are associated with poor clinical outcomes (Aulmann et al., 2006; Berns et al., 1992a; Berns et al., 1992b; Bonilla et al., 1988; Deming et al., 2000; Roux-Dosseto et al., 1992; Schlotter et al., 2003). For example, 8q24 gain has been found in the more aggressive phenotype of ductal carcinoma in situ (Aulmann et al., 2002) or in only the invasive component (Aulmann et al., 2006; Corzo et al., 2006; Robanus-Maandag et al., 2003). *PVT1* locus co-amplified with *MYC* in the 8q24 region and PVT1 transcripts have been implicated to participate in breast cancer progression as well (Guan et al., 2007). However, little evidence exists to support that role because most studies have concentrated on the oncogene, MYC. A clear functional role of 8q24 gain for breast

cancer pathophysiology still needs to be validated *in vivo*. Yet, most mouse models for breast cancer studies focus primarily on the effects of Myc overexpression in promoting mammary tumor formation (Boxer et al., 2004; D'Cruz et al., 2001; Schoenenberger et al., 1988; Stewart et al., 1984). For instance, the first transgenic Myc model, in which the oncogene was expressed under the control of the hormone responsive mouse mammary tumor virus (MMTV) promoter, developed mammary adenocarcinomas following their first pregnancy (Stewart et al., 1984). Subsequently, other transgenic models, including models in which Myc expression can be regulated (by Tet-on and Tet-off systems) have tried to elucidate the mechanisms by which deregulated MYC contributes to tumorigenesis, including regulatable tumors in the mammary tissue (Boxer et al., 2004; D'Cruz et al., 2001). Although these transgenic mouse models are very helpful in elucidating the role of MYC deregulation, no mouse model can truly recapitulate the increased copies of 8q24 region. To investigate the role of 8q24 gain in breast carcinogenesis, new approaches should be applied to improve current models.

Chromosome engineered mouse models mimic human genetic diseases

Chromosomal aberrations are frequently found in humans and could be disease-associated or phenotypically neutral. Validating the functional role of these aberrations and understanding how they contribute to the pathology of cancer are necessary for improvement in diagnosis and therapy. Because of genetic and physiologic similarities between mouse and human, mouse has proved to be an invaluable model organism in allowing understanding of the genomic landscape that results in human diseases. In addition, mice have many important advantages over other mammalian models, including

(1) small body size; (2) less expensive for maintaining; (3) fast reproduction and large litter size; (4) mature techniques for genetic manipulation. A novel method, chromosome engineering, which combines the power of gene targeting in mouse embryonic stem (ES) cells with Cre/loxP recombination, allows for the generation of mouse models that harbor large-scale rearrangements of specific chromosome regions (Mills and Bradley, 2001; Yu and Bradley, 2001). For example, the mouse models that were generated by chromosome engineering have several psychotic phenotypes similar to those seen in autism or schizophrenia patients with duplication of the 15q11-13 locus (Nakatani et al., 2009), deletion/duplication of the 16p11.2 (Horev et al., 2011), or microdeletion of the 22q11.2 (Merscher et al., 2001; Stark et al., 2008). In addition to these psychiatric disorders, chromosome engineered mouse models with loss or gain of genomic regions corresponding to human 1p36 successfully provide functional evidence that chromodomain helicase DNA binding 5 (*CHD5*) plays a tumor suppressive role in caner development (Bagchi et al., 2007). Thus, chromosome engineering offers a very powerful tool to mirror the gain of human 8q24 region as closely as possible in the mouse genome.

Her2 amplification is a common co-mutation with 8q24 gain in breast cancer

Cancer is frequently accompanied by multiple genetic alterations. As previously mentioned 8q24 region has been reported to be amplified in approximately 20% of breast cancers and appears to related to a poor prognosis. The 17q12 region, contains human epidermal growth factor receptor 2 (*HER2*) gene, is highly amplified (more than 200 copies) in around 30% of breast cancers and, therefore, leads to HER2 overexpression (Liang et al., 2008). Interestingly, many studies have reported that the 8q24 gain is

strongly associated with ERBB2/HER2/neu amplification in breast cancers (Al-Kuraya et al., 2004; Park et al., 2005; Persons et al., 1997; Sircoulomb et al., 2010). With cytogenetic analyses, for instance, more than 40% of 8q24 gain breast cancers co-amplified with *HER2* amplification (Janocko et al., 2001; Park et al., 2005; Persons et al., 1997). Adjuvant ERBB2-targeted therapy, trastuzumab, improves the overall survival rate of ERBB2-positive early cancer patients compared with chemotherapy alone (Perez et al., 2009). However, clinical outcome findings are inconsistent regarding the benefits from adjuvant trastuzumab therapy in ERBB2/8q24 amplifications patients (Kim et al., 2005; Perez et al., 2011). These indicate that several synergistic collaborations activate the ERBB2 pathway by increased copies of *MYC* or other gene deregulation, such as *PVT1* locus, located on the 8q24 interval. It is important to identify these relationships to develop alternative molecular targets and manage combination therapies.

Summary

Chromosomal abnormalities like deletions, translocations, and duplications/amplifications are hallmarks of almost all cancers. Increased copy number of the 8q24 region, such as a single-copy gain of 8q24, a locus that contains the proto-oncogene *MYC,* has been implicated in many human cancers, particularly in solid tumors. Importantly, this 8q24 gain is often associated with poor progonosis of breast cancer, indicating that 8q24 gain may not only play an important role in tumorigenesis but also contribute to tumor progression. Mouse models for studying the effects of Myc overexpression have been helpful in elucidating its in neoplastic transformation. However, these transgenic mouse models do not allow for examining the large-scale

genomic gain of 8q24 that is frequently found in human breast cancers, strongly suggesting the need for additional models to mirror the highly penetrant and aggressive tumors associated with 8q24 gain. Moreover, in many cancers, *MYC* is co-amplified with the neighboring genetic elements which have also been implicated in tumorigenesis in multiple studies. We argue that increased copies of MYC alone is not sufficient to result in the poor prognosis seen in the breast cancer patients with 8q24 gain, and we hypothesize that additional gene(s) in the 8q24 amplicon contributes substantially to the mammary tumor initiation and/or aggressive progression of neoplasia.

In this study, we sought to determine the contributions of a single-copy gain of 8q24 to oncogenic transformation in cancer. Our study focused on determining whether either gain of *MYC* alone is sufficient to drive tumor formation, or if other elements in the gene-desert region play a role in this process. To fully understand the role of 8q24 gain in cancer development, we developed genetically engineered mice with a single-copy number gain of an approximately 2 Mb interval that is syntenic to Hu 8q24.21. Next, to discern the contribution of *Myc* and the rest of region in cancer inception, we generated two additional genetically engineered mouse strains, one harboring a gain of *Myc* only and another with an extra copy of the rest of the region. Using these *in vivo* models and human breast cancer cell lines, we have uncovered a new oncogenic role for lncRNA PVT1, and demonstrate that it co-operates with MYC in oncogenic transformation.

Materials and Methods

Chromosome Engineering

The procedures of chromosome engineering were performed as previously described (Bagchi et al., 2007). In brief, AB2.2 ES cells (129S5 strain) were electroporated with 25 µg of the targeting vector (Table 1). These electroporated ES cells were cultured in G418 (180 µg/ml) or puromycin (3 µg/ml) for 7-10 days. Correctly targeted clones were identified by polymerase chain reaction (PCR) analysis. Double-targeted ES cells were electroporated with the transient Cre recombinase expression vector pOG231. After subsequent selection of recombinants by using hypoxanthine aminopterin thymidime (HAT) media for 7 days and then recovery of recombinants by using hypoxanthines and thymidine (HT) media for 2 days, the $H^RG^RP^R$ clones containing one mouse chromosome 15 with the targeted locus duplication (*dp*) and the other mouse chromosome 15 with the targeted locus deletion (*df*) were identified and confirmed by using fluorescence in situ hybridization (FISH) analysis.

Mouse Strains and Tumor Analysis

Correctly targeted *df*/*dp* ES clones were injected into C57BL/6J blastocysts to establish chimeric mice. The F1 *dp*/+ progeny generated from chimera crossed with C57BL/6J were genotyped by PCR and backcrossed three times to FVB/N mice. For tumor analysis, *dp*/+ mouse strains were crossed with FVB/N-Tg(MMTVneu)202Mul/J transgenic mice (purchased from The Jackson

Table 1. Gene targeting of mouse genome at the *Myc*^{L}, *Myc*^{R} and *Gsdmc*^{R} loci.

Engineering mouse		Target locus	MICER clone	Co-ordinates	LoxP direction	Gap size (kb)	Restricted enzyme	Linker (Yes/No)	Targeting efficiency
Myc-Gsdmc$^{dp/+}$	1st	Gsdmc^{R}	MHPN93A17	chr15:63,937,185-63,944,470	Centromere	0.3	SfiI + HpaI	Yes	12.50%
	2nd	Myc^{L}	MHPP129C23	chr15:61,954,800-61,965,870	Centromere	1.9	KpnI	No	26.04%
Myc$^{dp/+}$	1st	Myc^{R}	MHPP333E06	chr15:61,999,071-61,999,459	Centromere	1.4	AflII	No	14.14%
	2nd	Myc^{L}	MHPN129C23	chr15:61,954,800-61,965,870	Centromere	1.9	KpnI	No	55.56%
Pvt1-Gsdmc$^{dp/+}$	1st	Myc^{R}	MHPP333E06	chr15:61,999,071-61,999,459	Centromere	1.4	AflII	No	14.14%
	2nd	Gsdmc^{R}	MHPN93A17	chr15:63,937,185-63,944,470	Centromere	0.3	SfiI + HpaI	Yes	20.20%

Laboratory) to generate the control (hemizygous MMTVneu) and experimental (*dp*/+, hemizygous MMTVneu) animals. After 4 months, these mice were monitored weekly by palpation for tumor induction. Tumors were documented in a double blinded manner. Animal protocols were approved by the Institutional Animal Care and Use Committee of University of Minnesota and were conducted in accordance with the procedures in the Guide for Care and Use of Laboratory Animals.

Mammary Gland Isolation, Whole Mounts, and Measurement of Mammary Ductal Branching

Six-week-old and ten-week-old virgin mice were sacrificed for dissecting mammary glands. Mammary glands from at least three mice per genotype were analyzed. For the mammary ductal branching studies, inguinal (No. 4) mammary glands were spread out, fixed in 4% paraformaldehyde (Merck) for 2 hr, and then stained as described (Schwertfeger et al., 2006). Images were acquired using Lieca Application Suite software on a Leica dissecting microscope and analyzed using Adobe Photoshop and ImageJ software. Number of ductal branch point was measured from the 25 mm^2 area near the lymph node of mammary gland. All experimental mice and control mice were littermates with matching estrous cycles.

Histological Analysis and Tissue Immunofluorescence Staining

Histological analyses were performed on hematoxylin and erosin (H&E)-stained paraffin sections of paraformaldehyde-fix (4%) mammary glands and tumors. For immunofluorescence analyses, 5-µm sections were deparaffinzed and rehydrated, and

antigens were retrieved using the Antigen Unmasking Solution (Vector Laboratories). Section samples were washed with PBS and blocked using M.O.M. basic kit (Vector Laboratories) or 10% normal goat serum for 1 hr. Primary antibodies were incubated for overnight at 4 ^{0}C. For proliferation assays, mice were injected with 100 mg/kg BrdU drug (Sigma) 2 hr before sacrifice, and tissues were stained with anti-BrdU (Abcam) at 1:300 dilution as described previously [Reed et al., 2012], and sections were counter stained with diaminophenylindole (DAPI, Invitrogen). Other primary antibodies were diluted with M.O.M. diluent as the following conditions: cytokeratin 8 (1:100, Epitomics), cytokeratin 14 (1:150, Covance), ERα (1:50, Santa Cluz Biotechnology), and γH2AX (1:100, Cell Signaling). Each staining was performed in mammary gland sections dissected from at least three mice of experimental groups and control group. Fluorescent images were acquired using the fluorescence microscopy (Carl Zeiss Axio Obersever.Z1).

Cell Culture and Reagents

Primary mouse tumor cells or primary mouse mammary epithelial cells (MECs) were dissociated from mammary tumors or mammary glands by incubation with collagenase type I (Invitrogen) for 3 hr and then plated on fetuin (Sigma) in growth media (DMEM/F12 containing 10% fetal bovine serum (FBS, Gibco), 5 µg/ml insulin (Sigma), 1 µg/ml hydrocortisone (Sigma), 5 ng/ml EGF (Sigma), and 200U/ml pen/strep (Invitrogen)) as described previously [Schwertfeger et al., 2006]. After 3 days, mammary epithelial cells and tumor cells were collected and stored at -80 ^{0}C for further experiments. Only early passages of tumor cells were used for advanced assays. Human breast cancer cell lines SK-BR-3 and MDA-MB-231 were obtained from American Type Culture Collection (Manassas, VA). SK-BR-3 and MDA-MB-231 cells were cultured in McCoys5A (Lonza) containing 10% FBS and DMEM (Invitrogen) containing 10% FBS individually.

RNA Isolation, Reverse-Transcription, and RT-qPCR Analysis

Mouse mammary glands were removed at six and ten weeks of age and immediately stored in the liquid nitrogen. Frozen mammary tissue lysates were prepared in Trizol Reagent (Invitrogen) by using the SHREDDER SG3 system (Pressure BioSciences Inc.) as described by manufacturer. Cell lysates were collected from 6-well plates. RNA was isolated from the Trizol Reagent (Invitrogen), including a DNase digestion step (Qiagen), as described by manufacturer. Total RNA was quantified by NanoDrop (Thermo Fisher). RNA quality was estimated by running RNA on agarose gels. cDNA was synthesized from equal amounts of total RNA and followed the manufacturer's protocol using

SuperScript III reverse transcriptase (Invitrogen) with Random Hexamer primers. For real-time quantitative PCR (RT-qPCR), the 50 ng of cDNA was added in reactions carried out on an ep realplex S machine (Eppendorf) using SyberGreen master mix (Promega) and gene-specific primers (Table 2). Primers for all amplification were designed the location on exon-exon borders by using Primer3 software. Melting curve analysis was performed to confirm the specificity of primers. Amplifications were performed as technical duplicates and biological triplicates in 96-well plates.

Western Analysis

Mouse mammary tissues were collected as above and protein extracted by using the SHREDDER SG3 system (Pressure BioSciences Inc.) in RIPA lysis buffer (50 mM Tris-HCl pH 7.5; 150 mM NaCl; 1 mM EDTA; 1% Triton-X-100; 0.5% sodium deoxycholate; 0.1% SDS) with Complete Protease Inhibitor Cocktail (Roche Applied Science). Cell lysates were also prepared in RIPA lysis buffer at the indicated time points. Lysates were centrifuged 14,000 rpm at 4 ^{0}C for 30 min, supernatants were collected, and protein was quantified with the Bio-Rad protein assay kit. Equal amounts of protein were loaded and analyzed by SDS-PAGE. Immunoblotting was done using the following antibodies purchased from Cell Signaling, unless noted: c-Myc (Abcam), GAPDH, pERK1/2, ERK1/2, and P53. The signal intensity for protein of interest was normalized to that of GAPDH.

Table 2. Oligonucleotide sequences.

Primer	Sequence	Purpose
GsdmcR-linker-F	CGGCCAATGCGGCCGCTATG	Linker
GsdmcR-linker-R	CTAGCATAGCGGCCCGCATTGGCCGA	
GsdmcR-5S1	GGAAGAGCGCCCAATACGCAA	gene targeting
GsdmcR-gap-S1'	GTAACCGTACCCACTCATGCAA	
GsdmcR-5S2	GGACAGTTTCCACCACTGTCAA	gene targeting
GsdmcR-gap-S2'	GTGGGTACGGTTACAGTGATGAA	
MycL-3S1	AGGCTGCGCAACTGTTGGGAA	gene targeting
MycL-gap-S1'	GGAATACTGGTCACATCTGCCTT	
MycL-3S2	GTTGCCAGCCATCTGTTGTT	gene targeting
MycL-gap-S2'	AGCTTCTCATTTACTAACGGCAA	
MycR-3S1	AGGCTGCGCAACTGTTGGGAA	gene targeting
MycR-gap-S1'	TGAAGCCTGGGCTAGAGATG	
MycR-3S2	GTTGCCAGCCATCTGTTGTT	gene targeting
MycR-gap-S2'	GGAAGGGGAAGTGGATAGGA	
MycL-5S1	GGAAGAGCGCCCAATACGCAA	gene targeting
MycL-gap-S1'	GGAATACTGGTCACATCTGCCTT	
MycL-5S2	GGACAGTTTCCACCACTGTCAA	gene targeting
MycL-gap-S2'	AGCTTCTCATTTACTAACGGCAA	
Myc-Gsdmc-dp-F	AACTGGCTGAGTGACGCCCTTTAT	mouse genotyping PCR
Myc-Gsdmc-dp-R	TGAGACGTGCTACTTCCATTTGTC	
Myc-Gsdmc-df-F	ATCCAGCAGGTCAGCAAAGA	mouse genotyping PCR
Myc-Gsdmc-df-R	CTGGCGTCGTGATTAGTGATG	
Myc-dp-F	ATCCAGCAGGTCAGCAAAGA	mouse genotyping PCR
Myc-dp-R	CTGGCGTCGTGATTAGTGATG	
Pvt1-Gsdmc-dp-F	AACTGGCTGAGTGACGCCCTTTAT	mouse genotyping PCR
Pvt1-Gsdmc-dp-R	TGAGACGTGCTACTTCCATTTGTC	
Mus-c-Myc-F	GCATGAGGAGACACCGCCCA	qPCR
Mus-c-Myc-R	GGTTTGCCTCTTCTCCACAGA	
Mus-Pvt1-F	CTCAGCAGATGTCACACAGCG	qPCR
Mus-Pvt1-R	AGGGTCAGTATCATGGCTGGAT	
Mus-Gsdmc-F	CCAGTTGGATTTACCCTTCTGC	qPCR
Mus-Gsdmc-R	GCCTCAGTTTCTGGGATATGG	
Mus-B-actin-F	AGAGCTATGAGCTGCCTGACG	qPCR
Mus-B-actin-R	GTTTCATGGATGCCACAGGAT	
Hu-c-MYC-F	AGCTGCTTAGCGCTGGATTTT	qPCR
Hu-c-MYC-R	TCGAGGTCATAGTTCCTGTTGG	
Hu-PVT1-F	GCCCCTTCTATGGGAATCATA	qPCR
Hu-PVT1-R	GGGGCAGAGATGAAATCTAAT	
Hu-GSDMC-F	TCAGAGACAGAGGGGCTCTACA	qPCR
Hu-GSDMC-R	GTTGGAAGTCACTCAGCACCAT	
Hu-B-ACTIN-F	ACCCAGCACAATGAAGATCAAG	qPCR
Hu-B-ACTIN-R	GACTCGTCATATCCTGCTTGC	

siRNA Transfections and 3D Culture

siRNA against human *PVT1* and *c-MYC* as well as mouse *Pvt1* and *c-Myc* were designed and purchased from FlexiTube siRNA (Qiagen). Two siRNAs located different parts of *PVT1*/*Pvt1* mRNA sequence (Hs_PVT1_5 FlexiTube siRNA and Hs_PVT1_6 FlexiTube siRNA; Mm_Pvt1_1 FlexiTube siRNA and Mm_Pvt1_4 FlexiTube siRNA) and two siRNAs located different parts of *MYC*/*Myc* mRNA sequence (Hs_MYC_5 FlexiTube siRNA and Hs_MYC_7 FlexiTube siRNA; Mm_Myc_1 FlexiTube siRNA and Mm_Myc_4 FlexiTube siRNA) were used in this study. A predesigned siRNA (AllStars Neg. siRNA, Qiagen) were used for the negative control and conjugated with Alex-488 to confirm the transfection efficiency. Approximately 2 x 10^5 cells were plated to each well of a 6-well plate 24 hr before the transfection procedure and the cell confluency of each well were 50%. siRNA transfection was applied with DharmaFECT 4 (Thermo SCIENTIFIC) following the manufacturer's protocol. Cells were harvested for RNA isolation 48 hr after transfection and for protein extraction 72 hr after transfection. 5 μM siRNA were tranfected into cells. Each experiment was repeated at least three times. For the ki67 proliferation assay, cells were trypsinized from the well of a 6-well plate 24 hr after transfection, and 1 X 10^4 cells were replated in the three-dimensional (3D) on-top culture system to grow for 72 hr. For the 3D culture procedure, a total 1 X 10^4 cells were plated on growth-factor reduced matrigel (BD Bioscience) in the 8-well chamber slide as described previously (Lee et al., 2007). MECs were maintained in growth media with 2% matrigel for observing the morphology of acinus-like structures and measuring the size of acinus-like structures.

Determination of Protein Stability

Cells were separately transfected with the siRNA of PVT1 and negative control. After 24 hours siRNA transfection, the cells of each transfection group were treated with 10 μM cycloheximide (Sigma) at 0 (control sample), 15, 30, 45, 60 minutes for protein stability analysis. Cells were harvested in RIPA lysis buffer at indicated time points. The cell lysates (20 μg) were then applied to Western analysis to determine the MYC and GAPDH proteins. Protein intensities were quantified using ImageJ software. The densitometric result of MYC protein of each time point was normalized to its densitometric result of GAPDH protein. The ratio of MYC protein intensities to their internal controls were then divided by the ratio of MYC protein intensity to its internal control of control sample. Each experiment set was repeated at least three times.

Ki67 Proliferation Assay

Cell proliferation assays were performed in breast cancer cell lines as previously described (Kenny et al., 2007; Lee et al., 2007). In brief, cells were directly fixed in 8-well chamber slides with 4% paraformaldehyde after 96 hr siRNA treatments. Cells were blocked and stained with ki67 antibody (1:500, Vector Laboratories) and then counterstained with DAPI for the total number of cells as described previously (Lee et al., 2007). Ki67 index was assessed by counting the proportion of ki67 positive cells. The number of ki67 positive cells were divided by the total number of cells. The number of total nuclei counted per well was above 500 for each experimental assay.

Statistical Analysis

For Kaplan-Meier survival curves, statistical analyses were performed by using Prism 4 (GraphPad Software), and p values were calculated by the log-rank test. All other p values were calculated using Student's t test (unpaired, two-tailed, $p < 0.05$ was considered significant). Results are reported as mean ± SEM or mean ± SD. All experiments were performed at least three times.

Results

Generation of Mouse Strains with ~2 Mb Rearrangements Corresponding to Human 8q24.21

We sought to develop an *in vivo* system to elucidate the functional consequence of 8q24 gain in human cancer. Chromosome engineering of the mouse genome (Ramirez-Solis et al., 1995) was carried out to develop strains with gain and loss of the mouse genomic interval syntenic to Hu 8q24.21 (Ch8:128,718,315 to Ch8:130,831,134). This corresponds to an approximate 2Mb region on Chr15 in mouse from Ch15:61,954,800 (Myc^{L}) to Ch15:63,944,470 ($Gsdmc^{R}$) (Figure 1A). The *Myc-Gsdmc* interval is also a gene-desert region in the mouse. The highly conserved genomic synteny included annotated genes *Myc, PVT1* and *GSDMC* as well as other unannotated genomic elements (Figure 1B, Appendix A). Six cancer-related risk alleles have been identified in the *Myc-Gsdmc* region: rs2608053, rs2019960 (Enciso-Mora et al., 2010), rs1516982, rs10088218, rs10098821 (Goode et al., 2010) and rs55705857 (Jenkins et al., 2012). Syntenic homology for four out of these six risk alleles, rs2019960, rs1516982, rs10088218 and rs55705857, are found in the *Myc-Gsdmc* interval in the mouse (Figure 1B, Table 3). The *PVT1* locus also encodes five conserved miRNAs, miR-1204 – miR-1208 (Figure 1B, Table 3) (Beck-Engeser et al., 2008; Huppi et al., 2008). A putative transcript, CCDC26, is suspected to be involved in several malignancies (Jenkins et al., 2012). Though

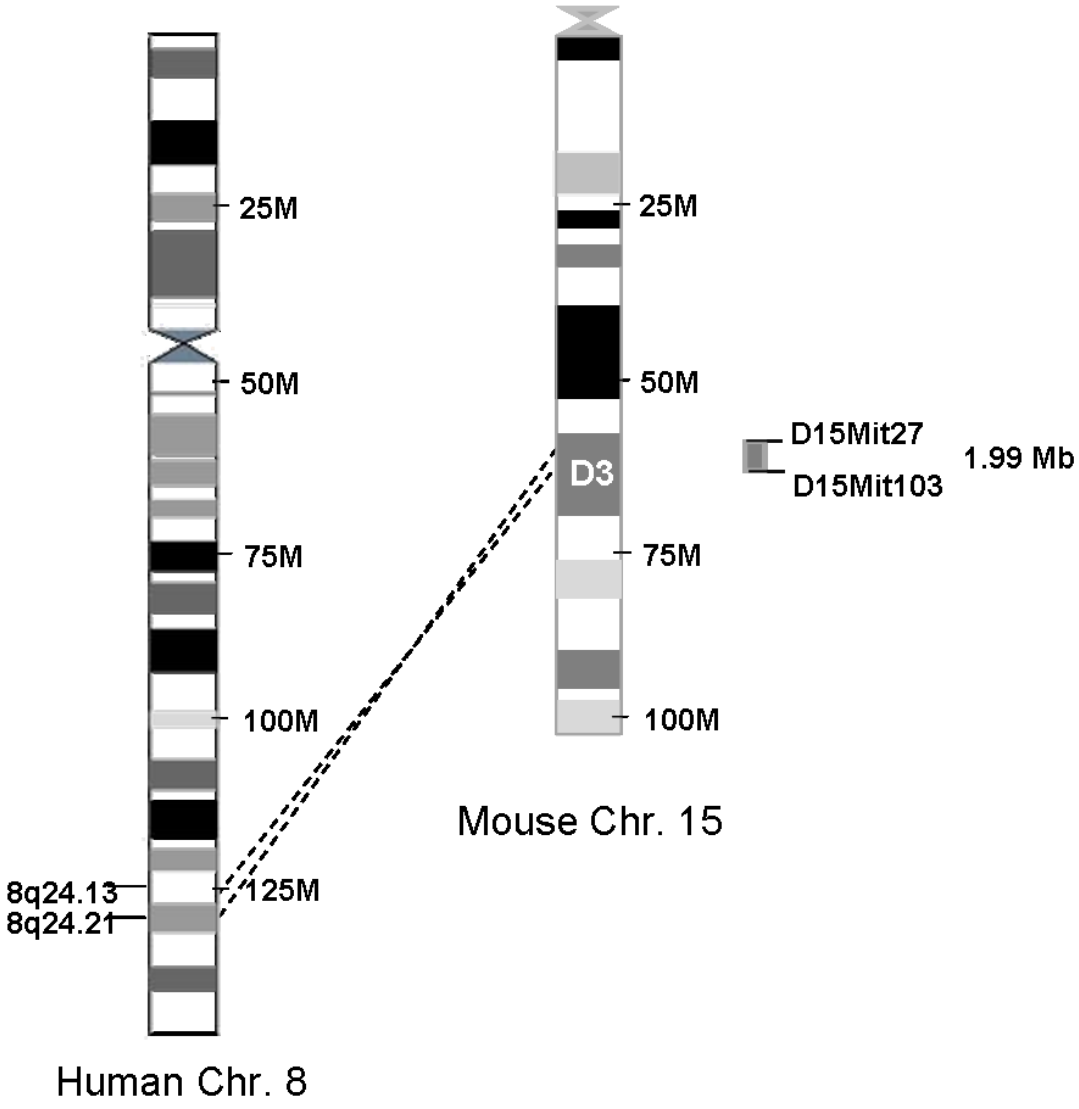

Figure 1 A. The sytenic region of Hu 8q24.21 is at Mus chromosome 15.

A ~ 2Mb genomic interval encompassing *MYC-GSDMC* on human 8q24.21 corresponds to a genomic region on mouse Chromosome 15 between D15Mit27-Mit103.

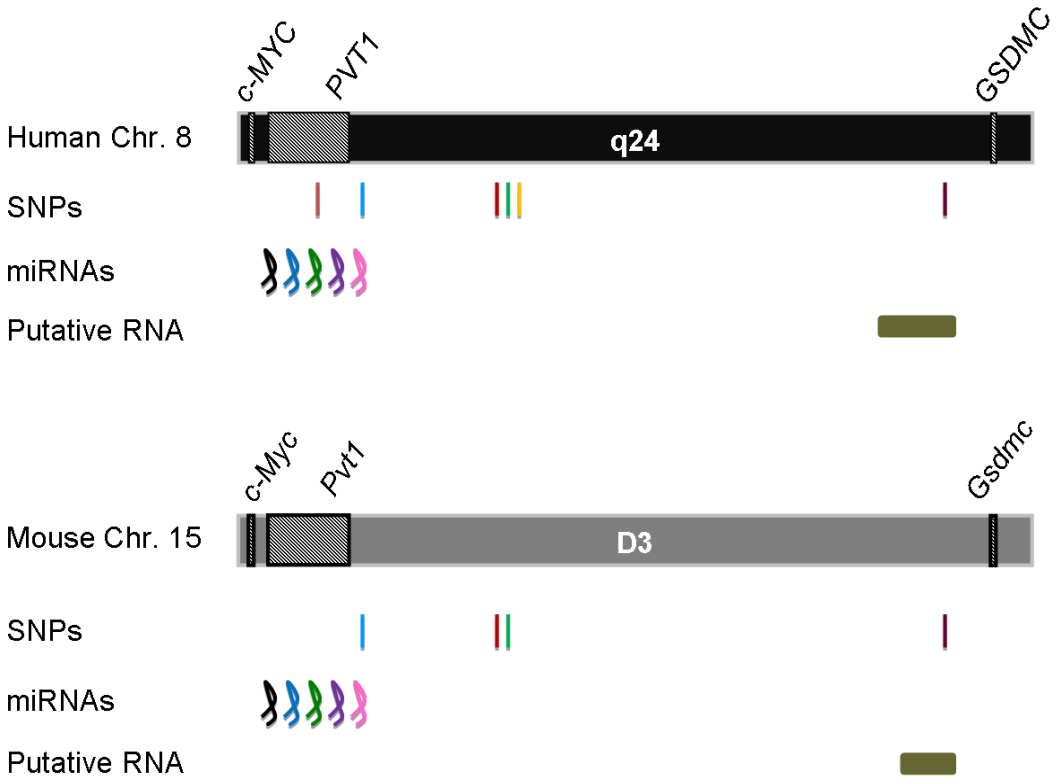

Figure 1 B. Genes and other structural features conserved between human and mouse in the *Myc-Gsdmc* interval.

See Table 3 and Appendix A for details. Cancer related risk alleles (SNPs): rs2608053 ( ), rs2019960 ( ), rs1516982 ( ), rs0088218 ( ), rs1098821 ( ) and rs55705857 ( ), miRNAs: miR-1204 ( ), miR-12[illegible] ( ), miR-12[illegible] ( ), miR-12[illegible] ( ) and miR-1[illegible]8 ( ) and putative transcript CCDC26 map in this region.

Table 3. Genetic elements shared between human and mouse in the *MYC-GSDMC* interval.

Genes and cancer related risk alleles	Co-ordinates in human genome	Co-ordinates in mouse genome
c-MYC[a]	chr8:128,748,315-128,752,723	chr15:61,985,341-61,990,361
PVT1[d]	chr8:128,806,779-129,113,499	chr15:62,037,987-62,250,975
GSDMC[a]	chr8:130,760,442-130,799,134	chr15:63,775,971-63,912,297
rs2608053[b]	chr8:129075807 129075858	-
rs2019960[b]	chr8:129,192,245-129,192,296	chr15:62,331,439-62,331,479
rs1516982[b]	chr8:129,533,620-129,533,671	chr15:62,669,784-62,669,831
rs10088218[b]	chr8:129,543,923-129,543,974	chr15:62,682,150-62,682,195
rs10098821[b]	chr8:129,559,202-129,559,253	-
rs55705857[b]	chr8:130,645,666-130,645,717	chr15:63,675,552-63,675,604
miR-1204[c]	chr8:128,808,208-128,808,274	chr15:62,039,394-62,039,465
miR-1205[c]	chr8:128,972,879-128,972,941	chr15:62,159,214-62,159,276
miR-1206[c]	chr8:129,021,144-129,021,202	chr15:62,188,081-62,188,132
miR-1207[c]	chr8:129,061,398-129,061,484	chr15:62,223,418-62,223,525
miR-1208[c]	chr8:129,162,362-129,162,434	chr15:62,301,237-62,301,299
CCDC26[d]	chr8:130,363,937-130,692,485	chr15:63,435,961-63,705,305

a: gene
b: single-nucleotide polymorphism
c: miRNA
d: non-coding RNA

a mouse homolog is yet to be identified, the genomic synteny is found to be conserved between the two species (Figure 1B, Table 3). These shared features indicate that the *Myc-Gsdmc* gene-desert is highly conserved between human and mouse.

Gene targeting was performed in AB2.2 mouse embryonic stem (ES) cells deficient in hypoxanthine guanine phosphoribosyl transferase (*Hprt*). The targeting vectors were obtained from the Mutagenic Insertion and Chromosome Engineering Resource (MICER) and were modified to facilitate detection of correctly targeted clones by Polymerase Chain Reaction (PCR) (Table 1). Targeting at $Gsdmc^{R}$ (distal to *Gsdmc*) (Figure 1C), occurred with a frequency of 12%. Germline-competent singly targeted clones were re-targeted at Myc^{L}, proximal to *Myc* (Figure 1D, Table 1), with an efficiency of 26%. Twelve doubly targeted ES cell clones were electroporated with a Cre-expressing construct and the clones were grown under HAT selection for recombined alleles (Figure 1E). To confirm the genomic rearrangements, we examined these ES cells by fluorescent in-situ hybridization (FISH) using bacterial artificial chromosome (BAC) probes. These probes which are specific for mouse Ch15 centromeric region (RP23-18H8) and the *Myc-Gsdmc* interval (RP24-78D24) affirmed the deficiency/duplication (*df/dp)* status of the *Myc-Gsdmc* interval in metaphase and interphase spreads (Figure 1F). Two independent *df/dp* clones were established as mouse strains (Figure 1G) and the offspring were genotyped by PCR. Each strain was backcrossed to the FVB background for three generations.

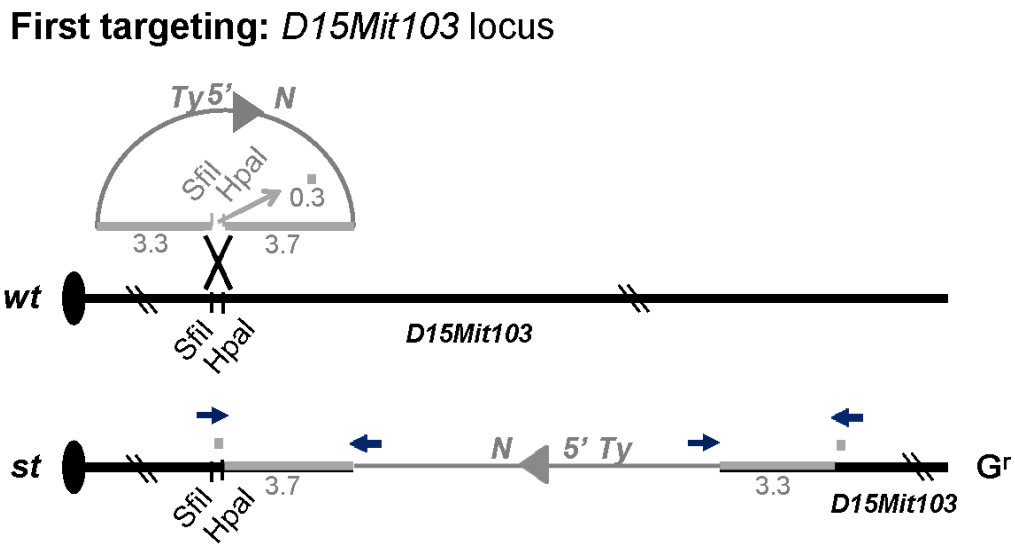

Figure 1 C. First gene targeting at D15Mit103 locus.

Gene targeting at D15Mit103 resulted in integration of a loxP site (triangle), a neomycin resistance cassette (N), the 5' half of the hprt locus (5'), and the Tyrosinase gene (Ty) at the endogenous (wild-type, wt) D15Mit103 locus (upper). Targeting was assessed by PCR analysis of G418-resistant (G^R) clones by using the primers specific for the gap and the targeting vector (see Table 2 for primers); a 3.7 kb or 3.3 kb PCR fragment is diagnostic for singly targeted (st) clones (lower).

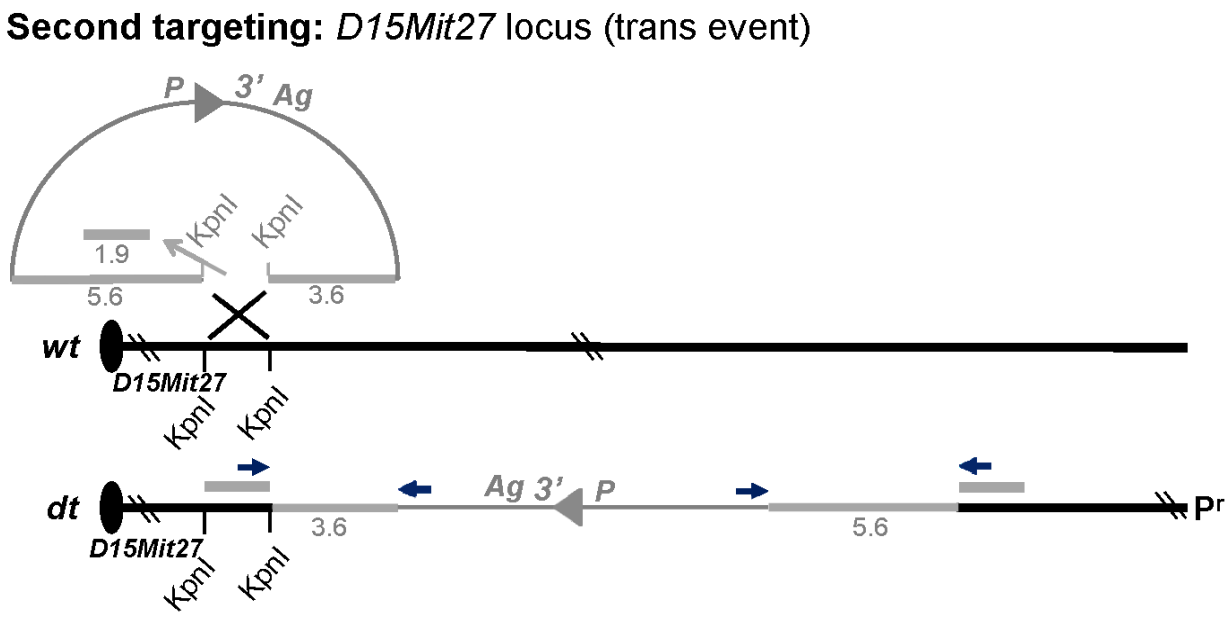

Figure 1 D. Second gene targeting at D15Mit27 locus.

Gene targeting in the st clone shown in (C) was performed to modify endpoint D15Mit27 to yield doubly targeted (dt) clones. Only the Trans-targeting event (in which both targeting events occur on different homologs) is shown here. The loxP site, a puromycin resistance cassette (P), the 3' half of the hprt locus (3'), and an Agouti transgene (Ag) were integrated at the D15Mit27 locus (upper). Accurate targeting of puromycin-resistant (P^R) clones was assessed by PCR using the gap and vector specific primers (See Table 2 for primers): a 5.6 kb or 3.6 kb PCR fragment is diagnostic for dt clones (lower).

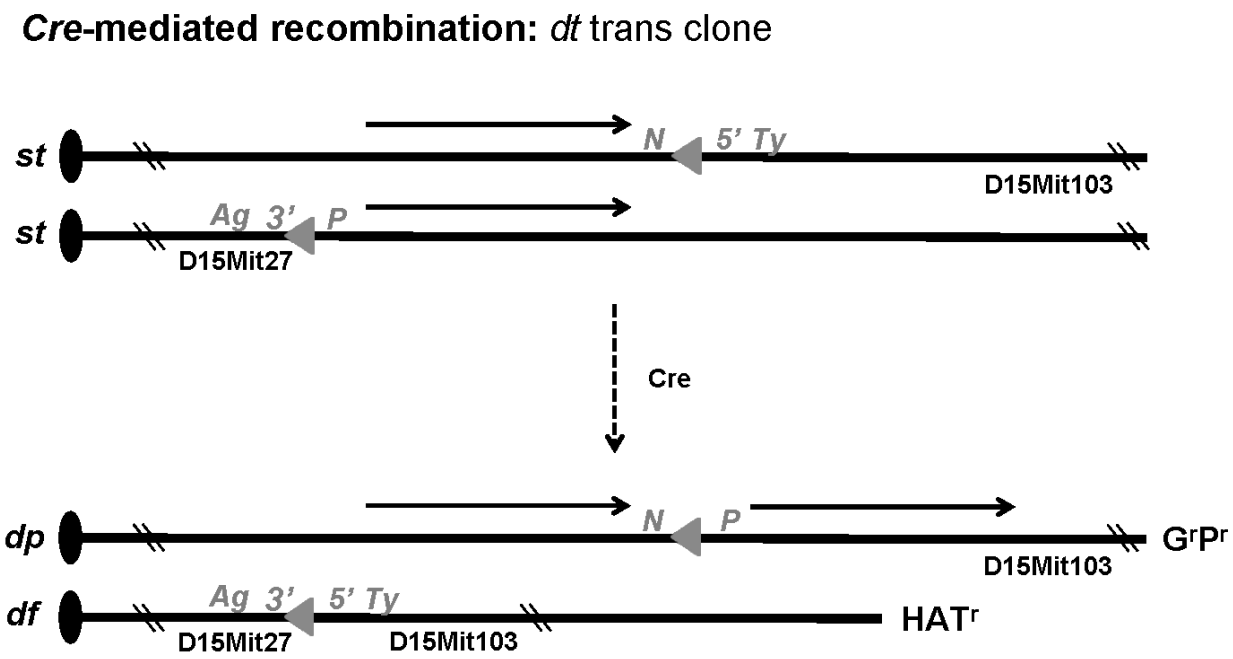

Figure 1 E. Cre-mediated recombination.

Trans-targeted dt clones generated hypoxanthine aminopterin thymidine (HAT)-resistant (H^R), G^R, P^R df/dp clones.

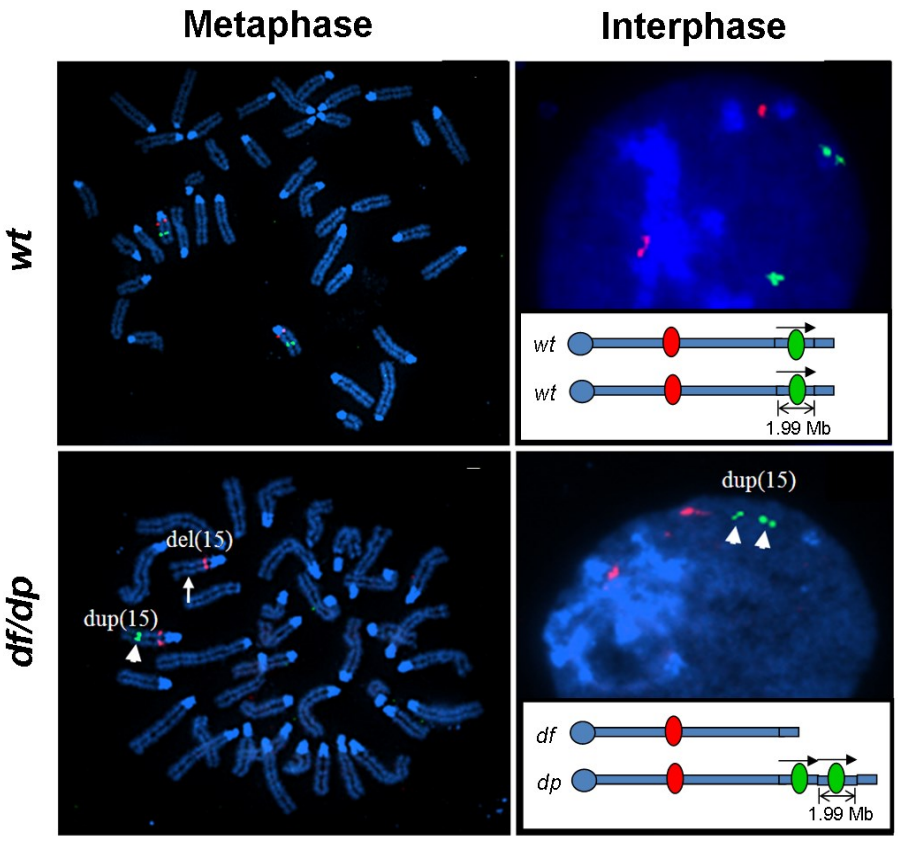

Figure 1 F. FISH analysis of *Myc-Gsdmc*$^{df/dp}$ ES cells.

Metaphase and interphase preparations from the engineered cells were probed with BAC clone specific for Chromosome 15 and located outside (RP23-18H8, red) and within (RP24-78D24, green) the engineered region. The alleles containing the deletion and the duplication are marked.

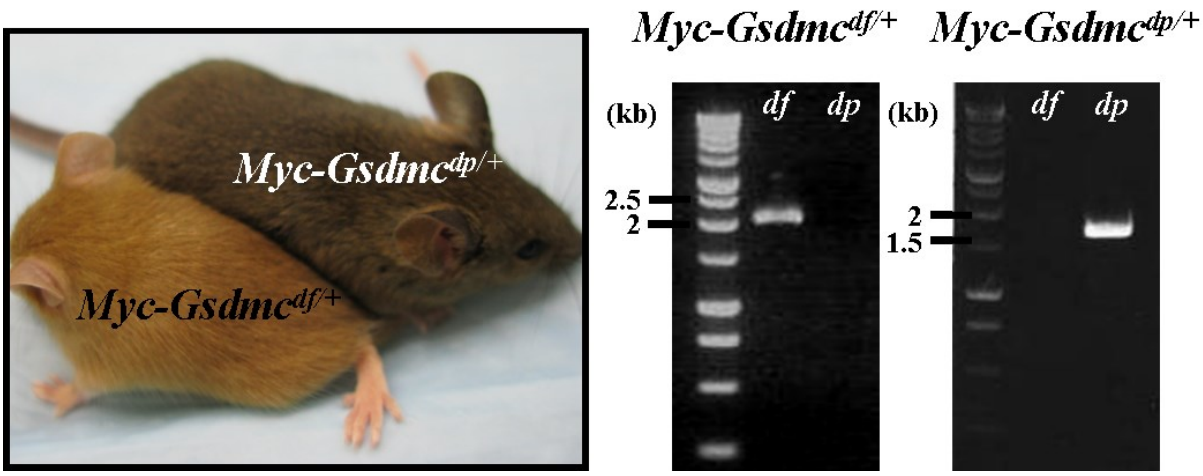

Figure 1 G. Germline transmission of engineered allele.

Germline transmission determined by PCR specific for *Myc-Gsdmc*$^{df/+}$ and *Myc-Gsdmc*$^{dp/+}$ alleles.

Single Copy Gain of *Myc-Gsdmc* Affects Mammary Structure, Proliferation and Differentiation

To determine how the copy number of the *Myc-Gsdmc* interval affected the morphogenesis of primary mammary epithelial cells (MEC), we isolated these cells from 6 week-old-virgin *Myc-Gsdmc*$^{df/+}$, wild type (wt), and *Myc-Gsdmc*$^{dp/+}$ mice and cultured them in recombinant basement membrane (Matrigel^{TM}). When normal epithelial cells are grown in a three dimensional (3D) Matrigel^{TM} environment, they form acinar structures that are characteristic of glandular development (Debnath and Brugge, 2005). During acinar development, a co-ordinated series of events involving cellular proliferation, apoptosis, and growth arrest results in an organized outer layer of quiescent epithelial cells surrounding a hollow luminal core (Mailleux et al., 2008; Reginato et al., 2005). We observed that the *Myc-Gsdmc*$^{dp/+}$ cells formed larger acinar structures, while those from *Myc-Gsdmc*$^{df/+}$ were smaller compared to the wild type acini after seven days of culture (Figure 2A-a), suggesting that the size of the acinar structures correlated with the dosage of *Myc-GsmdC* region. We further determined that the increase in acinar size in the *Myc-Gsdmc*$^{dp/+}$ MECs was due to increased cell-number and not due to cell-volume by counting the number of nuclei per structure after staining the acini with 4,6-diamidino-2-phenylindole (DAPI). Statistical analysis using two-way analysis of variance (ANOVA), demonstrated that acinar structures derived from *Myc-Gsdmc*$^{dp/+}$ MEC have significantly increased number of cells compared to the wild type, while the structures derived from *Myc-Gsdmc*$^{df/+}$ MECs have fewer cells (Figure 2A-b).

a

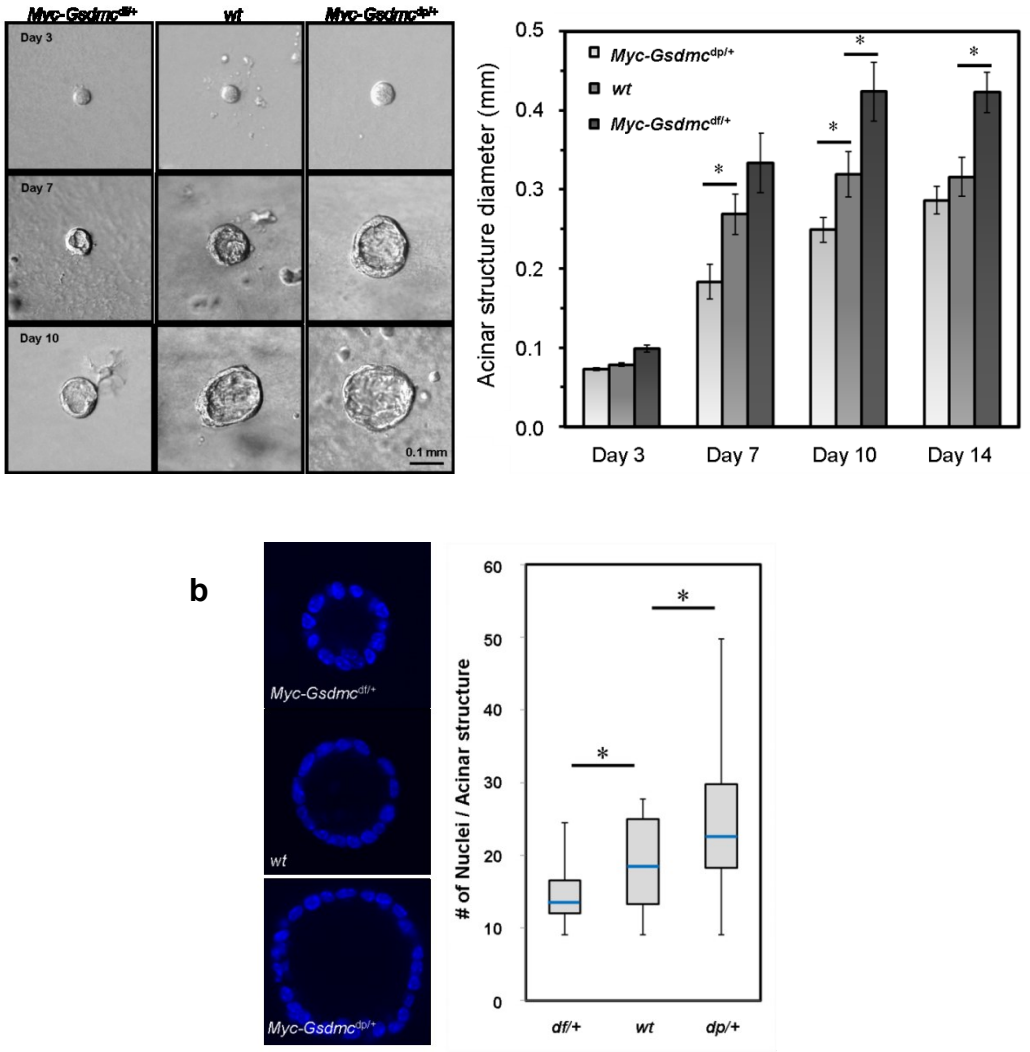

Figure 2 A. Mammary epithelial cells isolated from *Myc-Gsdmc*$^{dp/+}$ mice promote proliferation in 3D Matrigel cultures.

Equal amount of *Myc-Gsdmc*$^{df/+}$, wt, and *Myc-Gsdmc*$^{dp/+}$ mammary epithelial cells were grown for 14 days in 3D Matrigel cultures. (a) DIC images were taken at day 3 (top panel), day 7 (middle panel), and day 10 (bottom panel). The diameter of each acinar structure was measured at indicated time points. n=24, Error bars represent SE. *, $P < 0.05$. (b) Confocal images of day 10 acinar structures stained with DAPI to monitor nuclei (left panel). Number of nuclei per acinus was quantified for acini formed by *Myc-Gsdmc*$^{df/+}$, wt, and *Myc-Gsdmc*$^{dp/+}$ cells (right panel). Blue line, median value. Spread, 1.5 times the interquartile range. *, $P < 0.05$. Note that *Myc-Gsdmc*$^{dp/+}$ mammary epithelial cells grown in 3D Matrigel cultures show increased acinar structure size (a) and increased cell number per acinar structure (b).

These observations led us to hypothesize that gain of a single copy of *Myc-Gsdmc* can alter the cellular features of the mouse mammary gland which subsequently leads to malignancy. These features include common molecular links shared between mammary development and tumorigenesis, such as branching morphology of mammary ducts, cellular proliferation and differentiation of post-puberty quiescent MECs at steady state. Mouse mammary development involves three distinct stages. At the newborn stage, a few mammary ducts occupy a small portion of the mammary fat pad. During puberty (4-9 weeks old), rapid cellular proliferation of MECs results in lateral branching and ductal elongation at the sites of terminal end buds (TEB) which fill up the mammary fat pad (Watson and Khaled, 2008). Later, the TEBs disappear and the ducts enter a quiescent stage in virgin female mice until pregnancy. Aberrations in this cycle of mammary development have been observed in mouse models predisposed to mammary tumors (Medina, 2002). For example, MMTV-*Wnt1* transgenic mice and those with conditional inactivation of PTEN in mammary epithelium show increased lateral branching of mammary ducts and excessive proliferation of MECs, leading to mammary tumorigenesis with reduced latency (Tsukamoto et al., 1988, Li et al 2002). To investigate the effect of a gain of the *Myc-Gsdmc* region on branching morphology of mammary ducts, we performed whole-mount analyses of the inguinal mammary glands from *Myc-Gsdmc*$^{dp/+}$ and their wild type littermates with matching estrous cycles. Mammary glands from ten-week-old virgin female *Myc-Gsdmc*$^{dp/+}$ mice exhibited increased lateral branching compared to wild-type (Figure 2B). We observed a 150% increase in

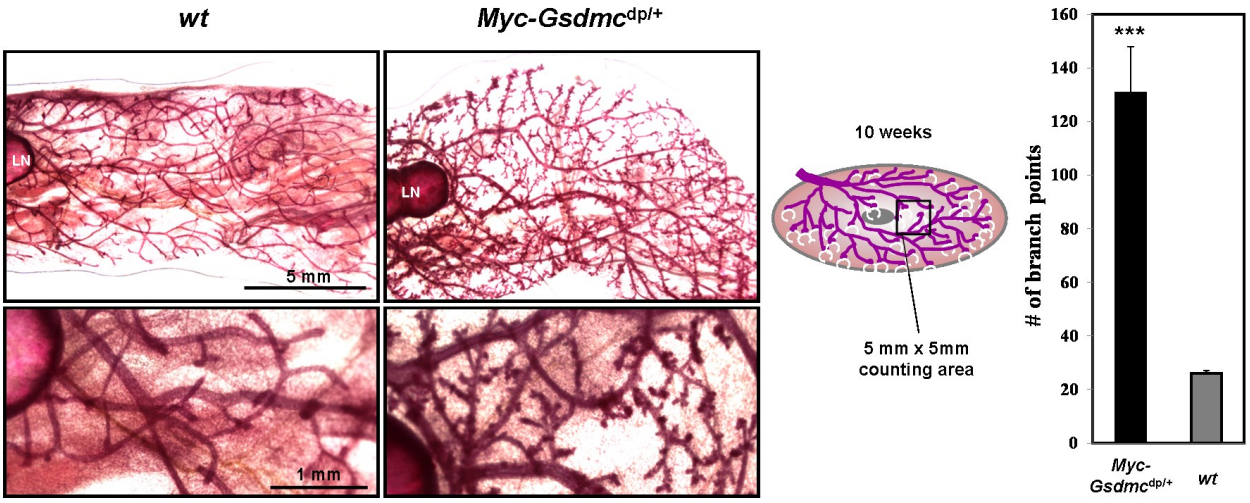

Figure 2 B . Excessive lateral branching in *Myc-Gsdmc*$^{dp/+}$ mammary glands.

Whole mount analysis of mammary glands from 10 weeks old wild type (wt) and *Myc-Gsdmc*$^{dp/+}$ littermates. *Myc-Gsdmc*$^{dp/+}$ mammary glands have excessive lateral branching of mammary ducts (n=3). Quantification of ductal branch points per 25 mm^2 area shown as bar graph. Data are presented as mean ± standard error (SE). Significance at *$p < 0.05$, **$p < 0.01$ and, ***$p < 0.001$ using two-tailed Student's t-test. LN, lymph node.

the lateral branch points within a 25 mm^2 area near the lymph node of the *Myc-Gsdmc*$^{dp/+}$ mammary glands compared to the wild type ones. Moreover, analysis of hematoxylin and eosin (H&E) stained sections of the mammary glands from *Myc-Gsdmc*$^{dp/+}$ mice revealed a precocious alveolar-like phenotype that was not observed in the wild-type mice (Figure 2C), indicating aberrant proliferation and differentiation of the *Myc-Gsdmc*$^{dp/+}$ MECs. To assess whether *Myc-Gsdmc* gain affected proliferation in MECs, we carried out bromodeoxyuridine (BrdU) incorporation analysis on glands from *Myc-Gsdmc*$^{dp/+}$ and their wild-type littermates. At 10 weeks of age, the MECs of virgin mice undergo relative replicative quiescence. Interestingly, we observed a greater number of BrdU-positive nuclei in ducts of *Myc-Gsdmc*$^{dp/+}$ mice compared to the wild-type (Figure 2D). More than 11.3% (± 1.7) of the MECs from *Myc-Gsdmc*$^{dp/+}$ mice had BrdU-positive epithelial nuclei compared to 0.6% (± 0.1) in the wild-type mice (Figure 2D, $n \geq 3$). These data suggest that a single-copy gain of *Myc-Gsdmc* leads to loss of proliferation arrest in the mammary epithelium of adult virgin mice.

To assess the effect of a gain of *Myc-Gsdmc* on the differentiation of the mammary epithelial cells, we carried out *immunofluorescence* studies using antibodies against specific mammary epithelial markers. The mouse mammary duct is defined by myoepithelial cells forming the outer layer while luminal cells constitute the inner layer (Tiede and Kang, 2011). Therefore, we examined the differentiation status of the cells in the mammary ducts from 10-week-old wild type and *Myc-Gsdmc*$^{dp/+}$ littermates by detecting the luminal marker keratin-8 (K8) and myoepithelial marker keratin-14 (K14). While the epithelium from wild-

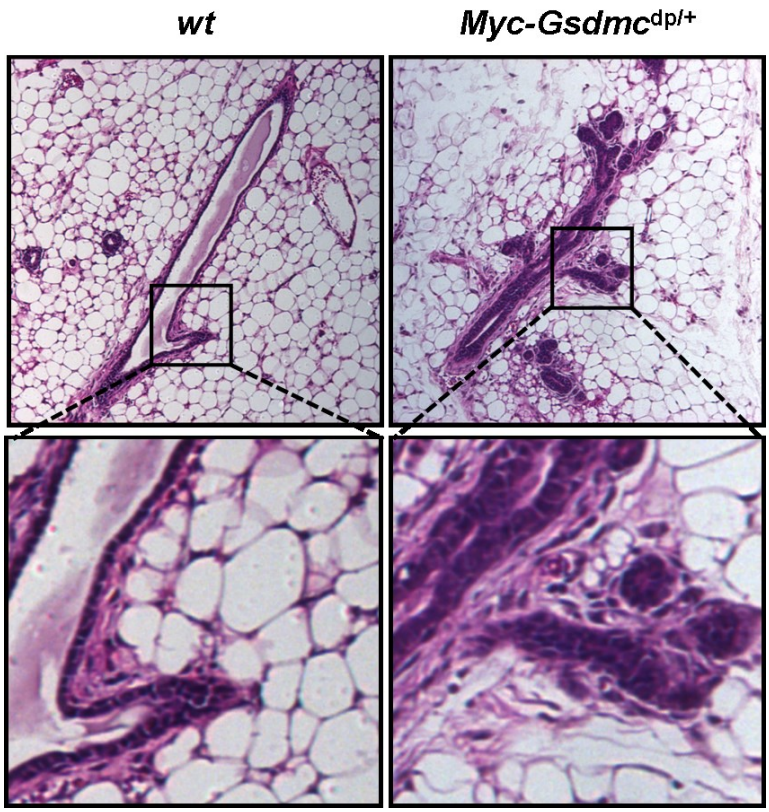

Figure 2 C. Precocious alveolar-like phenotype in *Myc-Gsdmc*$^{dp/+}$ mammary ducts.

H&E staining of the mammary ducts from wt and *Myc-Gsdmc*$^{dp/+}$ mice revealed precocious alveolar-like phenotype in the latter. The aberrant structure is shown at higher magnification in the bottom row.

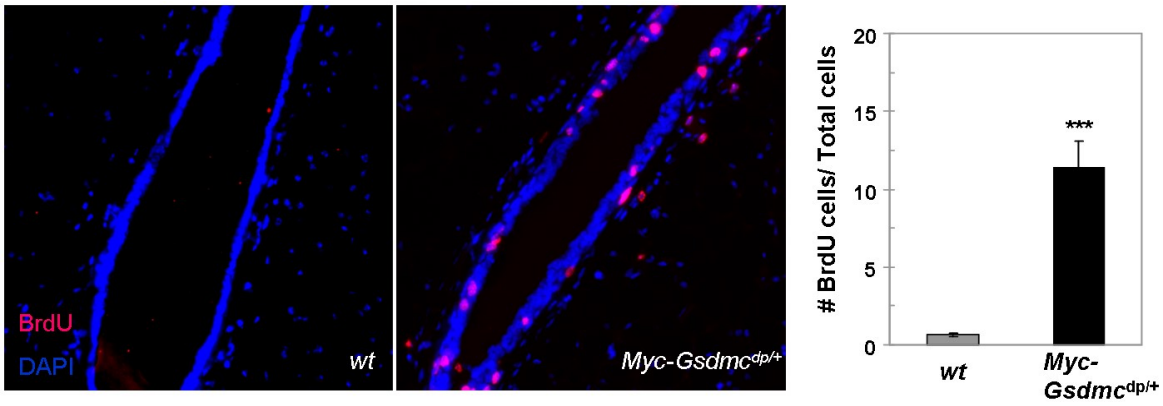

Figure 2 D. Loss of proliferation arrest in *Myc-Gsdmc*$^{dp/+}$ mammary glands.

BrdU incorporation assay in the mammary ducts of wt and *Myc-Gsdmc*$^{dp/+}$ littermates. BrdU-positive cells is shown in red. DAPI, used as a counterstain, is shown in blue. The percentage of BrdU-positive cells of ducts shown as bar graph. The values represent the average fraction of BrdU-positive epithelial cells per total number of epithelial cells of three different mice. Data are presented as mean ± standard error (SE). Significance at *p < 0.05, **p < 0.01 and, ***p <0.001 using two-tailed Student's t-test.

type mice exhibited an expected outer layer of myoepithelial cells (K14 positive) and an inner layer of luminal cells (K8 positive), a number of luminal cells in the *Myc-Gsdmc*$^{dp/+}$ mammary ducts were found to express myoepithelial (K14) markers, suggesting mis-expression of myoepithelial markers in *Myc-Gsdmc*$^{dp/+}$ luminal cells (Figure 2E). Strikingly, we observed multiple layers of luminal cells that filled the *Myc-Gsdmc*$^{dp/+}$ ducts (Figure 2E). To detect whether *Myc-Gsdmc* gain contributed to proliferation of myoepithelial and luminal cells, we co-stained the sections with antibodies against BrdU and K14. BrdU-positive signals were observed in both luminal and myoepithelial cells (Figure 2F). Because ERα-positive MECs are known not to undergo cell division (Lamote et al., 2004), we examined the number of ERα-positive MECs in *Myc-Gsdmc*$^{dp/+}$ and wild type mammary ducts. Consistent with the higher level of cellular proliferation observed in *Myc-Gsdmc*$^{dp/+}$ mammary epithelium, only 9.9% (± 1.2) *Myc-Gsdmc*$^{dp/+}$ MECs were ERα-positive (Figure 2G) compared to wild type. Taken together, these data indicate that an extra copy of *Myc-Gsdmc* can confer aberrant proliferation and differentiation of mammary epithelium *in vivo*.

Generation of *Myc*$^{dp/+}$ and *Pvt1-Gsdmc*$^{dp/+}$ mice

The *Myc-Gsdmc*$^{dp/+}$ mice fulfilled the need of a suitable animal model that mimics the copy-number gain of 8q24, and thus addresses its role in cancer. To investigate if *Myc* is the only gene that contributes to the aberrant phenotypes

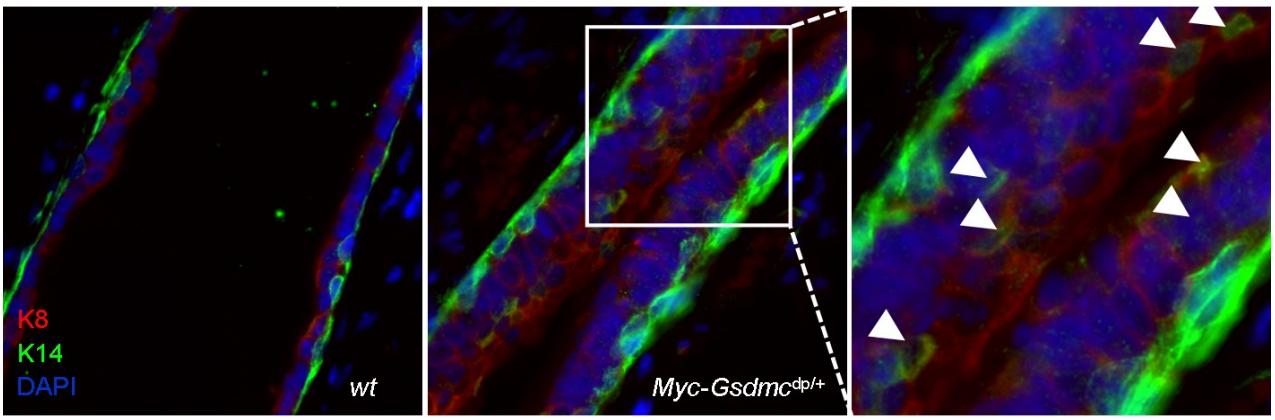

Figure 2 E. Aberrant differentiation of mammary epithelial cells in *Myc-Gsdmc*$^{dp/+}$ mice.

Immunofluorescence co-staining for luminal marker K8 (red) and myoepithelial marker K14 (green) in mice. Arrowheads indicate co-expression of K8 and K14.

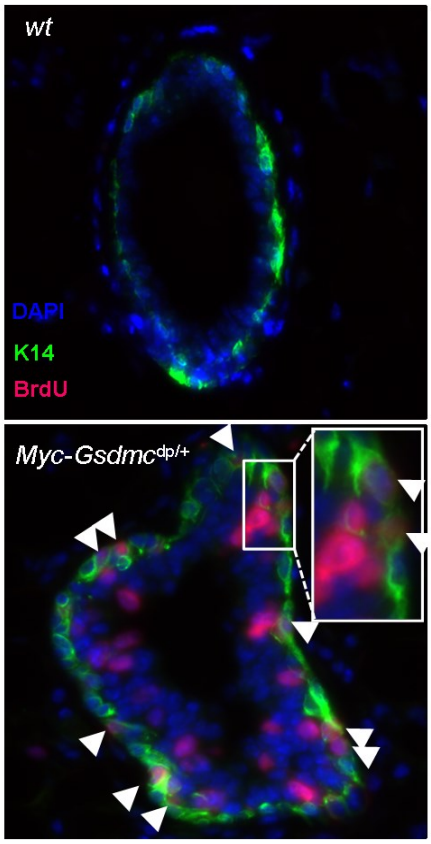

Figure 2 F. Excessive proliferation of myoepithelia cells and luminal cells in *Myc-Gsdmc*$^{dp/+}$ mammary ducts.

Color merged images of multi-labeled immunofluorescence fixed mammary ducts of wt and *Myc-Gsdmc*$^{dp/+}$ mice. Antibodies used against K14 (green) and BrdU (red). DAPI stained nuclei in blue. Arrowheads indicate co-localization of BrdU and K14 in *Myc-Gsdmc*$^{dp/+}$ mammary ducts.

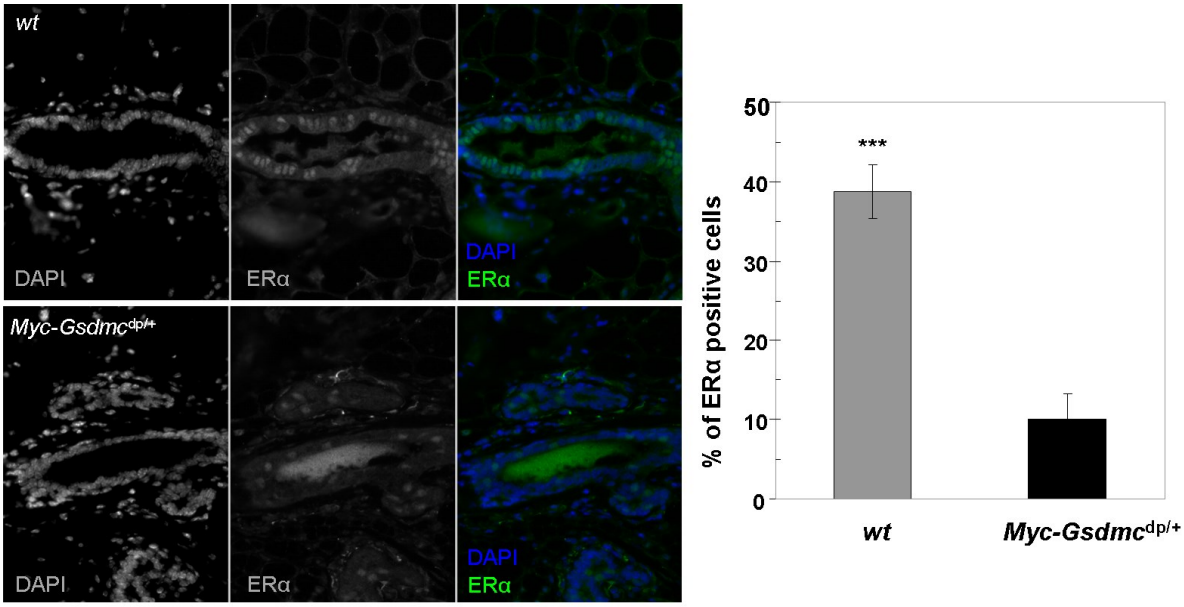

Figure 2 G. Reduced expansion of ERα^{+} cells in *Myc-Gsdmc$^{dp/+}$* mammary ducts.

Immunofluorescence analysis of ERα (green) on sections of mammary ducts. Cell nuclei positive for ERα were counted and the numbers were expressed as the percentage of total epithelial cell nuclei (DAPI, blue). Results are mean ± SD of nine determinations for each of three individual mammary tissues. Images shown are representative 3 mice per genotype.

observed in *Myc-Gsdmc*$^{dp/+}$ mammary gland, or if it collaborates with other gene(s) in the *Myc-Gsdmc* interval, we generated additional mouse strains. We employed chromosome engineering of mouse ES cells to develop mouse strains containing an additional copy of *Myc* (*Myc*$^{dp/+}$) and *Pvt1-Gsdmc* (*Pvt1-Gsdmc*$^{dp/+}$, Figure 3A). To develop ES cells with balanced rearrangement of the *Myc* locus (*Myc*$^{df/dp}$), gene-targeting was first carried out at ch15: 61,990,555 (*Myc*^{R}) distal to *Myc* (Figure 3B). Correctly targeted clones were identified by PCR analysis. Singly targeted, germline competent clones were retargeted at *Myc*^{L}, proximal to *Myc* gene. A dozen, doubly targeted clones were subjected to transient Cre-expression, as described before. Clones resistant to G418, puromycin and HAT were identified as *Myc*$^{df/dp}$ clones and further confirmed by PCR. Chimeras were derived from two independent *Myc*$^{df/dp}$ clones. Germline transmission of the *Myc*$^{dp/+}$ allele was obtained by crossing the chimeras with wild type females. The *Myc*$^{dp/+}$ were crossed to FVB wild-type mice for three subsequent generations. A similar procedure was employed to obtain *Pvt1-Gsdmc*$^{dp/+}$ mice (Figure 3C).

Gain of Myc or Pvt1-Gsdmc Alone is Insufficient to Produce Aberrant Phenotype in Mammary Epithelium

Our central objective is to functionally validate whether *Myc* co-operates with other genes in the Hu 8q24.21 locus for neoplastic transformation in breast cancer. If so, we expect that neither *Myc*$^{dp/+}$ nor *Pvt1-Gsdmc*$^{dp/+}$ should develop the aberrant phenotypes seen in *Myc-Gsdmc*$^{dp/+}$ mammary glands. To test this hypothesis, whole mounts of mammary glands from *Myc*$^{dp/+}$ and *Pvt1-Gsdmc*$^{dp/+}$

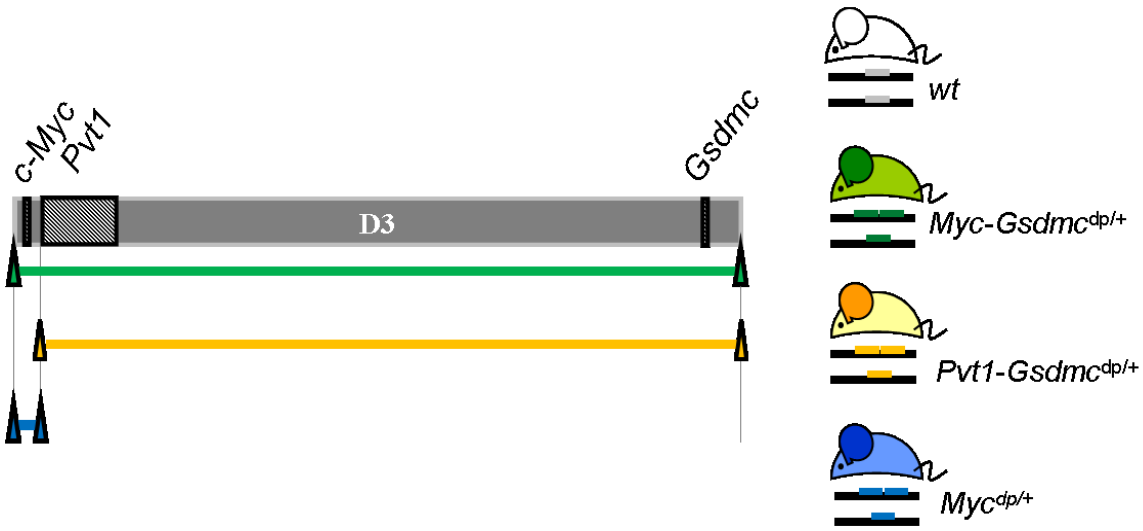

Figure 3 A. Chromosome engineered mouse for a single copy gain of *Myc* or *Pvt1-Gsdmc*.

Schematic of three chromosome engineered mouse strains: *Myc-Gsdmc*$^{dp/+}$, *Pvt1-Gsdmc*$^{dp/+}$ and *Myc*$^{dp/+}$ (See Figure 3B and 3C and Table 1 for details).

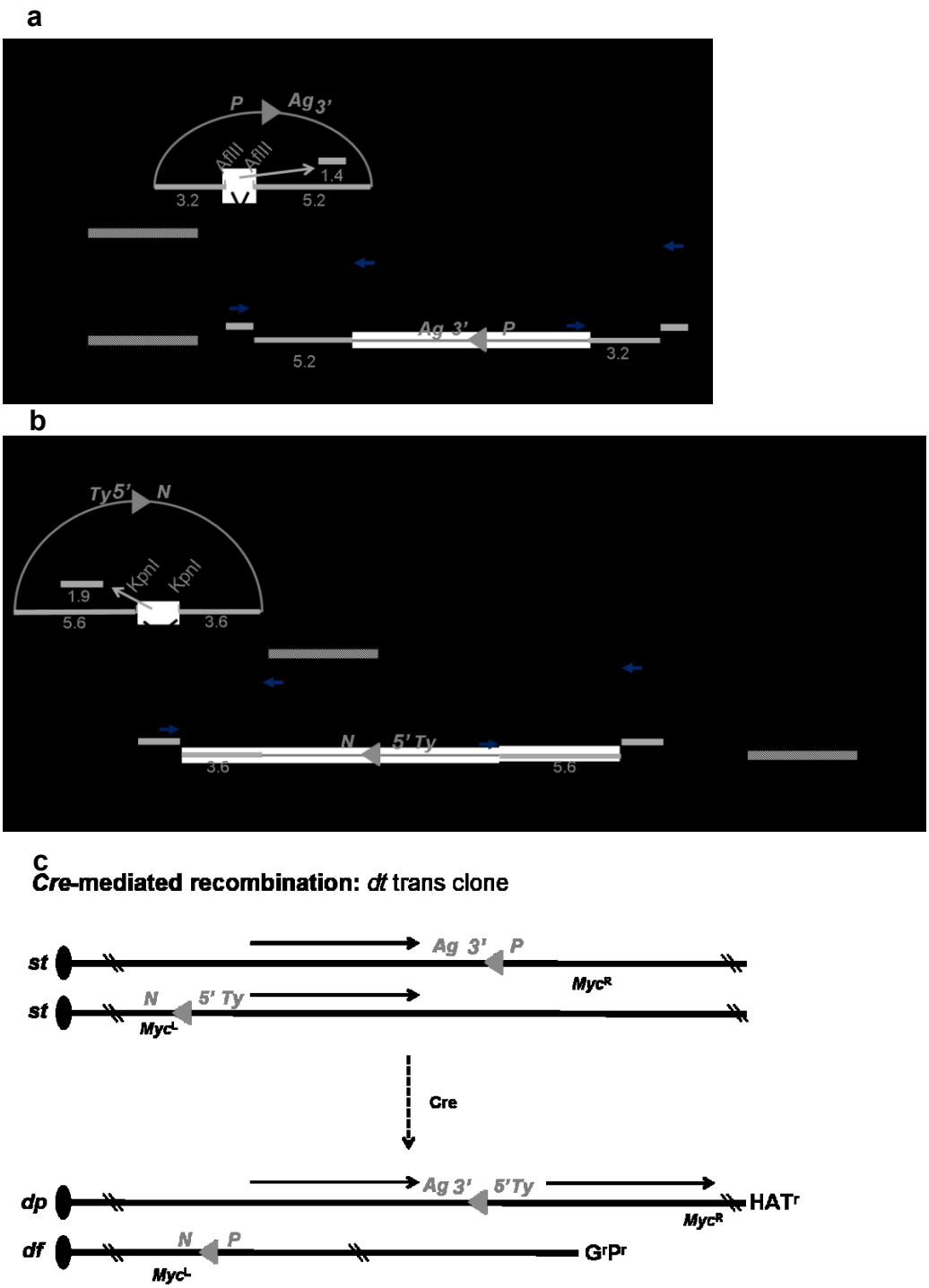

Figure 3 B. Engineering *Myc*$^{df/dp}$ allele in mouse ES cells.

(a) Gene targeting at *c-Myc*^{R} resulted in integration of a loxP site (triangle), a puromycin resistance cassette (P), the 3' half of the hprt locus (3'), and an Agouti gene (Ag) at the endogenous locus (upper). Targeting was assessed by PCR analysis of Puromycin-resistant clones by using the primers specific for the gap and the targeting vector (see

Table 2 for primers); a 5.2 kb or 3.2 kb PCR fragment is diagnostic for singly targeted (st) clones (lower). (B) Gene targeting in the st clone was performed at Myc^{L} to yield doubly targeted (dt) clones. Only the Trans-targeting event is shown here. The loxP site, a neomycin resistance cassette (N), the 5' half of the hprt locus (5'), and a Tyrosinase transgene (Ty) were integrated at the Myc^{L} locus (upper). Accurate targeting of G418-resistant clones was assessed by PCR using the gap and vector specific primers (See Table 2 for primers): a 5.6 kb or 3.6 kb PCR fragment is diagnostic for dt clones (lower). (C) Cre-mediated recombination. trans-targeted dt clones generated hypoxanthine aminopterin thymidine (HAT)-resistant (H^{R}), G^{R}, P^{R} df/dp clones.

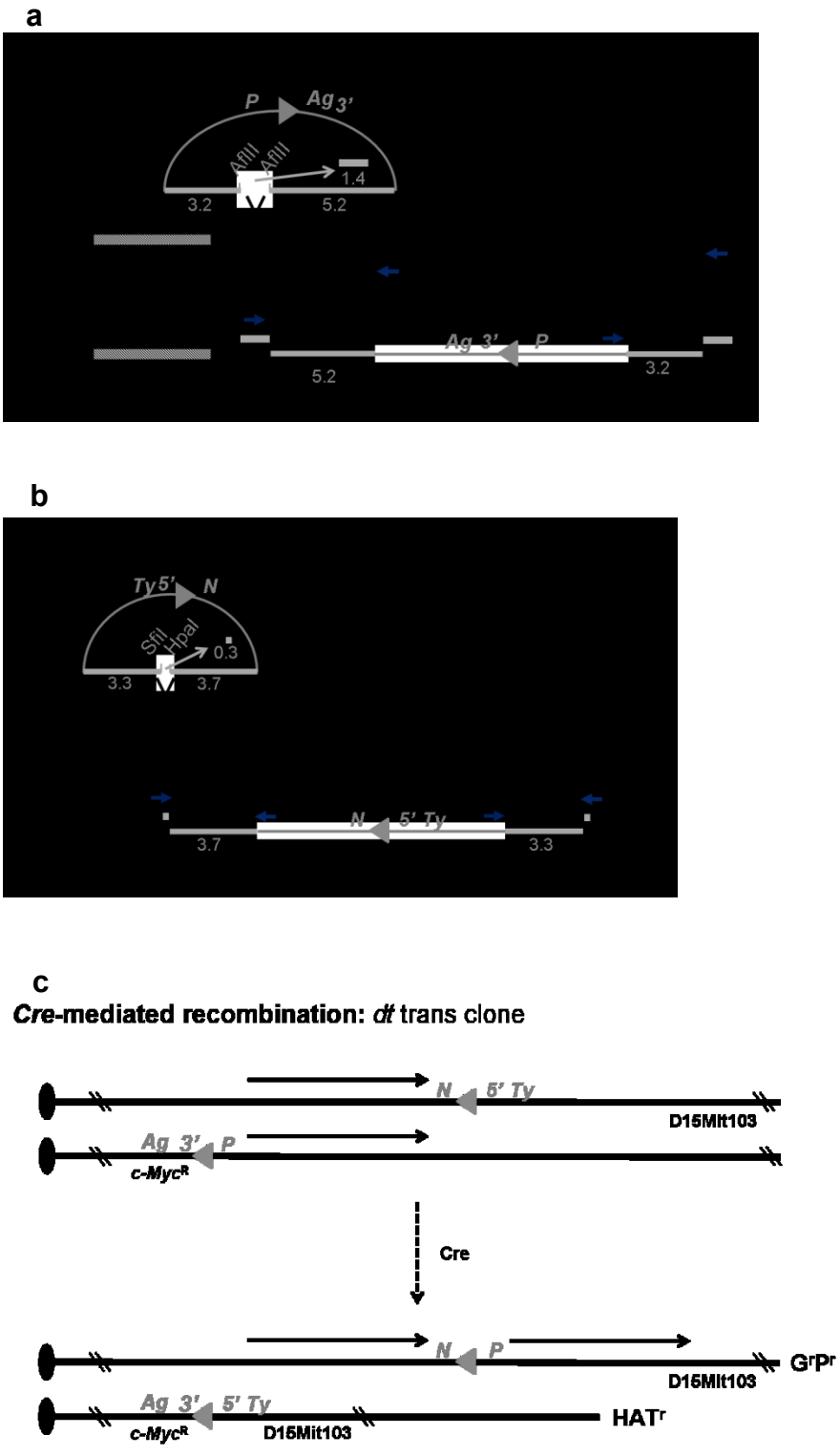

Figure 3 C. Engineering *Pvt1-Gsdmc*$^{df/dp}$ allele in mouse ES cells.

(a) Gene targeting at *Myc*^{R} discussed in Figure 3B-a. (b) Gene targeting in the *c-Myc*^{R} targeted clone was performed at *Gsdmc*^{R} to yield doubly targeted (dt) clones. Only the

Trans-targeting event is shown here. The loxP site, a neomycin resistance cassette (N), the 5' half of the hprt locus (5'), and a Tyrosinase transgene (Ty) were integrated at the *Gsdmc*^{R} locus (upper). Accurate targeting of G418-resistant clones was assessed by PCR using the gap and vector specific primers (See Table 2 for primers): a 3.7 kb or 3.3 kb PCR fragment is diagnostic for dt clones (lower). (c) Cre-mediated recombination. trans-targeted dt clones generated hypoxanthine aminopterin thymidine (HAT)-resistant (H^R), G^R, P^R df/dp clones.

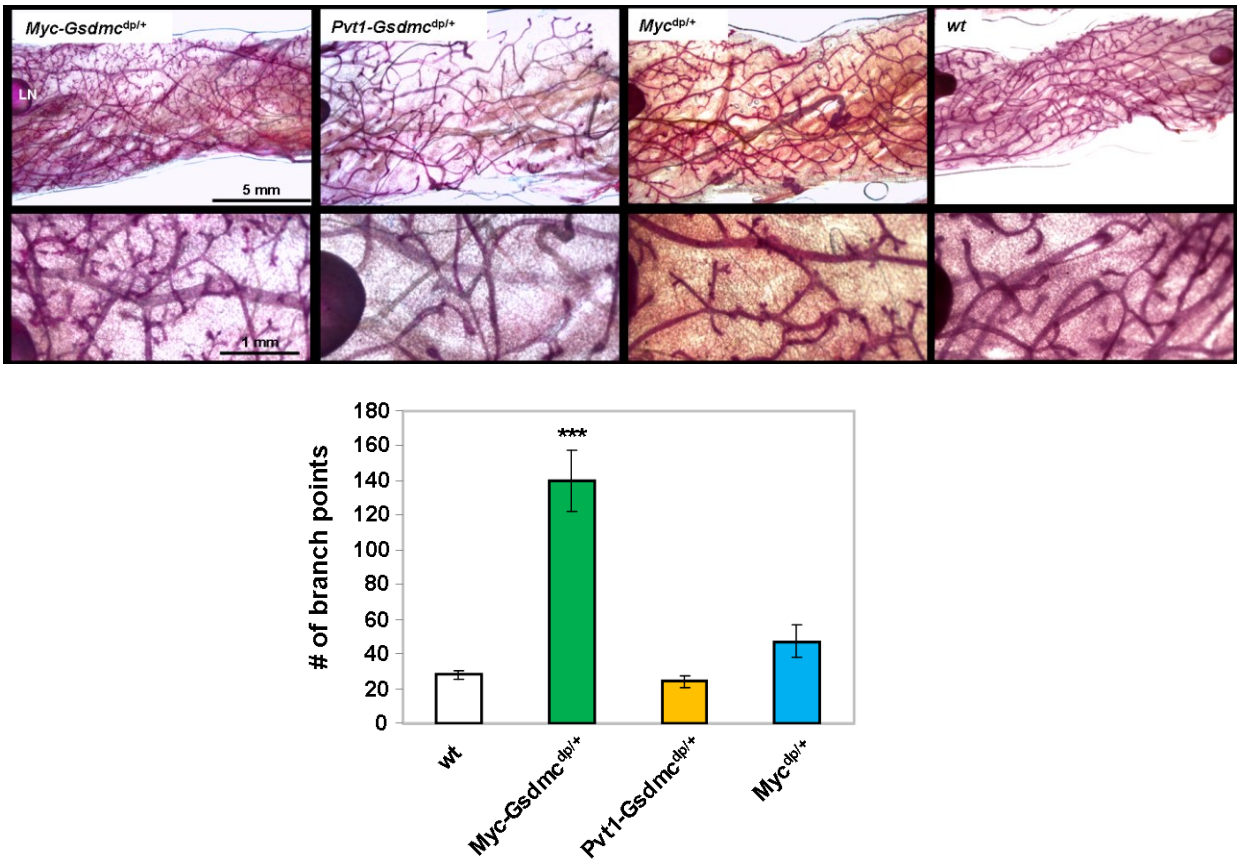

Figure 3 D. *Myc*$^{dp/+}$ and *Pvt1-Gsdmc*$^{dp/+}$ mice do not display mammary gland hyperplasia.

Whole mount analysis of mammary glands from 10 weeks-old *Myc-Gsdmc*$^{dp/+}$, *Pvt1-Gsdmc*$^{dp/+}$, *Myc*$^{dp/+}$ and wt virgin mice. The bottom panel shows images in higher-magnification. Branch points were enumerated at a 25 mm^2 area near the lymph node. Data are presented as mean ± standard error (SE). Significance at *p < 0.05, **p < 0.01 and, ***p <0.001 using two-tailed Student's t-test.

were examined for lateral branching and compared to those from *Myc-Gsdmc*$^{dp/+}$ mice (Figure 3D). At 10 weeks, careful enumeration and statistical analysis of branch points revealed that both *Myc*$^{dp/+}$ and *Pvt1-Gsdmc*$^{dp/+}$ mammary ducts had significantly less lateral branching compared to what we observed in *Myc-Gsdmc*$^{dp/+}$ mammary ducts (Figure 3D). Indeed, the lateral branching in mammary glands from *Myc*$^{dp/+}$ and *Pvt1-Gsdmc*$^{dp/+}$ mice were similar to that observed in wild-type mice (Figure 3D). These data suggest that neither gain of *Myc* nor *Pvt1-Gsdmc* was sufficient to produce excessive mammary branching in mice.

We then asked whether an extra copy of *Myc* or *Pvt1-Gsdmc* would be sufficient to cause aberrant proliferation in the mammary ducts. Mammary glands from 10 week-old *Myc*$^{dp/+}$, *Pvt1-Gsdmc*$^{dp/+}$, *Myc-Gsdmc*$^{dp/+}$, and wild-type mice were assayed for proliferation using BrdU. No incorporation of BrdU was found in wild-type, *Myc*$^{dp/+}$, and *Pvt1-Gsdmc*$^{dp/+}$mammary ducts, whereas, consistent with our previous finding, we observed a significant increase in BrdU incorporation in *Myc-Gsdmc*$^{dp/+}$ ducts (Figure 3E). These data indicate that *Myc* and *Pvt1-Gsdmc* synergize to mediate excessive lateral branching morphology and aberrant cellular proliferation in mammary ducts. To test the hypothesis of this excessive lateral branching structural aberration was caused by increased copy number gain of *Myc-Gsdmc* interval, we evaluated the phenotype of mammary glands from 10 weeks-old *Myc-Gsdmc*$^{dp/df}$ mice. *Myc-Gsdmc*$^{dp/df}$ mammary tissue exhibited normal mammary development (Figure 3F). There is no significant

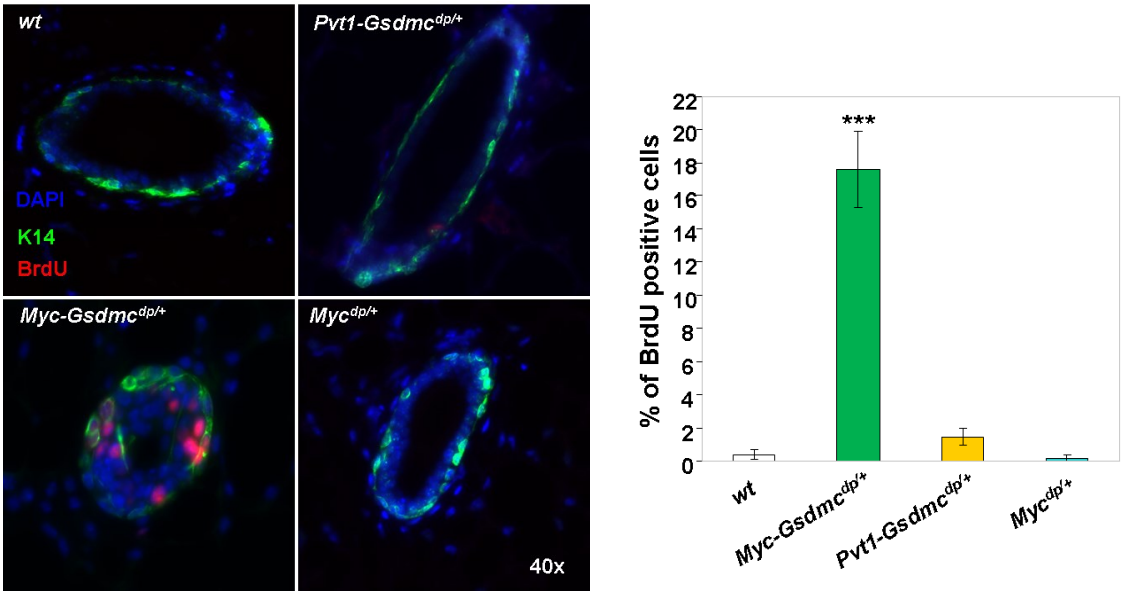

Figure 3 E. Neither *Myc* nor *Pvt1* alone are sufficient to inhibit proliferation arrest.

Immunofluorescence images of BrdU incorporation in mammary ducts of wild type, *Myc-Gsdmc*$^{dp/+}$, *Pvt1-Gsdmc*$^{dp/+}$, *Myc*$^{dp/+}$ mice. Antibodies against BrdU (red) and K14 (green) were used. Quantification of BrdU positive cells represented as a percentage of the total DAPI (blue) stained nuclei. (n=5 for each genotype, ***p<0.001).

increase in mammary ductal branching and BrdU-positive cells of the *Myc-Gsdmc*$^{dp/df}$ mammary glands compared with wild-type mice (Figure 3F and 3G), demonstrating that these aberrant phenotypes are due to increased dosage of *Myc-Gsdmc* interval.

Single Copy Gain of *Myc-Gsdmc* is an Oncogenic Aberration which Promotes Mouse Mammary Tumors

Human cancers with gain of 8q24.21 have been reported to express a high level of PVT1 transcripts (Haverty et al., 2009). To examine whether the genomic rearrangements in our three mouse models affect the expression of genes in the *Myc-Gsdmc* interval, we carried out real-time, quantitative reverse transcription-PCR (RT-qPCR) analysis using total RNA isolated from mammary glands of *Myc-Gsdmc*$^{dp/+}$, *Myc*$^{dp/+}$ and *Pvt1-Gsdmc*$^{dp/+}$ mice (virgin, 10 weeks of age). The level of Myc transcripts was approximately 2.7 (± 0.7) fold higher in *Myc-Gsdmc*$^{dp/+}$ and Myc$^{dp/+}$ mammary glands compared to the wild-type, while no change was found in the Pvt1-Gsdmc$^{dp/+}$ mice (Figure 4A). Interestingly, the Pvt1 transcripts were elevated in *Myc-Gsdmc*$^{dp/+}$ and *Myc*$^{dp/+}$ mammary glands, but not in *Pvt1-Gsdmc*$^{dp/+}$. Mammary glands of all these mice showed negligible expression of Gsdmc (Appendix B). We also assayed the protein levels of Myc in the mammary glands of these mice by western blotting (Figure 4B) and found it to be increased 3 (± 0.3) times higher in *Myc-Gsdmc*$^{dp/+}$, compared to *Myc*$^{dp/+}$ or *Pvt1-Gsdmc*$^{dp/+}$ mammary glands (Figure 4B). This suggests that the gain of one more copy of the *Myc-Gsdmc* interval leads to increased Myc protein in

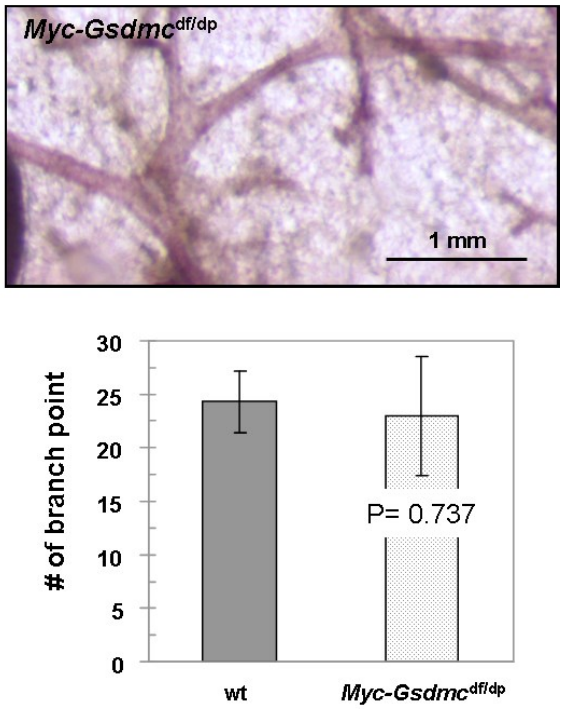

Figure 3 F. *Myc-Gsdmc*$^{df/dp}$ mammary ducts are as normal as wt.

Whole mount analysis of mammary glands from 10 weeks-old *Myc-Gsdmc*$^{df/dp}$ and wt virgin mice. Quantification of ductal branch points per 25 mm^2 area shown as bar graph. Data are presented as mean ± standard error (SE), n=3 for each genotype.

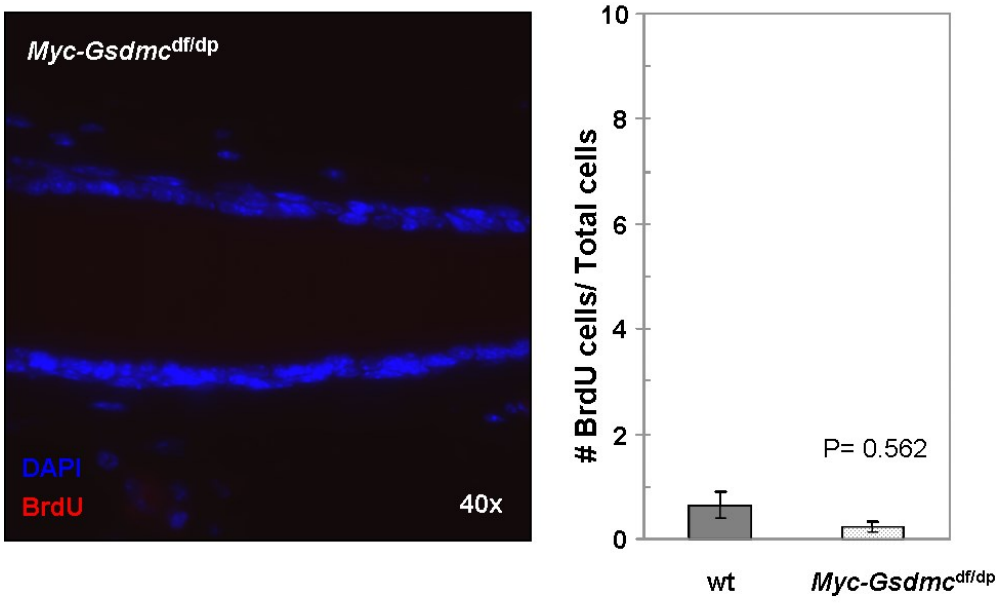

Figure 3 G. *Myc-Gsdmc*$^{df/dp}$ mammary epithelial cells (MECs) are quiescent.

Immunofluorescence images of BrdU incorporation in mammary ducts from 10 weeks-old virgin *Myc-Gsdmc*$^{df/dp}$ mice and wt mice. Antibodies against BrdU (red). DAPI stained nuclei in blue. Quantification of BrdU positive cells represented as a percentage of the total DAPI (blue) stained nuclei. (n=3 for each genotype).

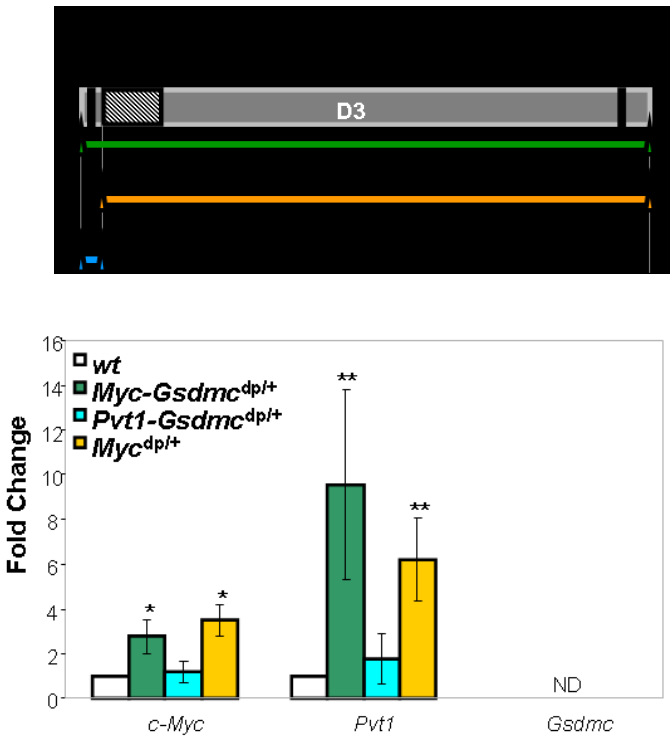

Figure 4 A. Quantitative RT-PCR analysis to assess the relative expression of Myc, Pvt1, and Gsdmc mRNA in mammary glands.

RT-qPCR analysis of *Myc*, *Pvt1* and *Gsdmc* in mammary glands of wild type, *Myc-Gsdmc*$^{dp/+}$, *Pvt1- Gsdmc*$^{dp/+}$ and *Myc*$^{dp/+}$ mice. Mammary glands were isolated from 10 weeks-old virgin mice. n=3 for each genotype. * $p < 0.05$, ** $p < 0.01$. ND, not detected because of low expression.

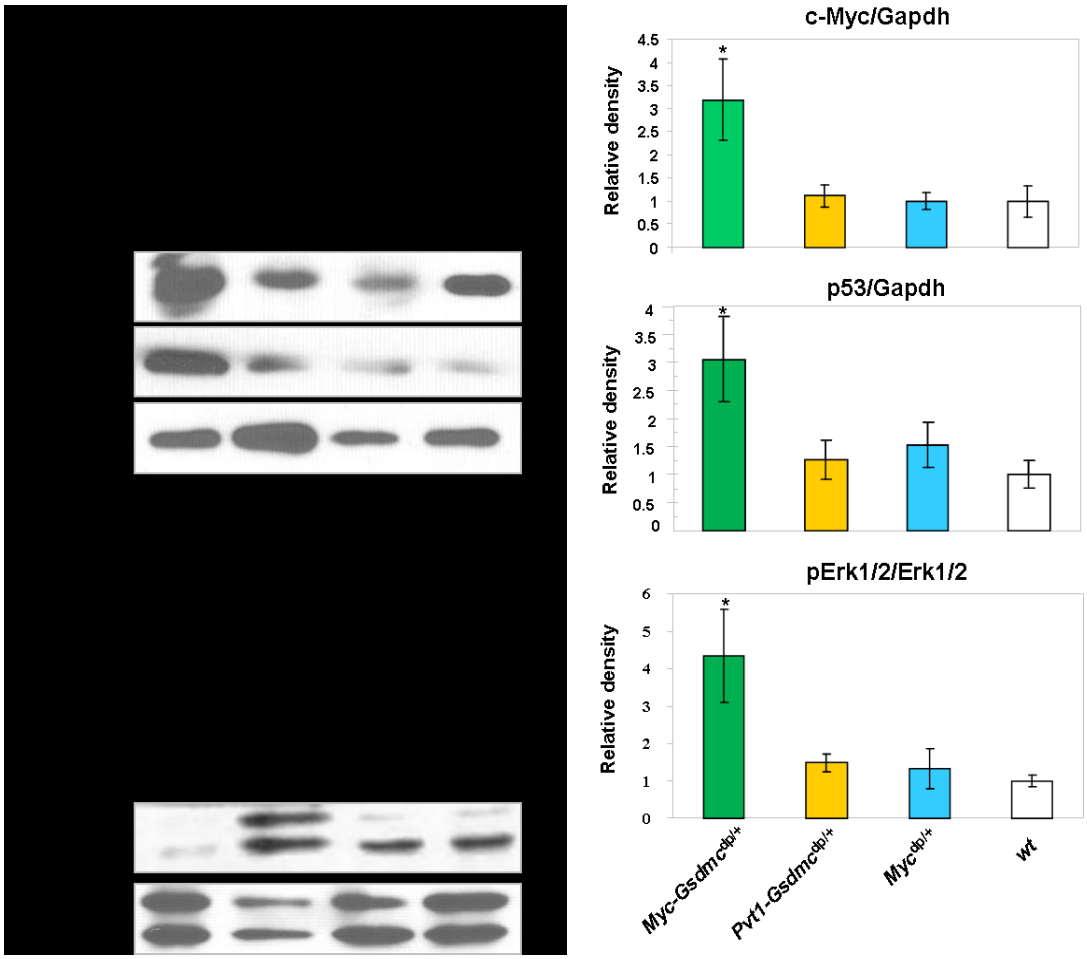

Figure 4 B. Western analysis of total protein lysates from mammary glands of indicated genotypes.

The relative densities of c-Myc and p53 were calculated by normalizing against the GAPDH intensities, and of p-ERK1/2 by normalizing against total ERK protein levels for each genotype. Data are presented as mean ± standard error (SE), n=3 for each genotype. * $p < 0.05$.

mammary glands. However, single-copy gain of *Myc* alone does not result into increased Myc protein.

A possible consequence of increased Myc protein levels is activation of pro-survival pathways that could explain the unregulated proliferation seen in *Myc-Gsdmc*$^{dp/+}$ mammary ducts. We carried out western blot analysis of total protein isolated from the mammary glands of *Myc-Gsdmc*$^{dp/+}$, *Myc*$^{dp/+}$, *Pvt1-Gsdmc*$^{dp/+}$, and wild type mice for pro-survival signaling. Indeed, phospho-ERK1/2 levels were 4.2 (± 1.6) fold elevated in *Myc-Gsdmc*$^{dp/+}$ mammary epithelium (Figure 4B), suggesting up-regulation of ERK1/2 signaling in the *Myc-Gsdmc*$^{dp/+}$ mammary gland but not in *Myc*$^{dp/+}$ or *Pvt1-Gsdmc*$^{dp/+}$. An increased level of Myc protein should also result in an oncogene-induced DNA-damage response (Vafa et al., 2002) . We observed a 3.0 (± 0.7) fold enrichment of p53, a key mediator of cellular stress response, in total protein lysates from *Myc-Gsdmc*$^{dp/+}$ mammary glands compared to *Myc*$^{dp/+}$ or *Pvt1-Gsdmc*$^{dp/+}$ (Figure 4B). Because p53 is a pro-apoptotic protein, we carried out a terminal deoxynucleotidyl transferase-dUTP nick-end-labeling (TUNEL) assay to determine the degree of apoptosis in *Myc-Gsdmc*$^{dp/+}$, *Myc*$^{dp/+}$, *Pvt1-Gsdmc*$^{dp/+}$, and wild type mammary gland sections. We detected more TUNEL- positive cells in *Myc-Gsdmc*$^{dp/+}$ mammary glands (1.7% ± 0.5) indicating increased cellular apoptosis due to elevated levels of Myc protein (Figure 4C). A critical feature of oncogene induced DNA damage response is the formation of γ-H2AX foci at the site of the DNA damage. Enhanced oncogene-induced DNA-damage response in *Myc-Gsdmc*$^{dp/+}$ mammary ducts was evident by the increased number of foci

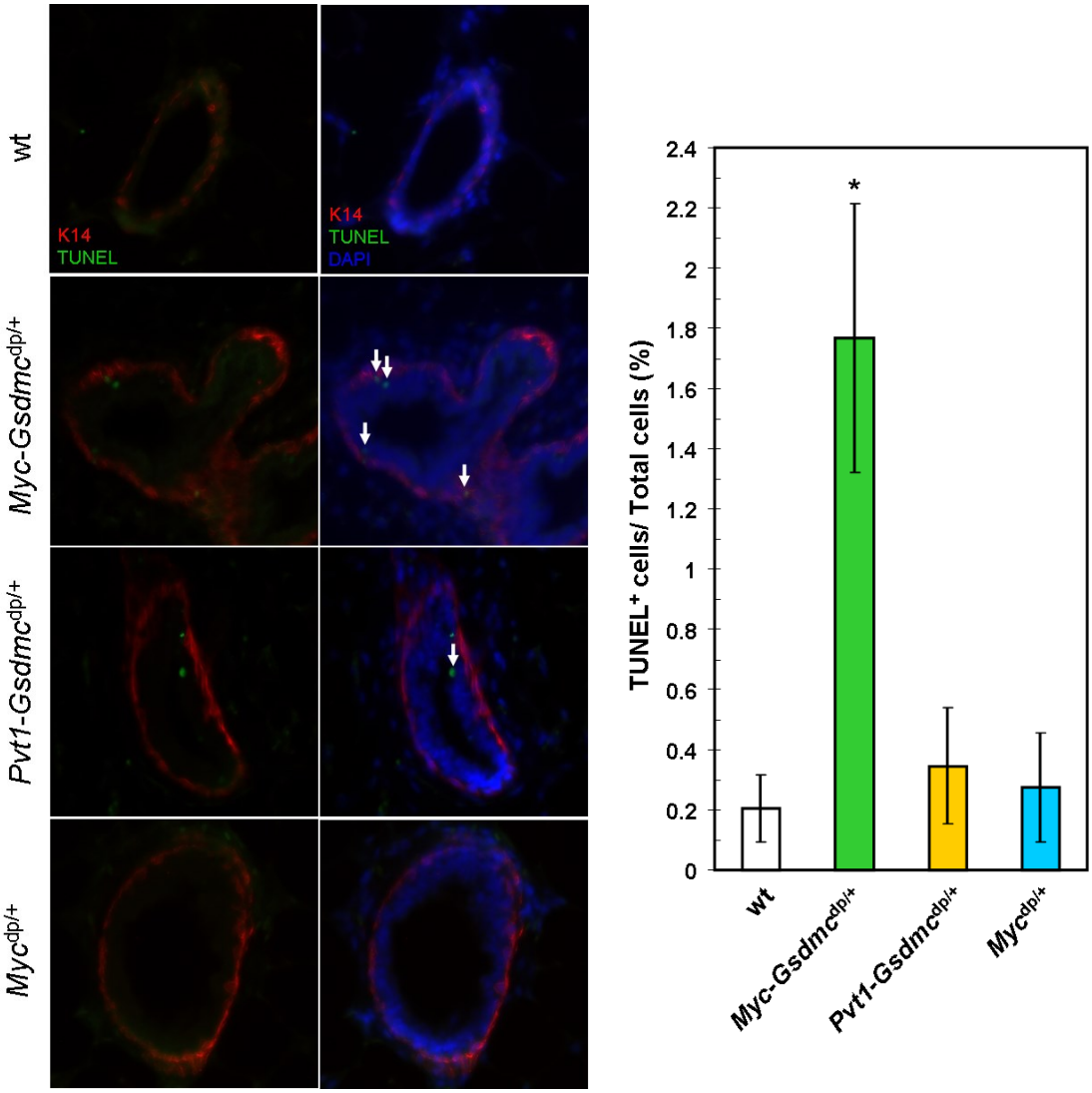

Figure 4 C. Increased apoptosis in mammary ducts of *Myc-Gsdmc*$^{dp/+}$ mice.

TUNEL assay was carried out on the mammary sections from wt, *Myc-Gsdmc*$^{dp/+}$, *Myc*$^{dp/+}$, and *Pvt1- Gsdmc*$^{dp/+}$ mice. Antibody against myoepithelial marker K14 (red) and TUNEL positive cells (green) are shown. DAPI (blue) used as counterstain. Three mice for each genotype was used. Nine mammary ducts for each mouse were examined. Arrows indicate TUNEL positive cell (green). Quantification of the number of TUNEL positive cells as a percentage of the total number of cells represented in bar graph, mean ± SE, *P < 0.05.

containing phosphorylated- γ-H2AX (160 foci per 100 ducts) compared those in *Myc*$^{dp/+}$ and *Pvt1-Gsdmc*$^{dp/+}$ mice (30 – 40 foci per 100 ducts) (Figure 4D). These data suggest that a single copy gain of the *Myc-Gsdmc* interval can lead to increased Myc protein levels resulting oncogenic activation by pro-survival signaling and DNA-damage response.

The above experiments indicated that gain of *Myc-Gsdmc* may predispose cells to tumorigenesis, while gain of either the *Myc* or *Pvt1-Gsdmc* alone is insufficient to do so. In breast and ovarian cancer, gain of 8q24 has been reported to be co-incident with amplification of ERBB2/HER2 in chromosome 17q12 (Al-Kuraya et al., 2004; Korkola and Gray; Park et al., 2005). About 40% of HER2-positive breast cancers have gain of the 8q24 locus, suggesting co-mutations of these two loci in some cancer patients (Perez et al., 2011; Sircoulomb et al., 2010). Patients with breast cancer who had gain of 8q24 with concurrent amplification of HER2 were observed to have substantially worse outcomes than patients who had only amplification of HER2 (Al-Kuraya et al., 2004). We crossed *Myc-Gsdmc*$^{dp/+}$, *Myc*$^{dp/+}$ and *Pvt1-Gsdmc*$^{dp/+}$ with mice harboring an un-activated *neu* (rat) transgene under the transcriptional control of the mouse mammary tumor virus promoter/enhancer (MMTV-neu/+,(Guy et al., 1992) (Figure 4E). To investigate the contribution of *Myc-Gsdmc* gain in mammary epithelial transformation, we carried out 3-D culture analysis of MECs isolated from 10 weeks old MMTV-neu/+ and *Myc-Gsdmc*$^{dp/+}$, MMTV-neu/+ mice. At day 14, we found that 71.8% (± 1.4) of the *Myc-Gsdmc*$^{dp/+}$, MMTV-neu/+ MECs displayed transformed acinar phenotypes in 3-D culture, compared to only

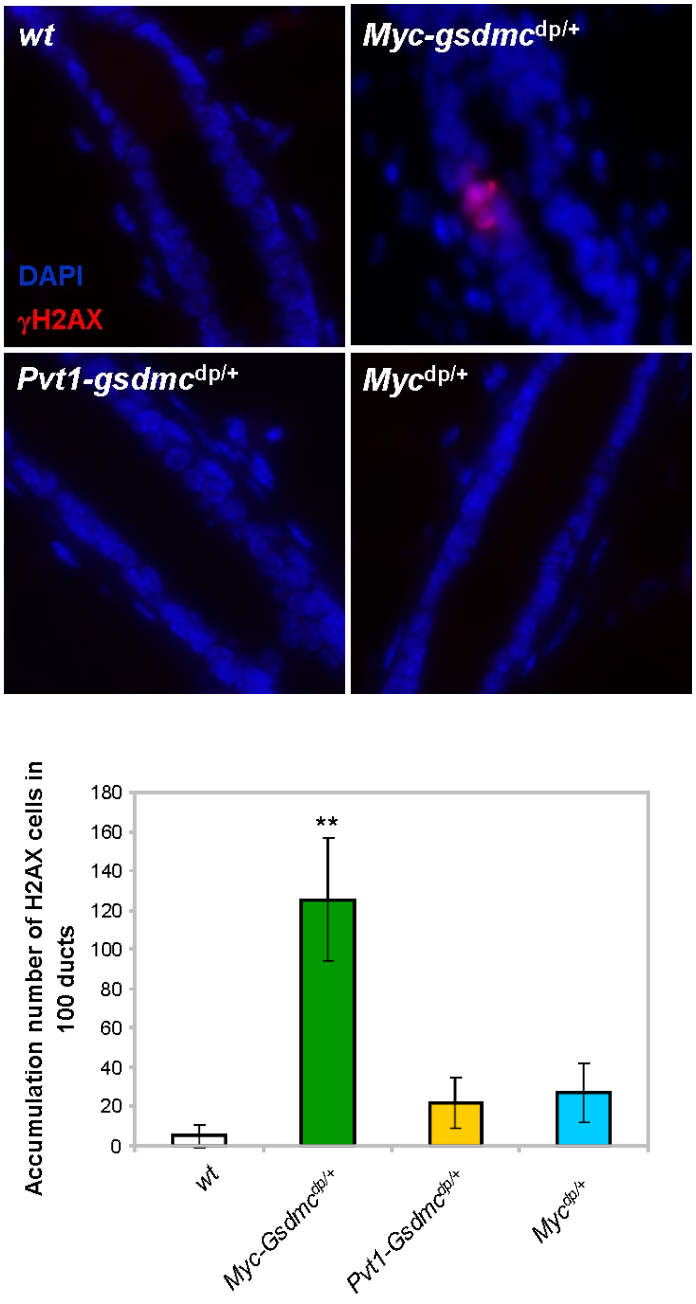

Figure 4 D. IF staining for γ-H2AX foci.

Fluorescence images of γ-H2AX foci formation in mammary epithelium (in red). One hundred ducts from each genotype were examined. The bar graph represents cumulative numbers of γ-H2AX foci from each genotype. n=3 for each genotype. Significance at **$p < 0.01$ using two-tailed Student's t-test.

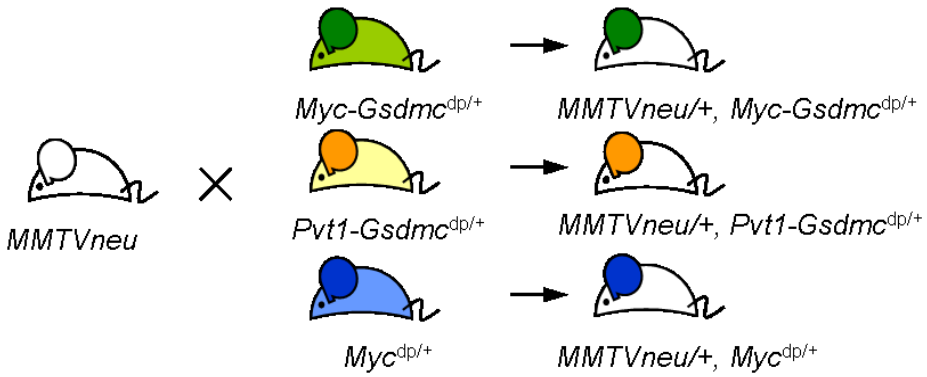

Figure 4 E. Generation of mouse with double mutations by crossing the duplication and MMTVneu lines.

Schematic of generating the *Myc-Gsdmc*$^{dp/+}$,MMTV-neu/+, *Pvt1-Gsdmc* $^{dp/+}$,MMTV-neu/+, and *Myc* $^{dp/+}$,MMTVneu/+ mice.

48.5% (± 2.3) of the MMTV-neu/+ MECs (Figure 4F). We also performed transwell migration assays to determine the migratory response of these MECs to different concentrations of epidermal growth factor (EGF). *Myc-Gsdmc*$^{dp/+}$, MMTV-neu/+ MECs exhibited nearly twice the migratory response to EGF compared to MMTVneu/+ cells (Figure 4G). These *in vitro* studies suggest that a single-copy gain of the *Myc-Gsdmc* interval may contribute to increased neoplastic transformation in the *Myc-Gsdmc*$^{dp/+}$, MMTV-neu/+ MECs. To determine the effect of *Myc-Gsdmc* gain in cellular transformation *in vivo*, we carried out a whole-mount analysis of mammary glands from 14 week old *Myc-Gsdmc*$^{dp/+}$, MMTV-neu/+ and MMTV-neu/+ mice. *Myc-Gsdmc*$^{dp/+}$, MMTV-neu/+ mammary glands revealed structures that looked consistent with hyperplastic alveolar nodules (HAN) which were not found in MMTV-neu/+ mice (Figure 4H). Usually, HAN structures are precancerous lesions found in neoplastic mammary glands (Harkness et al., 1957). Taken together, these data provided strong evidence in support of our hypothesis that *Myc-Gsdmc* gain could predispose mammary epithelium for oncogenic transformation.

We carried out a mammary tumor latency study using 1) *Myc-Gsdmc*$^{dp/+}$, MMTV-neu/+; 2) *Myc*$^{dp/+}$, MMTV-neu/+; 3) *Pvt1-Gsdmc*$^{dp/+}$, MMTV-neu/+; and 4) MMTV-neu/+ mice. Mice with mean tumor diameters of 1 cm were enrolled for tumor onset. The log-rank test was performed on the Kaplan–Meier tumor-free curves. The *Myc-Gsdmc*$^{dp/+}$, MMTV-neu/+ mice showed 90% penetrance of mammary tumors with a median latency of 224 days. In comparison, only half of

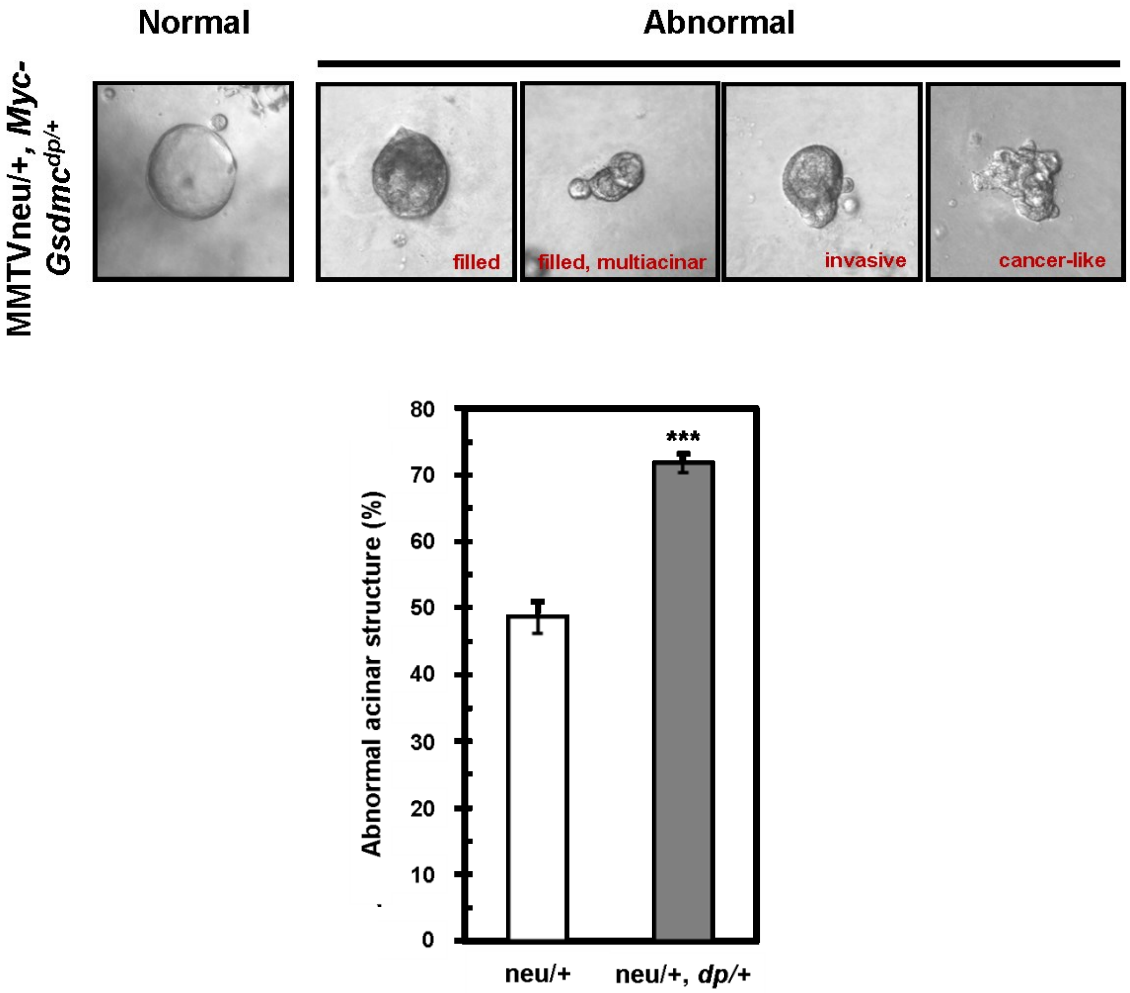

Figure 4 F. *Myc-Gsdmc*$^{dp/+}$, MMTVneu/+ MECs exhibit increased number of abnormal acinar structure than MMTVneu/+ MECs in 3-D culture.

c-Myc-Gsdmc$^{dp/+}$, MMTVneu/+ and MMTVneu/+ MECs were grown for 14 days in 3-D Matrigel cultures. Representative DIC images of normal and abnormal acinar structures are shown in the top panel. 200 acinar structures of each genotype were examined in a double blinded study. Number of acini exhibiting abnormal features for each genotype were scored. Data presented as mean ± SE, ***P< 0.001.

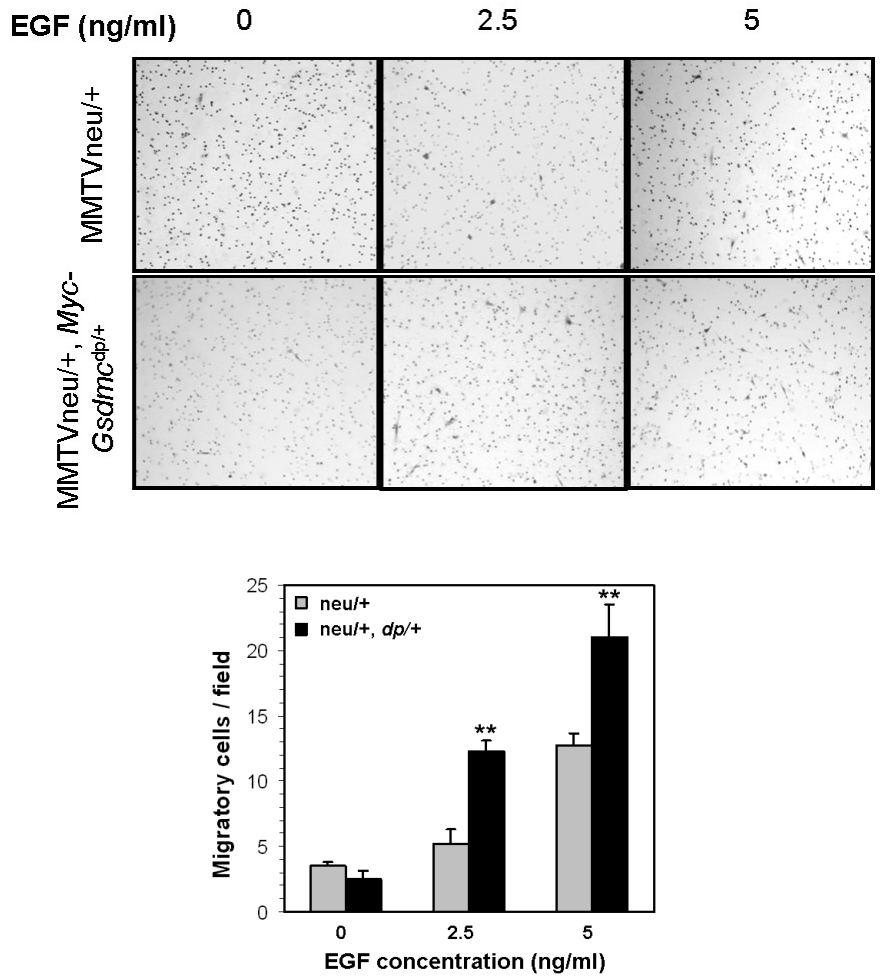

Figure 4 G. Transwell migration assay shows the MMTVneu/+, *Myc-Gsdmc*$^{dp/+}$ mammary epithelial cells has a higher migratory ability to EGF compared to the MMTVneu cells.

Primary mammary epithelial cells were isolated from mammary glands of MMTVneu, *Myc-Gsdmc*$^{dp/+}$ or MMTVneu virgin littermates at ages of 12 weeks. Equal amount of MMTVneu, *Myc-Gsdmc*$^{dp/+}$ and MMTneu cells were plated in the top chamber with the non-coated membrane. Cells were plated in medium without serum and growth factors, and medium supplemented with EGF was used as a chemoattractant in the lower chamber for 24 hr incubation. (Top panel) Bright-field images of MMTVneu, *Myc-Gsdmc*$^{dp/+}$ and MMTVneu cells stained with hymatoxyline to measure migratory cells. Four bright-field images were taken of each transwell membrane. Magnification, 200X. (Lower panel) Quantitative representation of migratory cell numbers from each field. Data are presented as mean ± SE, **, $P < 0.005$.

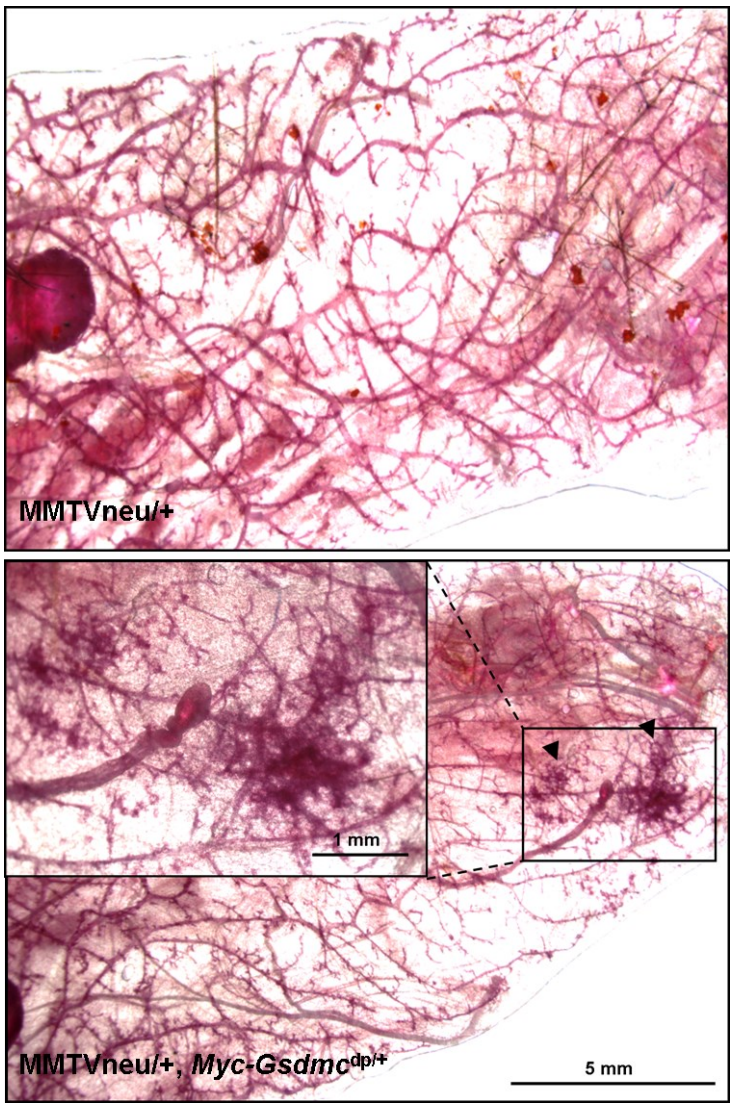

Figure 4 H. Early onset of hyperplastic alveolar nodules (HAN) like structures in MMTVneu/+, *Myc-Gsdmc*$^{dp/+}$ mammary glands.

Whole mount preparations of mammary glands from 14 weeks old virgin MMTVneu/+ and MMTVneu/+, *Myc-Gsdmc*$^{dp/+}$ are compared. The inset in the lower panel shows the HAN like structure in the MMTVneu/+, *Myc-Gsdmc*$^{dp/+}$ mammary glands.

the *Myc*$^{dp/+}$, MMTV-neu/+; and MMTV-neu/+ cohorts developed mammary tumors at a median latency of 345 days (Figure 4I). Neither *Myc*$^{dp/+}$, MMTV-neu/+ nor *Pvt1-Gsdmc*$^{dp/+}$, MMTV-neu/+mice exhibited abbreviated latency in mammary tumorigenesis similar to *Myc-Gsdmc*$^{dp/+}$, MMTV-neu/+. These results strongly suggest co-operation between Myc and other potential genes or regulatory sequences in the *Myc-Gsdmc* interval contribute to the reduced latency of mammary tumorigenesis. The *Myc-Gsdmc*$^{dp/+}$, MMTV-neu/+ tumors presented a spectrum of morphologies from poorly encapsulated, solid, nodular, masses (Fig 4J) to solid masses containing pools of eosinophilic secretory material, to more differentiated masses with alveoli containing secretory material. Additional features included a high mitotic index (Fig 4J-b, arrow) particularly involving the solid masses, or variably sized areas of necrosis. Some of these masses were locally invasive, or in places invaded adjacent thin walled blood vessels (Fig 4J-a, arrow) consistent with adenocarcinomas. These data strongly indicate that gain of just one copy of the *Myc-Gsdmc* region is an oncogenic aberration and can drive early tumorigenesis in mouse mammary glands.

Non-coding RNA PVT1 Controls Cellular Proliferation in Mammary Tumors

It is evident from the above experiments that Myc co-operates with other genes in the *Myc-Gsdmc* interval in the neoplastic transformation of *Myc-*

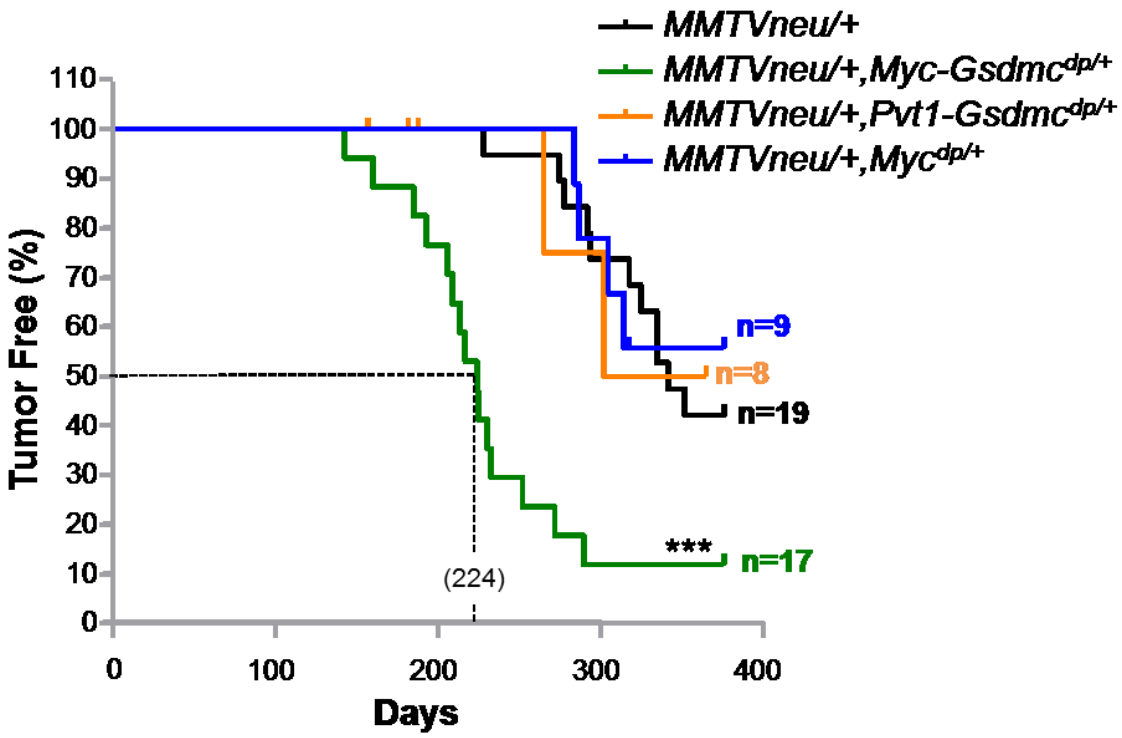

Figure 4 I. Kaplan–Meier analysis of mammary tumor free among the different genotypes.

Highly significant difference (*** $p < 0.001$, logrank test) in the tumor latency between *Myc-Gsdmc*$^{dp/+}$,MMTV-neu/+ and the other genotypes.

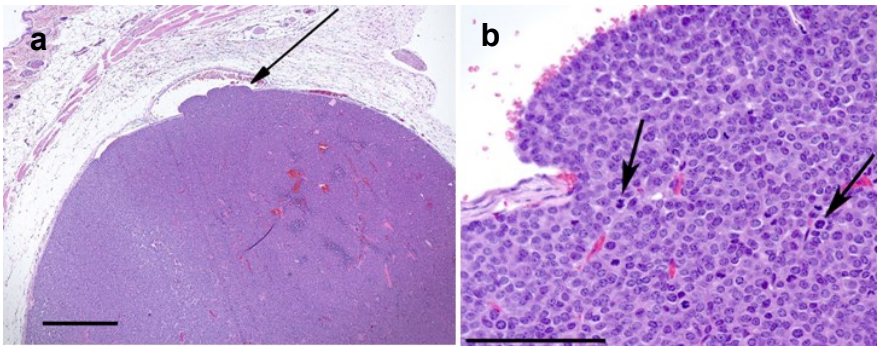

Figure 4 J. Representative histopathology of mammary tumors from *Myc-Gsdmc*$^{dp/+}$,MMTV-neu/+ mice.

Panel a shows a solid, expansile tumor that is invading a small blood vessel (arrow), bar = 1000 µm. Panel b shows numerous mitotic figures (arrows), bar = 100 µm.

Gsdmc$^{dp/+}$, MMTV-neu/+ mammary epithelium. Since the *Myc-Gsdmc* interval is a gene desert region and *Gsdmc* transcripts were barely detectable in mouse mammary glands, we investigated the possible role of *Pvt1* in the *Myc-Gsdmc*$^{dp/+}$, MMTV-neu/+ mammary tumors. We reasoned that if *Myc* or *Pvt1* is contributing to the neoplastic transformation of *Myc-Gsdmc*$^{dp/+}$, MMTV-neu/+ cells, then depleting either *Myc* or *Pvt1* will result reduction in proliferation of these cells. Two independent tumors, YYT 549-t and YYT 402-t, each of 1-cm diameter were harvested from *Myc-Gsdmc*$^{dp/+}$, MMTV-neu/+ mice. Cells isolated from these tumors were grown in 2-dimensional (2-D) culture for 2-3 days. Transfection of these tumor cells was carried out with respective si-RNAs to knockdown either *Myc* (si-Myc), *Pvt1* (si-Pvt1), or both (si-Myc + si-Pvt1) (Figure 5A). The transfection efficiencies of the si-RNAs were monitored by fluorescent emission of Alexa 488, which was conjugated with a control si-RNA. We obtained at least 90% transfection efficiency in these cells growing in 2-D culture for 16 hrs (data not shown). These cells were then grown in 3-D culture for 72 hrs, stained for proliferative marker Ki67, and the proliferating cells were enumerated (Figure 5A). Depletion of *Pvt1* resulted in 55% reduction in proliferation in these cells (percentage of Ki67 positive cells - YYT549-t: 43.3 ± 2.5%, YYT402-t: 47.5 ± 8.9%) (Figure 5B). Similarly, knock down of *Myc* led to 65% decrease in the Ki67 positive *Myc-Gsdmc*$^{dp/+}$, MMTV-neu/+ cells compared to the control (YYT549-t: 34.9 ± 1.8%, YYT402-t: 37.7 ± 3.3%) (Figure 5B). This conclusively shows that both Pvt1 and Myc contribute to the proliferation of *Myc-Gsdmc*$^{dp/+}$, MMTV-neu/+ tumors. Surprisingly, knock down of both *Myc* and *Pvt1* in the *Myc-Gsdmc*$^{dp/+}$,

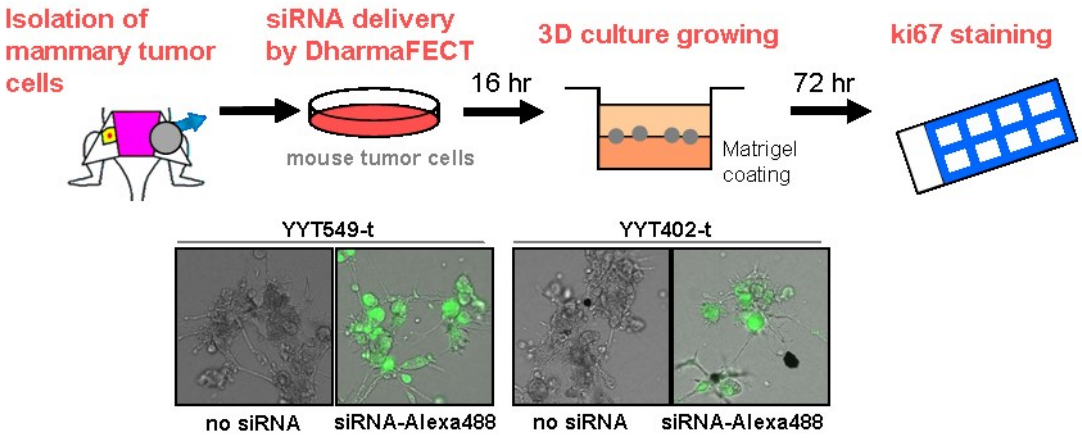

Figure 5 A. Schematic of proliferation assay for *Myc-Gsdmc*$^{dp/+}$, MMTV-neu/+ mammary tumor derived cells obtained from two mice, YYT549 and YYT409.

Cells were transfected with siRNA against *Myc* (si-Myc), *Pvt1* (si-Pvt1), and Ctrl (si-Ctrl). Transfection efficiency was confirmed by si-Ctrl conjuigated with Alex-488 (green). After growing the transfected cells in 3-D culture system, the cells were stained using antibody against Ki-67. Images were taken under the microscope (magnification ×20).

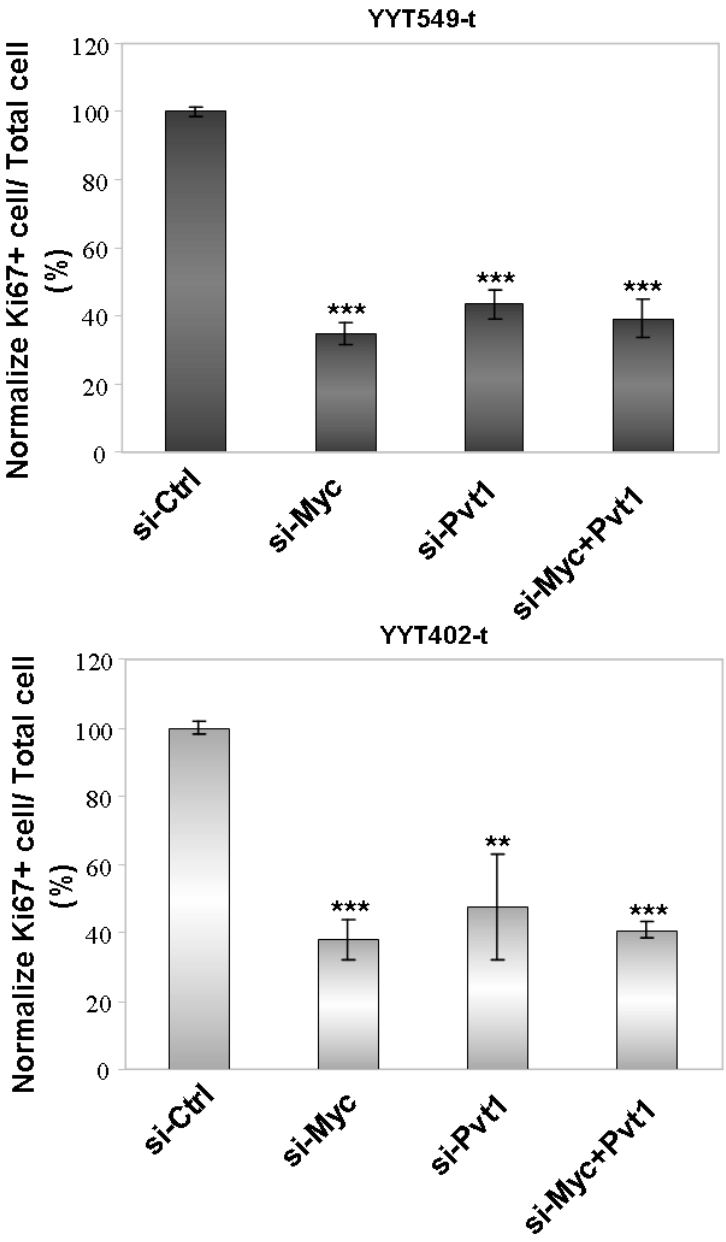

Figure 5 B. Ki-67 proliferation indexes from siRNA mediated silencing of Myc, Pvt1, and Myc+Pvt1 in primary mammary tumor cells.

Quantification of the number of cells undergoing proliferation in 3-D culture is measured by their Ki-67 index. n = 3 for each transfected cell line (top: YYT549, bottom: YYT402). Significance at **p < 0.01 and, ***p <0.001 using two-tailed Student's t-test.

MMTV-neu/+ tumor cells led to an identical (YYT549-t: 39.2 ± 3.2%, YYT402-t: 40.7 ± 1.4%) decreases in proliferation as observed when either *Myc* or *Pvt1* was knocked down separately (Figure 5B). We verified the specificity and the efficiency of the si-RNAs by RT-qPCR analysis of *Myc* and *Pvt1* in these cells (Figure 5C). Knocking down *Myc* or *Pvt1* transcripts with their respective si-RNAs were specific and did not affect the transcript levels of the other, or vice versa (Figure 5C). From these data we inferred that *Myc* and *Pvt1* were mediating their oncogenic activity through the same pathway, which may explain why depletion of *Myc* and *Pvt1* together would result in identical proliferative inhibition in *Myc-Gsdmc*$^{dp/+}$, MMTV-neu/+ tumor cells as when they are knocked down separately.

To determine if PVT1 has a similar role in human breast cancers, we carried out identical experiments in human breast cancer cell lines that have a gain of 8q24.21. Breast cancer cell lines SK-BR-3 and MDA-MB-231 harbor copy number gains of 8q24.21 (Guan et al., 2007; Huppi et al., 2008). We knocked down either *MYC* (si-MYC) or *PVT1* (si-PVT1) or both (si-MYC + si-PVT1) in SK-BR-3 and MDA-MB-231 as described above. The transfection efficiency in each cell line was optimized using a control si-RNA with Alexa 488. Under the conditions in which at least 90% transfection efficiency was achieved (Figure 5D), the cell lines were transfected with si-MYC, si-PVT1, or si-MYC + si-PVT1. The cells were allowed to grow in 2-D for 16 hrs, following which they were plated on 3-D Matrigel^{TM} and allowed to grow for 72 hrs. As before, the Ki67 index for each cell line was taken as a measure of its proliferative potential. In SK-BR-3, proliferation was reduced by 29.4% (± 0.9), 37.3 % (± 5), and 29.3% (±

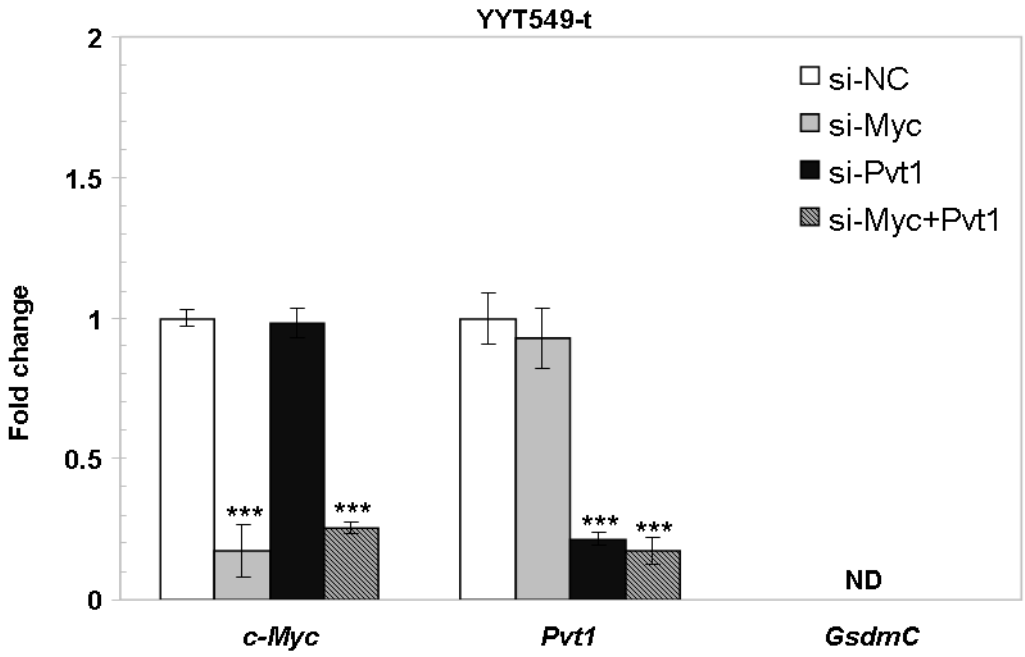

Figure 5 C. Quantitative RT-PCR analysis to assess the relative expression of Myc, Pvt1, and Gsdmc mRNA in primary mammary tumor cells after siRNA mediated silencing.

Relative mRNA expression of *Myc*, *Pvt1* and *Gsdmc* in *Myc-Gsdmc*$^{dp/+}$, MMTV-neu/+ mammary tumor cells transfected with the si-RNAs. ND, not detected because of low expression. Significance at ***p <0.001 using two-tailed Student's t-test.

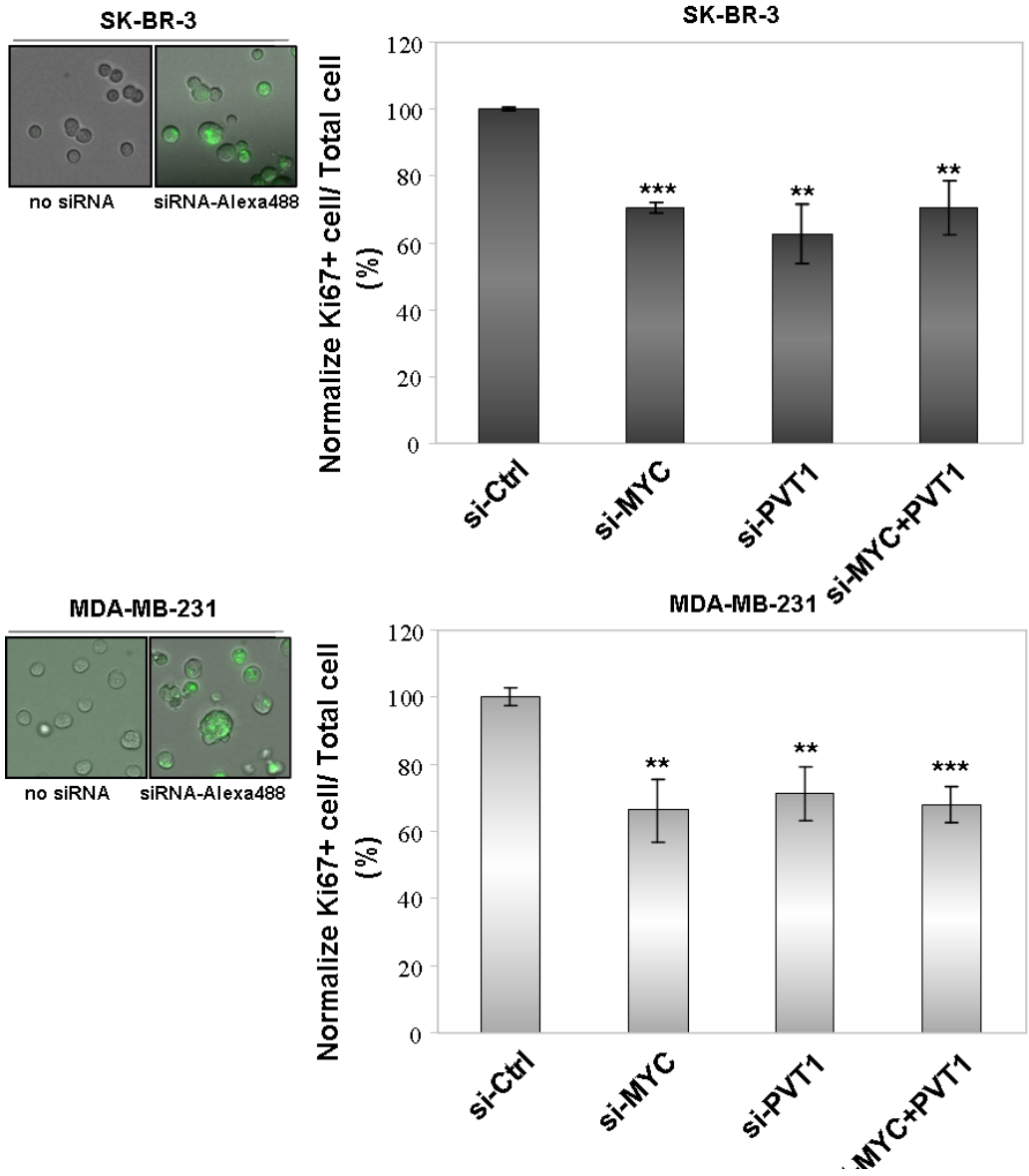

Figure 5 D. Ki-67 proliferation indexes from siRNA mediated silencing of MYC, PVT1, and MYC+PVT1 in human breast cancer cells.

Proliferation assay of human breast cancer cell lines SK-BR-3 (top) and MDA-MB-231 (bottom) growing in 3-D culture after the cell lines were transfected with si-Ctrl, si-MYC, si-PVT1 and (si-MYC + si-PVT1). Transfection in each cell line was confirmed as mentioned in (A). n = 3 for each transfected cell line. Significance at **p < 0.01 and, ***p <0.001 using two-tailed Student's t-test.

4.7) in cells transfected with si-MYC, si-PVT1, and si-MYC + si-PVT1 respectively (Figure 5D). Similarly, for MDA- MB-231 cells transfected with si-MYC, si-PVT1, and si-MYC + si-PVT1, reduction in Ki67 index was observed by 33.8% (± 5.4), 28.9% (± 4.6) and 31.9% (± 3.2) respectively (Figure 5D). Once again, we found the similar level of proliferation arrest in both the cell lines with reduced levels of *MYC*, *PVT*1, or *MYC* + *PVT1*. Efficiency and specificity of the si-RNAs in reducing the *MYC*, *PVT1*, or *MYC+PVT1* transcript levels were confirmed by RT-qPCR in both the cell lines (Figure 5E). These data suggest that *PVT1* and MYC can control proliferation of mouse and human breast cancer cell lines through a shared pathway.

PVT1 Regulates MYC Stability in Human Breast Cancer

An Increase in Myc protein level in the *Myc-Gsdmc*$^{dp/+}$ mammary glands was found (Figure 4B) with concomitant increases in *Pvt1* transcripts. To investigate whether a similar correlation could be observed in the human breast cancer cell lines with 8q24.21-gain, we quantified the levels of *PVT1* transcripts and MYC protein in SK-BR-3 and MDA-MB-231 cell lines and compared them with untransformed breast cell line MCF-10A. RT-qPCR analysis revealed that *PVT1* transcript was enriched 6.2-fold (± 0.3) in SK-BR-3 cells and 15.7-fold in MDA-MB-231 cell lines compared to the level of *PVT1* in MCF-10A (Figure 6A). Using Western blot analysis, we also detected a higher protein level of MYC in SK-BR-3 and MDA-MB-231 cell lines compared to MCF-10A (Figure 6B). This

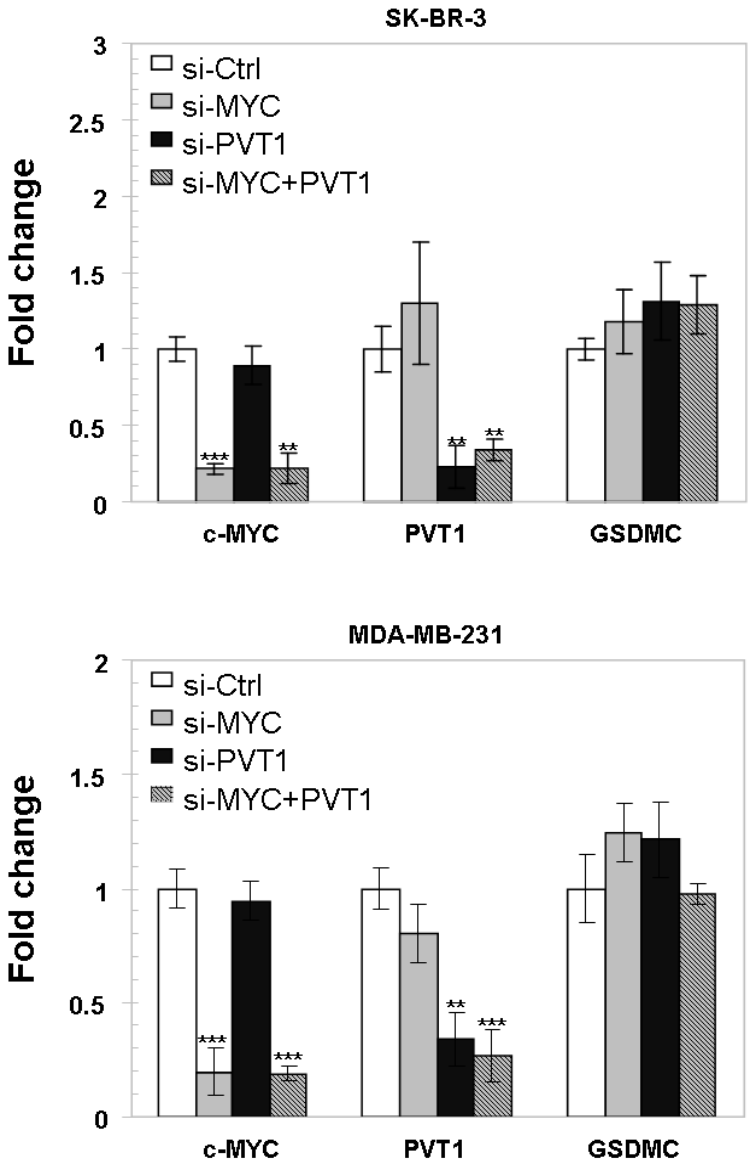

Figure 5 E. Quantitative RT-PCR analysis to assess the relative expression of MYC, PVT1, and GSDMC mRNA in human breast cancer cells after siRNA mediated silencing.

Relative mRNA expression of MYC, PVT1, and GSDMC in SK-BR-3 (top) and MDA-MB-231 (bottom) breast cancer cells transfected with the respective si-RNAs. Each bar represents the mean ± SE of triplicate experiments. ** $p < 0.01$, *** $p < 0.001$.

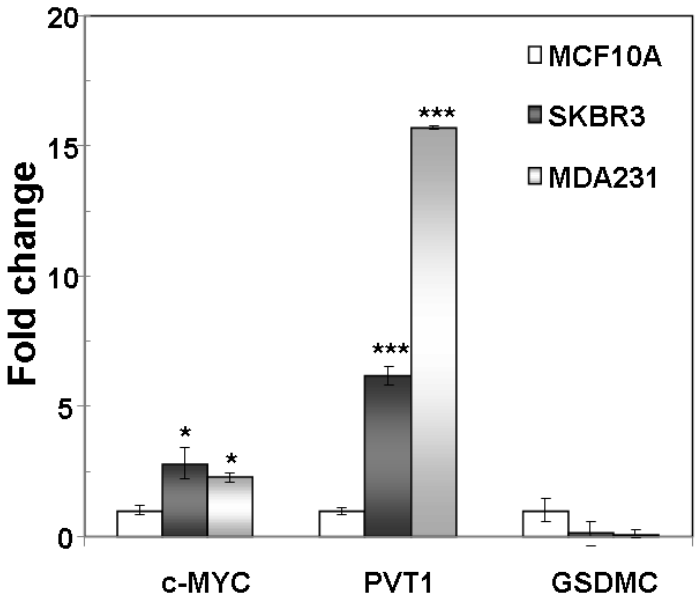

Figure 6 A. Quantitative RT-PCR analysis to assess the relative expression of MYC, PVT1, and GSDMC mRNA in human breast cancer cells.

Relative expression of MYC, PVT1 and GSDMC transcripts in SK-BR-3 and MDA-MB-231 (with 8q24 gain) and MCF10A (without 8q24 gain). Significance at *$p < 0.05$ and, ***$p < 0.001$ using two-tailed Student's t-test.

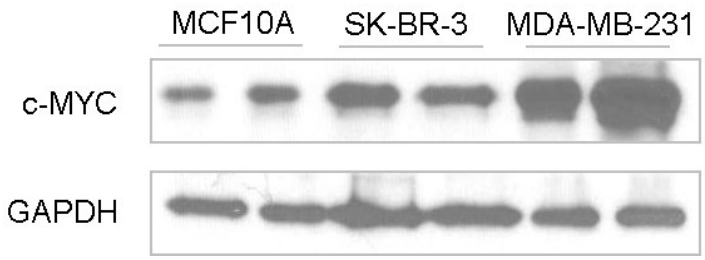

Figure 6 B. SK-BR-3 and MDA-MB-231 cells express higher level of MYC protein compared to MCF10A.

Western analysis for MYC expression in MCF10A, SK-BR-3, and MDA-MB-231 cell lines.

observation corroborates with our finding that *Pvt1* transcript and Myc protein are increased in mouse mammary epithelia with a gain of the *Myc-Gsdmc* interval. In addition, functional analyses of *Myc-Gsdmc*$^{dp/+}$, MMTV-neu/+ mammary tumors as well as in human cancer cell lines SK-BR-3 and MDA-MB-231, *PVT1* and MYC seemed to control proliferation via same pathway (Figure 5B and 5D). Accordingly, we hypothesized that *PVT1* regulates MYC protein levels in the SK-BR-3 and MDA-MB-231 cell lines. To address this, we knocked down *MYC* (si-MYC), *PVT1* (si-PVT1) or both (si-MYC + si-PVT1) in SK-BR-3 and MB-MDA-231 cell lines. Western blot analyses showed that a depletion of *PVT1* led to strong reduction of MYC protein in SK-BR-3 (35.7 ± 7.4%) and in MB-MDA-231(61.9 ± 3.5%) (Figure 6C). These data suggest that the *PVT1* co-operates with MYC in these human breast cancer cell lines by regulating its protein level.

Because the depletion of *PVT1* did not affect the *MYC* mRNA level (Figure 5E), we investigated whether *PVT1* regulates MYC protein level in these cells by modulating its stability. A recent study has shown that Myc half-life is significantly longer in SK-BR-3 cell line, ranging from 80 to 90 minutes, compared to MCF10A, which ranged from 16 to 20 minutes (Zhang et al., 2012). SK-BR-3 cells were transfected with si-PVT1 for 16 hrs and were treated with 10 μM of cycloheximide, a protein synthesis inhibitor, for 0, 15, 30, 45 and 60 minutes. A non-specific si-RNA (si-Ctrl) was used as a control. Following the cycloheximide treatment, both si-PVT1 and si-Ctrl transfected cells were harvested at the above mentioned time points and whole cell lysates were subjected to Western blot analysis for MYC and GAPDH. We observed a rapid degradation of MYC in

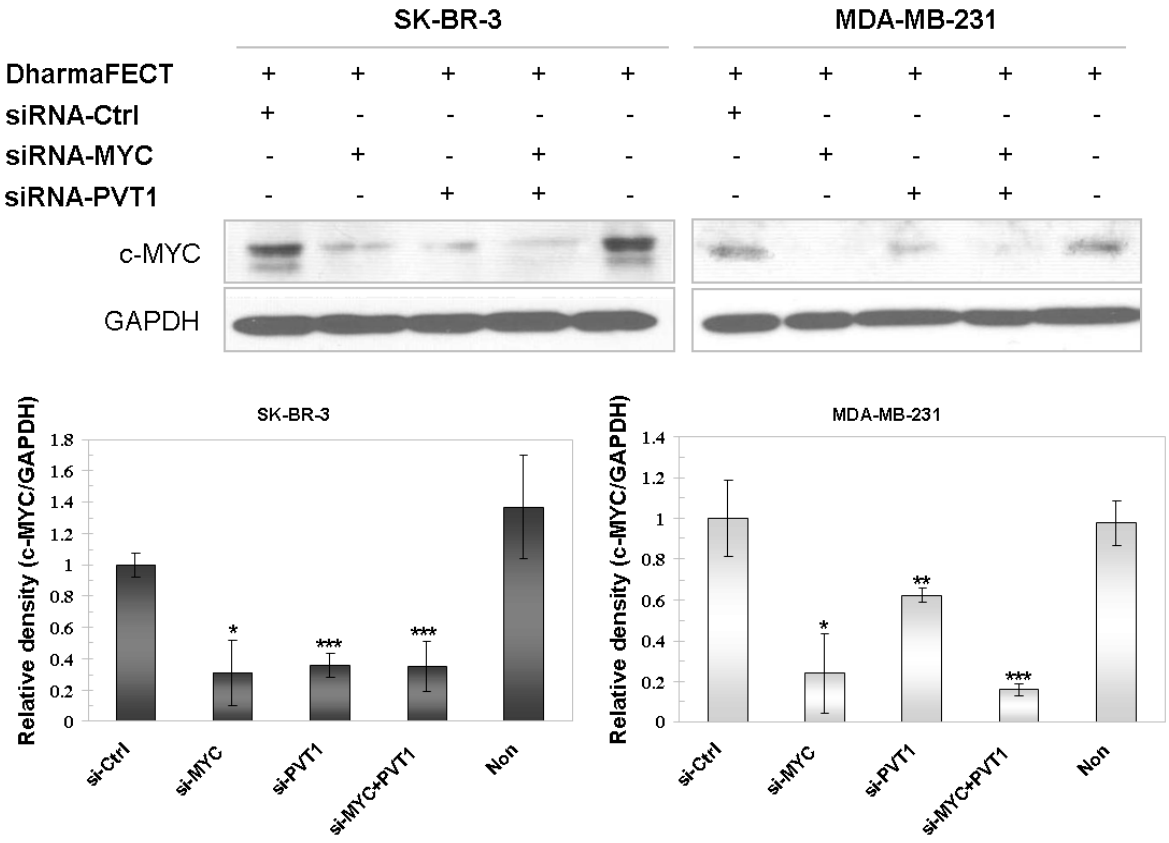

Figure 6 C. Western analysis for MYC protein in the total lysates obtained from SK-BR-3 and MDA-MB-231 cell lines transfected with different si-RNAs.

The relative density for each category was determined by normalizing against the intensity of the GAPDH band. Data are presented as mean ± standard error (SE). Significance at *p < 0.05, **p < 0.01 and, ***p <0.001 using two-tailed Student's t-test.

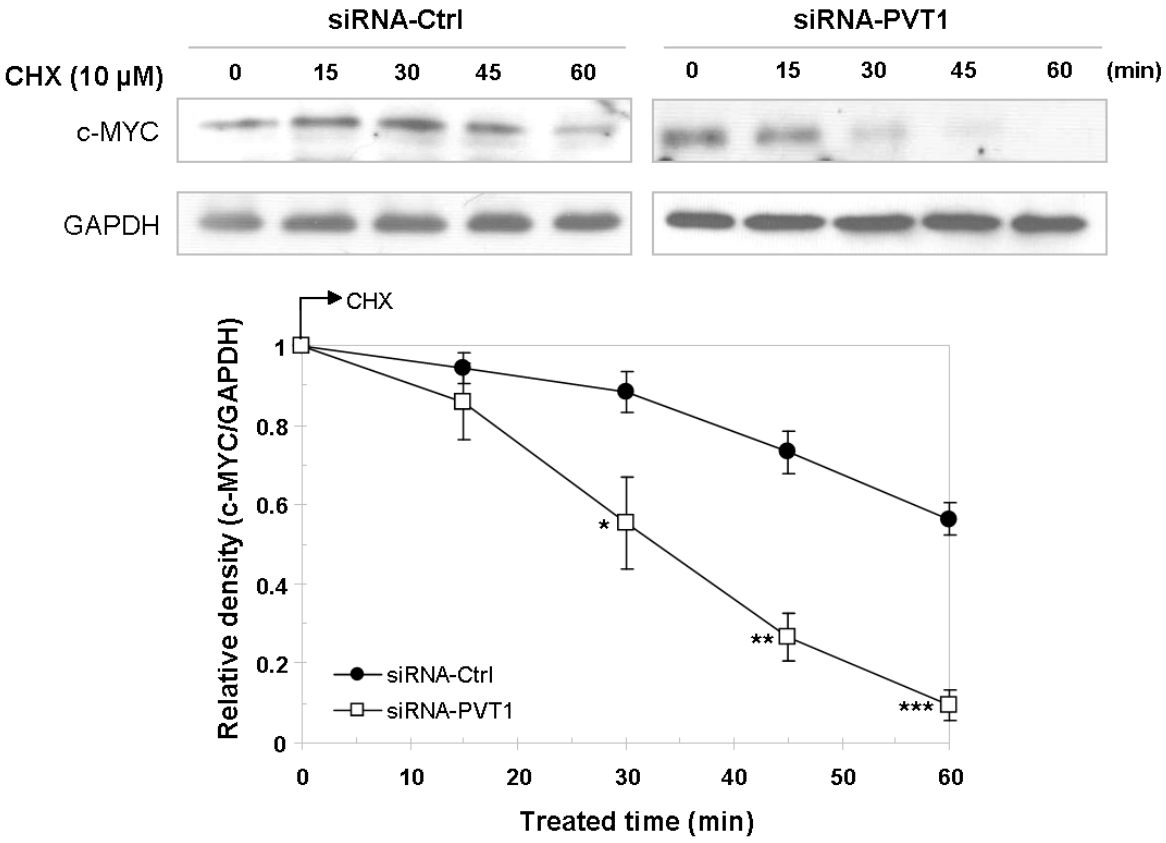

Figure 6 D. PVT1 regulates MYC stability in SK-BR-3 breast cancer cells.

Stability of c-MYC protein in SK-BR-3 transfected with si-Ctrl and si-PVT1 and treated with 10 μM cycloheximide (CHX) for different time points (top row). The relative density was determined by comparing against the GAPDH level (bottom row). Each bar represents the mean ± SE of triplicate experiments. * $p < 0.05$, ** $p < 0.01$, *** $p < 0.001$.

PVT1 depleted cells (si-PVT1) compared to the control (si-Ctrl) after cycloheximide treatment (Figure 6D). A quantitative analysis revealed that 45.7% of MYC was degraded at the 30 minutes time point after cycloheximide treatment in *PVT1* depleted cells, while 88.5% of the MYC protein was still intact in si-Ctrl transfected cells. Taken together, these results provide strong evidence that *PVT1* regulates MYC protein stability in human breast cancer cells with 8q24.21 gain.

Discussion

There are several important findings in this study. First, we found that gain of a single copy of an approximately 2Mb gene-desert on 8q24 can lead to oncogenesis. In mammary tissues of *Myc-Gsdmc*$^{dp/+}$ mice, we observe striking anomalies in mammary duct morphology that includes increased lateral branching and failure to undergo replicative quiescence in post- pubertal virgin females. The mammary epithelial cells of these mice show abnormal differentiation and readily co-operate with Neu to undergo transformation. Low copy-number gain of 8q24, which includes *PVT1*, has been observed in several cancers including sarcomas (Hattinger et al., 2002; Zielenska et al., 2001) (Afify and Mark, 1999) (Sandberg and Bridge, 2002), prostate cancer (Chen et al.; Lapointe et al., 2007; Sato et al., 1999), colorectal cancer (Douglas et al., 2004; Liu et al., 2007; Nakao et al.), cervical cancer (Zhang et al., 2002), medulloblastoma (Zitterbart et al., 2011), glioblastoma (Nishizaki et al., 1998), ovarian cancer (Noack et al., 2004; Osterberg et al., 2009), esophageal adenocarcinoma (Rygiel et al., 2008), small cell lung carcinoma (Kang et al., 2008; Yamada et al., 2000), hepatocellular carcinoma (Chochi et al., 2009; Wang et al., 2001) and acute myeloid leukemia (AML) (Grimwade et al., 1998; Le Beau et al., 2002). In human breast cancers, low copy-number gain of the 8q24 region is found in 15% of the patients (Chin et al., 2006; Guan et al., 2007; Liao and Dickson, 2000) and is associated with poor prognosis (Bergamaschi et al., 2006; Borg et al., 1992). It has also been suggested that a difference in high versus low copy-number gains in 8q24 may contribute to differences in clinico-pathological parameters in ovarian cancer (Dimova et al., 2006). Moreover, tumors in several genetically engineered mouse models for cancer develop spontaneous low copy-number gains, including trisomy of whole or

part of chromosome 15 that is syntenic with Hu 8q24. In the mouse model for acute promyelocytic leukemia (APL), in which tumor formation is driven by a PML-RARα fusion gene in the myeloid cells, 64% of the tumor bearing mice are found to harbor trisomy of chromosome 15 that is syntenic to Hu8q24 (Jones et al., 2010; Le Beau et al., 2002). Mice harboring a hypomorphic allele of *Dnmt1,* which develop early onset of T lymphoma, also exhibit gain of chromosome 15 at high frequency (10 out of 12) (Gaudet et al., 2003). Our results functionally verify these observations and suggest that gain of a single copy of 8q24 can predispose cells for transformation.

Secondly, our data suggest that gain of just one copy of *Myc* is insufficient to drive tumorigenesis. Rather, oncogenesis requires co-operation from other participants in the 8q24 region. Though *MYC* has been considered the best candidate for cancer in the 8q24 region, emerging evidences indicate other functional elements in the region that can influence the pathological outcome. For example, Myc-335 mice with deletion of a genomic region containing rs6983267, a common SNP found in several cancers and located 500 kb upstream of Myc, have been reported to be resistant to *APCmin* driven intestinal cancer (Sur et al., 2012). The gene-desert region surrounding MYC may harbor several unidentified candidates which can facilitate tumor pathophysiology. Our mouse strains provide a mechanistic understanding of co-operation between multiple genes in the 8q24.21 'gene desert' locus and advances our knowledge regarding a poorly understood mutation which is common in all major cancers. Copy-number gain of 8q24 in human cancers presents a characteristic challenge in understanding the functional consequences associated with structural variations in human cancer. Although *MYC* is the most prominent gene in this region and garners obvious attention, the role of the genomic

segments adjoining *MYC* that are also co-amplified in almost every cancer remains unexplained. Our results unequivocally show that in addition to *Myc*, an additional gene in the *Myc-Gsdmc* locus, the *Pvt1* non-coding RNA,co-operate to drive cellular transformation when this region is gained. We observed up regulation of pro-survival pathways as well as increased DNA damage response in the *Myc-Gsdmc*$^{dp/+}$, but not in *Myc*$^{dp/+}$ or *Pvt1-Gsdmc*$^{dp/+}$ mammary tissues. This suggests that gain of *Myc-Gsdmc* can result in sufficient activation of oncogenic events necessary for tumorigenesis, namely activation of cellular stress markers and pro-survival pathways that cannot be mediated by single-copy gain of *Myc* alone.

This co-operative activity may have important implications in our understanding of the mechanisms underlying cellular transformation in the cancer cells where 8q24 is gained. Known to be genomically unstable, this region is considered to be a hot spot to undergo structural mutations (Huppi et al., 2008). Our work demonstrates that a simple duplication of about 2 Mb in this region renders the cell vulnerable to cellular transformation. It has been previously speculated that changes caused by gain of human 8q24 or the corresponding locus in mouse chromosome 15, such as increased copy-number of *TRIB1*, *PVT1*, *CCDC26* and other genes in this region may impact tumorigenesis in collaboration with *MYC* (Guan et al., 2007; Jones et al., 2010; Radtke et al., 2009; Rothlisberger et al., 2007). Tumorigenesis facilitated by gain of *Myc-Gsdmc*, which encompasses, in addition to *MYC*, the genomic locus syntenic to *PVT1* and *CCDC26* in the human, and harbors several risk alleles found in human cancers, is a direct proof of this hypothesis. Though we have identified Pvt1 as an oncogene that co-operates with Myc in the tumors in the *Myc-Gsdmc*$^{dp/+}$,MMTV-neu/+ mice, it is possible

that other functional elements in the *Myc-Gsdmc* region can also play a role in the tumorigenesis. Thus, these mice will be useful as functional models to illuminate the importance of 8q24.21 in tumorigenesis.

Thirdly, we identified a novel role of a lncRNA in 8q24, *PVT1*, in tumorigenesis and regulation of MYC in human breast cancer cells. Knock-down of *PVT1* reduced proliferation of *Myc-Gsdmc*$^{dp/+}$,MMTV-neu/+ tumor cells as well as in human breast cancer cell lines, SK-BR-3 and MDA-MB-231. Additionally, since knock-down of either *MYC*, *PVT1*, or both resulted in similar reduction in proliferation, we reasoned that *PVT1* and *MYC* affect the same oncogenic pathway. The presence of increased Myc protein in *Myc-Gsdmc*$^{dp/+}$, but not in *Myc*$^{dp/+}$ or *Pvt1-Gsdmc*$^{dp/+}$ mammary epithelial cells led us to conclude that *Pvt1* can regulate Myc levels in these cells, thereby sensitizing them for transformation. This was supported by knocking down *PVT1* which resulted in reduction of MYC in both SK-BR-3 and MDA-MB-231.

PVT1 is a lncRNA with unknown function. It is a hotspot for translocation that has been observed in many cancers including Burkitt's lymphoma (Graham and Adams, 1986; Mengle-Gaw and Rabbitts, 1987), multiple myeloma (Nagoshi et al., 2012), and medulloblastoma (Northcott et al., 2012). Overexpression and/or gain of *PVT1* and some of its miRNAs have been reported in several malignancies, including breast cancer and it has been suggested to contribute to suppression of apoptosis in these cells (Bakkus et al., 1990; Beck-Engeser et al., 2008; Guan et al., 2007; Huppi et al., 1993; Huppi et al., 2008; Meyer et al.; Shtivelman and Bishop, 1989; Sugawara et al., 2011). Recently *PVT1* has been reported to regulate gemcitabine-sensitivity in human pancreatic cells (You et al., 2011) and to provide resistance to cyclolignan picropodophyllin (PPP), a new anticancer

drug with tumor-inhibitory effects (Hashemi et al., 2011). However, no mechanistic explanation for any of its functions has been reported. Here we show that *PVT1* helps maintain MYC level in human breast cancer cells with gain of 8q24, thus establishing a feedback mechanism for MYC protein in these cancer cells. This can eventually cause the affected cells to be addicted to higher protein levels of MYC. Therefore, knocking down *PVT1* in human breast cancer cell lines results in reduction of MYC protein. Surprisingly, *PVT1* ablation leads to decreased stability of MYC in SK-BR-3 cells, providing a mechanistic insight to the co-operation of adjacent genes, *MYC* and *PVT1*, in cellular transformation. To our knowledge, this is the first data showing the role of a lncRNA in maintaining the MYC protein by regulating its stability in cancer cells.

Additionally, we suggest that a detailed understanding of how *PVT1* regulates MYC protein in cancer cells can be exploited therapeutically. Soucek et al. have shown that MYC ablation can result in apoptosis in cancer cells, but not in normal cells, and can cause regression of K-ras mediated lung cancer in mice (Soucek et al., 2008) thereby demonstrating the central importance of MYC in human cancer. However, so far it has not been possible to target MYC directly. Recent development of JQ1, a small molecule inhibitor of Bromodomain 4 has been found to indirectly inhibit MYC (Delmore et al., 2011; Zuber et al., 2011). But although JQ1 has shown promise in blood-related cancers, it has not been effective in breast cancer. This example highlights the difference in contexts and the driver mutations that stabilize MYC in different cancers (Mertz et al., 2011). Our findings suggest a novel mechanism by which *PVT1* can contribute to MYC stability in breast cancers. We propose that *PVT1* could be a potential target for inhibiting MYC in breast cancer for patients with gain of 8q24.

Bibliography

Adams, J.M., Harris, A.W., Pinkert, C.A., Corcoran, L.M., Alexander, W.S., Cory, S., Palmiter, R.D., and Brinster, R.L. (1985). The c-myc oncogene driven by immunoglobulin enhancers induces lymphoid malignancy in transgenic mice. Nature *318*, 533-538.

Afify, A., and Mark, H.F. (1999). Trisomy 8 in embryonal rhabdomyosarcoma detected by fluorescence in situ hybridization. Cancer Genet Cytogenet *108*, 127-132.

Aguirre, A.J., Brennan, C., Bailey, G., Sinha, R., Feng, B., Leo, C., Zhang, Y., Zhang, J., Gans, J.D., Bardeesy, N.*, et al.* (2004). High-resolution characterization of the pancreatic adenocarcinoma genome. Proceedings of the National Academy of Sciences of the United States of America *101*, 9067-9072.

Al-Kuraya, K., Schraml, P., Torhorst, J., Tapia, C., Zaharieva, B., Novotny, H., Spichtin, H., Maurer, R., Mirlacher, M., Kochli, O.*, et al.* (2004). Prognostic relevance of gene amplifications and coamplifications in breast cancer. Cancer research *64*, 8534-8540.

Aulmann, S., Adler, N., Rom, J., Helmchen, B., Schirmacher, P., and Sinn, H.P. (2006). c-myc amplifications in primary breast carcinomas and their local recurrences. Journal of clinical pathology *59*, 424-428.

Aulmann, S., Bentz, M., and Sinn, H.P. (2002). C-myc oncogene amplification in ductal carcinoma in situ of the breast. Breast cancer research and treatment *74*, 25-31.

Bagchi, A., Papazoglu, C., Wu, Y., Capurso, D., Brodt, M., Francis, D., Bredel, M., Vogel, H., and Mills, A.A. (2007). CHD5 is a tumor suppressor at human 1p36. Cell *128*, 459-475.

Bakkus, M.H., Brakel-van Peer, K.M., Michiels, J.J., van 't Veer, M.B., and Benner, R. (1990). Amplification of the c-myc and the pvt-like region in human multiple myeloma. Oncogene *5*, 1359-1364.

Barsotti, A.M., Beckerman, R., Laptenko, O., Huppi, K., Caplen, N.J., and Prives, C. (2012). p53-Dependent induction of PVT1 and miR-1204. J Biol Chem *287*, 2509-2519.

Beck-Engeser, G.B., Lum, A.M., Huppi, K., Caplen, N.J., Wang, B.B., and Wabl, M. (2008). Pvt1-encoded microRNAs in oncogenesis. Retrovirology *5*, 4.

Bergamaschi, A., Kim, Y.H., Wang, P., Sorlie, T., Hernandez-Boussard, T., Lonning, P.E., Tibshirani, R., Borresen-Dale, A.L., and Pollack, J.R. (2006). Distinct patterns of DNA copy number alteration are associated with different clinicopathological features and gene-expression subtypes of breast cancer. Genes Chromosomes Cancer *45*, 1033-1040.

Berns, E.M., Foekens, J.A., van Putten, W.L., van Staveren, I.L., Portengen, H., de Koning, W.C., and Klijn, J.G. (1992a). Prognostic factors in human primary breast cancer: comparison of c-myc and HER2/neu amplification. The Journal of steroid biochemistry and molecular biology *43*, 13-19.

Berns, E.M., Klijn, J.G., van Putten, W.L., van Staveren, I.L., Portengen, H., and Foekens, J.A. (1992b). c-myc amplification is a better prognostic factor than HER2/neu amplification in primary breast cancer. Cancer research *52*, 1107-1113.

Beroukhim, R., Mermel, C.H., Porter, D., Wei, G., Raychaudhuri, S., Donovan, J., Barretina, J., Boehm, J.S., Dobson, J., Urashima, M.*, et al.* (2010). The landscape of somatic copy-number alteration across human cancers. Nature *463*, 899-905.

Bonilla, M., Ramirez, M., Lopez-Cueto, J., and Gariglio, P. (1988). In vivo amplification and rearrangement of c-myc oncogene in human breast tumors. Journal of the National Cancer Institute *80*, 665-671.

Borg, A., Baldetorp, B., Ferno, M., Olsson, H., and Sigurdsson, H. (1992). c-myc amplification is an independent prognostic factor in postmenopausal breast cancer. Int J Cancer *51*, 687-691.

Boxer, R.B., Jang, J.W., Sintasath, L., and Chodosh, L.A. (2004). Lack of sustained regression of c-MYC-induced mammary adenocarcinomas following brief or prolonged MYC inactivation. Cancer cell *6*, 577-586.

Boyd, L.K., Mao, X., Xue, L., Lin, D., Chaplin, T., Kudahetti, S.C., Stankiewicz, E., Yu, Y., Beltran, L., Shaw, G.*, et al.* (2012). High-resolution genome-wide copy-number analysis suggests a monoclonal origin of multifocal prostate cancer. Genes, chromosomes & cancer *51*, 579-589.

Carrasco, D.R., Tonon, G., Huang, Y., Zhang, Y., Sinha, R., Feng, B., Stewart, J.P., Zhan, F., Khatry, D., Protopopova, M.*, et al.* (2006). High-resolution genomic profiles define distinct clinico-pathogenetic subgroups of multiple myeloma patients. Cancer cell *9*, 313-325.

Chen, H., Liu, W., Roberts, W., Hooker, S., Fedor, H., DeMarzo, A., Isaacs, W., and Kittles, R.A. 8q24 allelic imbalance and MYC gene copy number in primary prostate cancer. Prostate Cancer Prostatic Dis *13*, 238-243.

Chin, K., DeVries, S., Fridlyand, J., Spellman, P.T., Roydasgupta, R., Kuo, W.L., Lapuk, A., Neve, R.M., Qian, Z., Ryder, T.*, et al.* (2006). Genomic and transcriptional aberrations linked to breast cancer pathophysiologies. Cancer Cell *10*, 529-541.

Chochi, Y., Kawauchi, S., Nakao, M., Furuya, T., Hashimoto, K., Oga, A., Oka, M., and Sasaki, K. (2009). A copy number gain of the 6p arm is linked with advanced hepatocellular carcinoma: an array-based comparative genomic hybridization study. J Pathol *217*, 677-684.

Corzo, C., Corominas, J.M., Tusquets, I., Salido, M., Bellet, M., Fabregat, X., Serrano, S., and Sole, F. (2006). The MYC oncogene in breast cancer progression: from benign epithelium to invasive carcinoma. Cancer genetics and cytogenetics *165*, 151-156.

Crowther-Swanepoel, D., Broderick, P., Di Bernardo, M.C., Dobbins, S.E., Torres, M., Mansouri, M., Ruiz-Ponte, C., Enjuanes, A., Rosenquist, R., Carracedo, A.*, et al.* (2010).

Common variants at 2q37.3, 8q24.21, 15q21.3 and 16q24.1 influence chronic lymphocytic leukemia risk. Nature genetics *42*, 132-136.

D'Cruz, C.M., Gunther, E.J., Boxer, R.B., Hartman, J.L., Sintasath, L., Moody, S.E., Cox, J.D., Ha, S.I., Belka, G.K., Golant, A.*, et al.* (2001). c-MYC induces mammary tumorigenesis by means of a preferred pathway involving spontaneous Kras2 mutations. Nature medicine *7*, 235-239.

Debnath, J., and Brugge, J.S. (2005). Modelling glandular epithelial cancers in three-dimensional cultures. Nat Rev Cancer *5*, 675-688.

Degenhardt, Y.Y., Wooster, R., McCombie, R.W., Lucito, R., and Powers, S. (2008). High-content analysis of cancer genome DNA alterations. Current opinion in genetics & development *18*, 68-72.

Delmore, J.E., Issa, G.C., Lemieux, M.E., Rahl, P.B., Shi, J., Jacobs, H.M., Kastritis, E., Gilpatrick, T., Paranal, R.M., Qi, J.*, et al.* (2011). BET bromodomain inhibition as a therapeutic strategy to target c-Myc. Cell *146*, 904-917.

Deming, S.L., Nass, S.J., Dickson, R.B., and Trock, B.J. (2000). C-myc amplification in breast cancer: a meta-analysis of its occurrence and prognostic relevance. British journal of cancer *83*, 1688-1695.

Dimova, I., Raitcheva, S., Dimitrov, R., Doganov, N., and Toncheva, D. (2006). Correlations between c-myc gene copy-number and clinicopathological parameters of ovarian tumours. Eur J Cancer *42*, 674-679.

Douglas, E.J., Fiegler, H., Rowan, A., Halford, S., Bicknell, D.C., Bodmer, W., Tomlinson, I.P., and Carter, N.P. (2004). Array comparative genomic hybridization analysis of colorectal cancer cell lines and primary carcinomas. Cancer Res *64*, 4817-4825.

Easton, D.F., and Eeles, R.A. (2008). Genome-wide association studies in cancer. Human molecular genetics *17*, R109-115.

Enciso-Mora, V., Broderick, P., Ma, Y., Jarrett, R.F., Hjalgrim, H., Hemminki, K., van den Berg, A., Olver, B., Lloyd, A., Dobbins, S.E*., et al.* (2010). A genome-wide association study of Hodgkin's lymphoma identifies new susceptibility loci at 2p16.1 (REL), 8q24.21 and 10p14 (GATA3). Nat Genet *42*, 1126-1130.

Engler, D.A., Gupta, S., Growdon, W.B., Drapkin, R.I., Nitta, M., Sergent, P.A., Allred, S.F., Gross, J., Deavers, M.T., Kuo, W.L*., et al.* (2012). Genome wide DNA copy number analysis of serous type ovarian carcinomas identifies genetic markers predictive of clinical outcome. PloS one *7*, e30996.

Erikson, J., Nishikura, K., ar-Rushdi, A., Finan, J., Emanuel, B., Lenoir, G., Nowell, P.C., and Croce, C.M. (1983). Translocation of an immunoglobulin kappa locus to a region 3' of an unrearranged c-myc oncogene enhances c-myc transcription. Proc Natl Acad Sci U S A *80*, 7581-7585.

Ferber, M.J., Montoya, D.P., Yu, C., Aderca, I., McGee, A., Thorland, E.C., Nagorney, D.M., Gostout, B.S., Burgart, L.J., Boix, L*., et al.* (2003). Integrations of the hepatitis B virus (HBV) and human papillomavirus (HPV) into the human telomerase reverse transcriptase (hTERT) gene in liver and cervical cancers. Oncogene *22*, 3813-3820.

Gaudet, F., Hodgson, J.G., Eden, A., Jackson-Grusby, L., Dausman, J., Gray, J.W., Leonhardt, H., and Jaenisch, R. (2003). Induction of tumors in mice by genomic hypomethylation. Science *300*, 489-492.

Ghoussaini, M., Song, H., Koessler, T., Al Olama, A.A., Kote-Jarai, Z., Driver, K.E., Pooley, K.A., Ramus, S.J., Kjaer, S.K., Hogdall, E*., et al.* (2008). Multiple loci with different cancer specificities within the 8q24 gene desert. Journal of the National Cancer Institute *100*, 962-966.

Goode, E.L., Chenevix-Trench, G., Song, H., Ramus, S.J., Notaridou, M., Lawrenson, K., Widschwendter, M., Vierkant, R.A., Larson, M.C., Kjaer, S.K*., et al.* (2010). A genome-wide association study identifies susceptibility loci for ovarian cancer at 2q31 and 8q24. Nature genetics *42*, 874-879.

Graham, M., and Adams, J.M. (1986). Chromosome 8 breakpoint far 3' of the c-myc oncogene in a Burkitt's lymphoma 2;8 variant translocation is equivalent to the murine pvt-1 locus. EMBO J *5*, 2845-2851.

Grimwade, D., Walker, H., Oliver, F., Wheatley, K., Harrison, C., Harrison, G., Rees, J., Hann, I., Stevens, R., Burnett, A.*, et al.* (1998). The importance of diagnostic cytogenetics on outcome in AML: analysis of 1,612 patients entered into the MRC AML 10 trial. The Medical Research Council Adult and Children's Leukaemia Working Parties. Blood *92*, 2322-2333.

Guan, Y., Kuo, W.L., Stilwell, J.L., Takano, H., Lapuk, A.V., Fridlyand, J., Mao, J.H., Yu, M., Miller, M.A., Santos, J.L.*, et al.* (2007). Amplification of PVT1 contributes to the pathophysiology of ovarian and breast cancer. Clin Cancer Res *13*, 5745-5755.

Gudmundsson, J., Sulem, P., Manolescu, A., Amundadottir, L.T., Gudbjartsson, D., Helgason, A., Rafnar, T., Bergthorsson, J.T., Agnarsson, B.A., Baker, A.*, et al.* (2007). Genome-wide association study identifies a second prostate cancer susceptibility variant at 8q24. Nat Genet *39*, 631-637.

Gurel, B., Iwata, T., Koh, C.M., Jenkins, R.B., Lan, F., Van Dang, C., Hicks, J.L., Morgan, J., Cornish, T.C., Sutcliffe, S.*, et al.* (2008). Nuclear MYC protein overexpression is an early alteration in human prostate carcinogenesis. Modern pathology : an official journal of the United States and Canadian Academy of Pathology, Inc *21*, 1156-1167.

Guy, C.T., Webster, M.A., Schaller, M., Parsons, T.J., Cardiff, R.D., and Muller, W.J. (1992). Expression of the neu protooncogene in the mammary epithelium of transgenic mice induces metastatic disease. Proc Natl Acad Sci U S A *89*, 10578-10582.

Hanahan, D., and Weinberg, R.A. (2000). The hallmarks of cancer. Cell *100*, 57-70.

Harkness, M.N., Bern, H.A., Alfert, M., and Goldstein, N.O. (1957). Cytochemical studies of hyperplastic alveolar nodules in the mammary gland of the C3H/He CRGL mouse. J Natl Cancer Inst *19*, 1023-1033.

Hartmann, S., Martin-Subero, J.I., Gesk, S., Husken, J., Giefing, M., Nagel, I., Riemke, J., Chott, A., Klapper, W., Parrens, M.*, et al.* (2008). Detection of genomic imbalances in microdissected Hodgkin and Reed-Sternberg cells of classical Hodgkin's lymphoma by array-based comparative genomic hybridization. Haematologica *93*, 1318-1326.

Hashemi, J., Worrall, C., Vasilcanu, D., Fryknas, M., Sulaiman, L., Karimi, M., Weng, W.H., Lui, W.O., Rudduck, C., Axelson, M.*, et al.* (2011). Molecular characterization of acquired tolerance of tumor cells to picropodophyllin (PPP). PLoS One *6*, e14757.

Hattinger, C.M., Potschger, U., Tarkkanen, M., Squire, J., Zielenska, M., Kiuru-Kuhlefelt, S., Kager, L., Thorner, P., Knuutila, S., Niggli, F.K.*, et al.* (2002). Prognostic impact of chromosomal aberrations in Ewing tumours. Br J Cancer *86*, 1763-1769.

Haverty, P.M., Hon, L.S., Kaminker, J.S., Chant, J., and Zhang, Z. (2009). High-resolution analysis of copy number alterations and associated expression changes in ovarian tumors. BMC medical genomics *2*, 21.

Hirano, T., Ike, F., Murata, T., Obata, Y., Utiyama, H., and Yokoyama, K.K. (2008). Genes encoded within 8q24 on the amplicon of a large extrachromosomal element are selectively repressed during the terminal differentiation of HL-60 cells. Mutation research *640*, 97-106.

Horev, G., Ellegood, J., Lerch, J.P., Son, Y.E., Muthuswamy, L., Vogel, H., Krieger, A.M., Buja, A., Henkelman, R.M., Wigler, M.*, et al.* (2011). Dosage-dependent phenotypes in models of 16p11.2 lesions found in autism. Proceedings of the National Academy of Sciences of the United States of America *108*, 17076-17081.

Horlings, H.M., Lai, C., Nuyten, D.S., Halfwerk, H., Kristel, P., van Beers, E., Joosse, S.A., Klijn, C., Nederlof, P.M., Reinders, M.J.*, et al.* (2010). Integration of DNA copy number alterations and prognostic gene expression signatures in breast cancer patients. Clinical cancer research : an official journal of the American Association for Cancer Research *16*, 651-663.

Huppi, K., Pitt, J.J., Wahlberg, B.M., and Caplen, N.J. (2012). The 8q24 gene desert: an oasis of non-coding transcriptional activity. Front Genet *3*, 69.

Huppi, K., Siwarski, D., Shaughnessy, J.D., Jr., and Mushinski, J.F. (1993). Co-amplification of c-myc/pvt-1 in immortalized mouse B-lymphocytic cell lines results in a novel pvt-1/AJ-1 transcript. Int J Cancer *53*, 493-498.

Huppi, K., Volfovsky, N., Runfola, T., Jones, T.L., Mackiewicz, M., Martin, S.E., Mushinski, J.F., Stephens, R., and Caplen, N.J. (2008). The identification of microRNAs in a genomically unstable region of human chromosome 8q24. Mol Cancer Res *6*, 212-221.

Janocko, L.E., Brown, K.A., Smith, C.A., Gu, L.P., Pollice, A.A., Singh, S.G., Julian, T., Wolmark, N., Sweeney, L., Silverman, J.F.*, et al.* (2001). Distinctive patterns of Her-2/neu, c-myc, and cyclin D1 gene amplification by fluorescence in situ hybridization in primary human breast cancers. Cytometry *46*, 136-149.

Jenkins, R.B., Xiao, Y., Sicotte, H., Decker, P.A., Kollmeyer, T.M., Hansen, H.M., Kosel, M.L., Zheng, S., Walsh, K.M., Rice, T.*, et al.* (2012). A low-frequency variant at 8q24.21 is strongly associated with risk of oligodendroglial tumors and astrocytomas with IDH1 or IDH2 mutation. Nat Genet *44*, 1122-1125.

Jones, L., Wei, G., Sevcikova, S., Phan, V., Jain, S., Shieh, A., Wong, J.C., Li, M., Dubansky, J., Maunakea, M.L.*, et al.* Gain of MYC underlies recurrent trisomy of the MYC chromosome in acute promyelocytic leukemia. J Exp Med *207*, 2581-2594.

Jones, L., Wei, G., Sevcikova, S., Phan, V., Jain, S., Shieh, A., Wong, J.C., Li, M., Dubansky, J., Maunakea, M.L.*, et al.* (2010). Gain of MYC underlies recurrent trisomy of the MYC chromosome in acute promyelocytic leukemia. J Exp Med *207*, 2581-2594.

Kang, J.U., Koo, S.H., Kwon, K.C., Park, J.W., and Jung, S.S. (2008). Gain of the EGFR gene located on 7p12 is a frequent and early event in squamous cell carcinoma of the lung. Cancer Genet Cytogenet *184*, 31-37.

Kenny, P.A., Lee, G.Y., Myers, C.A., Neve, R.M., Semeiks, J.R., Spellman, P.T., Lorenz, K., Lee, E.H., Barcellos-Hoff, M.H., Petersen, O.W.*, et al.* (2007). The morphologies of breast cancer cell lines in three-dimensional assays correlate with their profiles of gene expression. Mol Oncol *1*, 84-96.

Kiemeney, L.A., Thorlacius, S., Sulem, P., Geller, F., Aben, K.K., Stacey, S.N., Gudmundsson, J., Jakobsdottir, M., Bergthorsson, J.T., Sigurdsson, A.*, et al.* (2008). Sequence variant on 8q24 confers susceptibility to urinary bladder cancer. Nature genetics *40*, 1307-1312.

Kim, H.K., Choi, I.J., Kim, C.G., Kim, H.S., Oshima, A., Yamada, Y., Arao, T., Nishio, K., Michalowski, A., and Green, J.E. (2012). Three-gene predictor of clinical outcome for gastric cancer patients treated with chemotherapy. The pharmacogenomics journal *12*, 119-127.

Kim, R., Tanabe, K., Emi, M., Uchida, Y., and Toge, T. (2005). Modulation of tamoxifen sensitivity by antisense Bcl-2 and trastuzumab in breast carcinoma cells. Cancer *103*, 2199-2207.

Kim, Y.H., Girard, L., Giacomini, C.P., Wang, P., Hernandez-Boussard, T., Tibshirani, R., Minna, J.D., and Pollack, J.R. (2006). Combined microarray analysis of small cell lung cancer reveals altered apoptotic balance and distinct expression signatures of MYC family gene amplification. Oncogene *25*, 130-138.

Korkola, J., and Gray, J.W. Breast cancer genomes--form and function. Curr Opin Genet Dev *20*, 4-14.

Kraehn, G.M., Utikal, J., Udart, M., Greulich, K.M., Bezold, G., Kaskel, P., Leiter, U., and Peter, R.U. (2001). Extra c-myc oncogene copies in high risk cutaneous malignant melanoma and melanoma metastases. British journal of cancer *84*, 72-79.

Kraus, I., Driesch, C., Vinokurova, S., Hovig, E., Schneider, A., von Knebel Doeberitz, M., and Durst, M. (2008). The majority of viral-cellular fusion transcripts in cervical

carcinomas cotranscribe cellular sequences of known or predicted genes. Cancer research *68*, 2514-2522.

Lamote, I., Meyer, E., Massart-Leen, A.M., and Burvenich, C. (2004). Sex steroids and growth factors in the regulation of mammary gland proliferation, differentiation, and involution. Steroids *69*, 145-159.

Lapointe, J., Li, C., Giacomini, C.P., Salari, K., Huang, S., Wang, P., Ferrari, M., Hernandez-Boussard, T., Brooks, J.D., and Pollack, J.R. (2007). Genomic profiling reveals alternative genetic pathways of prostate tumorigenesis. Cancer Res *67*, 8504-8510.

Le Beau, M.M., Bitts, S., Davis, E.M., and Kogan, S.C. (2002). Recurring chromosomal abnormalities in leukemia in PML-RARA transgenic mice parallel human acute promyelocytic leukemia. Blood *99*, 2985-2991.

Lee, G.Y., Kenny, P.A., Lee, E.H., and Bissell, M.J. (2007). Three-dimensional culture models of normal and malignant breast epithelial cells. Nat Methods *4*, 359-365.

Letessier, A., Sircoulomb, F., Ginestier, C., Cervera, N., Monville, F., Gelsi-Boyer, V., Esterni, B., Geneix, J., Finetti, P., Zemmour, C.*, et al.* (2006). Frequency, prognostic impact, and subtype association of 8p12, 8q24, 11q13, 12p13, 17q12, and 20q13 amplifications in breast cancers. BMC cancer *6*, 245.

Liang, Z., Zeng, X., Gao, J., Wu, S., Wang, P., Shi, X., Zhang, J., and Liu, T. (2008). Analysis of EGFR, HER2, and TOP2A gene status and chromosomal polysomy in gastric adenocarcinoma from Chinese patients. BMC cancer *8*, 363.

Liao, D.J., and Dickson, R.B. (2000). c-Myc in breast cancer. Endocr Relat Cancer *7*, 143-164.

Liu, X.P., Kawauchi, S., Oga, A., Sato, T., Ikemoto, K., Ikeda, E., and Sasaki, K. (2007). Chromosomal aberrations detected by comparative genomic hybridization predict outcome in patients with colorectal carcinoma. Oncol Rep *17*, 261-267.

Lochhead, P., Ng, M.T., Hold, G.L., Rabkin, C.S., Vaughan, T.L., Gammon, M.D., Risch, H.A., Lissowska, J., Mukhopadhya, I., Chow, W.H.*, et al.* (2011). Possible association between a genetic polymorphism at 8q24 and risk of upper gastrointestinal cancer. Eur J Cancer Prev *20*, 54-57.

Mailleux, A.A., Overholtzer, M., and Brugge, J.S. (2008). Lumen formation during mammary epithelial morphogenesis: insights from in vitro and in vivo models. Cell Cycle *7*, 57-62.

Mangano, R., Piddini, E., Carramusa, L., Duhig, T., Feo, S., and Fried, M. (1998). Chimeric amplicons containing the c-myc gene in HL60 cells. Oncogene *17*, 2771-2777.

Medina, D. (2002). Biological and molecular characteristics of the premalignant mouse mammary gland. Biochim Biophys Acta *1603*, 1-9.

Mengle-Gaw, L., and Rabbitts, T.H. (1987). A human chromosome 8 region with abnormalities in B cell, HTLV-I+ T cell and c-myc amplified tumours. EMBO J *6*, 1959-1965.

Merscher, S., Funke, B., Epstein, J.A., Heyer, J., Puech, A., Lu, M.M., Xavier, R.J., Demay, M.B., Russell, R.G., Factor, S.*, et al.* (2001). TBX1 is responsible for cardiovascular defects in velo-cardio-facial/DiGeorge syndrome. Cell *104*, 619-629.

Mertz, J.A., Conery, A.R., Bryant, B.M., Sandy, P., Balasubramanian, S., Mele, D.A., Bergeron, L., and Sims, R.J., 3rd (2011). Targeting MYC dependence in cancer by inhibiting BET bromodomains. Proc Natl Acad Sci U S A *108*, 16669-16674.

Meyer, K.B., Maia, A.T., O'Reilly, M., Ghoussaini, M., Prathalingam, R., Porter-Gill, P., Ambs, S., Prokunina-Olsson, L., Carroll, J., and Ponder, B.A. A Functional Variant at a Prostate Cancer Predisposition Locus at 8q24 Is Associated with PVT1 Expression. PLoS Genet *7*, e1002165.

Mills, A.A., and Bradley, A. (2001). From mouse to man: generating megabase chromosome rearrangements. Trends in genetics : TIG *17*, 331-339.

Mitelman, F. (2005). Cancer cytogenetics update 2005. Atlas Genet Cytogenet Oncol Haematol.

Nagoshi, H., Taki, T., Hanamura, I., Nitta, M., Otsuki, T., Nishida, K., Okuda, K., Sakamoto, N., Kobayashi, S., Yamamoto-Sugitani, M.*, et al.* (2012). Frequent PVT1 Rearrangement and Novel Chimeric Genes PVT1-NBEA and PVT1-WWOX Occur in Multiple Myeloma with 8q24 Abnormality. Cancer Res *72*, 4954-4962.

Nakao, M., Kawauchi, S., Uchiyama, T., Adachi, J., Ito, H., Chochi, Y., Furuya, T., Oga, A., and Sasaki, K. DNA copy number aberrations associated with the clinicopathological features of colorectal cancers: Identification of genomic biomarkers by array-based comparative genomic hybridization. Oncol Rep *25*, 1603-1611.

Nakatani, J., Tamada, K., Hatanaka, F., Ise, S., Ohta, H., Inoue, K., Tomonaga, S., Watanabe, Y., Chung, Y.J., Banerjee, R.*, et al.* (2009). Abnormal behavior in a chromosome-engineered mouse model for human 15q11-13 duplication seen in autism. Cell *137*, 1235-1246.

Nishizaki, T., Ozaki, S., Harada, K., Ito, H., Arai, H., Beppu, T., and Sasaki, K. (1998). Investigation of genetic alterations associated with the grade of astrocytic tumor by comparative genomic hybridization. Genes Chromosomes Cancer *21*, 340-346.

Noack, F., Schmidt, H., Buchweitz, O., Malik, E., and Horny, H.P. (2004). Genomic imbalance and onco-protein expression of ovarian endometrioid adenocarcinoma arisen in an endometriotic cyst. Anticancer Res *24*, 151-154.

Northcott, P.A., Shih, D.J., Peacock, J., Garzia, L., Morrissy, A.S., Zichner, T., Stutz, A.M., Korshunov, A., Reimand, J., Schumacher, S.E.*, et al.* (2012). Subgroup-specific structural variation across 1,000 medulloblastoma genomes. Nature *488*, 49-56.

Osterberg, L., Levan, K., Partheen, K., Staaf, J., Sundfeldt, K., and Horvath, G. (2009). High-resolution genomic profiling of carboplatin resistance in early-stage epithelial ovarian carcinoma. Cytogenet Genome Res *125*, 8-18.

Park, K., Kwak, K., Kim, J., Lim, S., and Han, S. (2005). c-myc amplification is associated with HER2 amplification and closely linked with cell proliferation in tissue microarray of nonselected breast cancers. Human pathology *36*, 634-639.

Perez, E.A., Jenkins, R.B., Dueck, A.C., Wiktor, A.E., Bedroske, P.P., Anderson, S.K., Ketterling, R.P., Sukov, W.R., Kanehira, K., Chen, B.*, et al.* (2011). C-MYC alterations and association with patient outcome in early-stage HER2-positive breast cancer from the north central cancer treatment group N9831 adjuvant trastuzumab trial. J Clin Oncol *29*, 651-659.

Perez, E.A., Palmieri, F.M., and Brock, S.M. (2009). Trastuzumab. Cancer treatment and research *151*, 181-196.

Persons, D.L., Borelli, K.A., and Hsu, P.H. (1997). Quantitation of HER-2/neu and c-myc gene amplification in breast carcinoma using fluorescence in situ hybridization. Modern pathology : an official journal of the United States and Canadian Academy of Pathology, Inc *10*, 720-727.

Peter, M., Rosty, C., Couturier, J., Radvanyi, F., Teshima, H., and Sastre-Garau, X. (2006). MYC activation associated with the integration of HPV DNA at the MYC locus in genital tumors. Oncogene *25*, 5985-5993.

Radtke, I., Mullighan, C.G., Ishii, M., Su, X., Cheng, J., Ma, J., Ganti, R., Cai, Z., Goorha, S., Pounds, S.B.*, et al.* (2009). Genomic analysis reveals few genetic alterations in pediatric acute myeloid leukemia. Proc Natl Acad Sci U S A *106*, 12944-12949.

Ramirez-Solis, R., Liu, P., and Bradley, A. (1995). Chromosome engineering in mice. Nature *378*, 720-724.

Reginato, M.J., Mills, K.R., Becker, E.B., Lynch, D.K., Bonni, A., Muthuswamy, S.K., and Brugge, J.S. (2005). Bim regulation of lumen formation in cultured mammary epithelial acini is targeted by oncogenes. Mol Cell Biol *25*, 4591-4601.

Robanus-Maandag, E.C., Bosch, C.A., Kristel, P.M., Hart, A.A., Faneyte, I.F., Nederlof, P.M., Peterse, J.L., and van de Vijver, M.J. (2003). Association of C-MYC amplification

with progression from the in situ to the invasive stage in C-MYC-amplified breast carcinomas. The Journal of pathology *201*, 75-82.

Rothlisberger, B., Heizmann, M., Bargetzi, M.J., and Huber, A.R. (2007). TRIB1 overexpression in acute myeloid leukemia. Cancer Genet Cytogenet *176*, 58-60.

Roux-Dosseto, M., Romain, S., Dussault, N., Desideri, C., Piana, L., Bonnier, P., Tubiana, N., and Martin, P.M. (1992). c-myc gene amplification in selected node-negative breast cancer patients correlates with high rate of early relapse. Eur J Cancer *28A*, 1600-1604.

Rygiel, A.M., Milano, F., Ten Kate, F.J., Schaap, A., Wang, K.K., Peppelenbosch, M.P., Bergman, J.J., and Krishnadath, K.K. (2008). Gains and amplifications of c-myc, EGFR, and 20.q13 loci in the no dysplasia-dysplasia-adenocarcinoma sequence of Barrett's esophagus. Cancer Epidemiol Biomarkers Prev *17*, 1380-1385.

Sandberg, A.A., and Bridge, J.A. (2002). Updates on the cytogenetics and molecular genetics of bone and soft tissue tumors. Synovial sarcoma. Cancer Genet Cytogenet *133*, 1-23.

Santarius, T., Shipley, J., Brewer, D., Stratton, M.R., and Cooper, C.S. (2010). A census of amplified and overexpressed human cancer genes. Nature reviews Cancer *10*, 59-64.

Sato, K., Qian, J., Slezak, J.M., Lieber, M.M., Bostwick, D.G., Bergstralh, E.J., and Jenkins, R.B. (1999). Clinical significance of alterations of chromosome 8 in high-grade, advanced, nonmetastatic prostate carcinoma. J Natl Cancer Inst *91*, 1574-1580.

Schlotter, C.M., Vogt, U., Bosse, U., Mersch, B., and Wassmann, K. (2003). C-myc, not HER-2/neu, can predict recurrence and mortality of patients with node-negative breast cancer. Breast cancer research : BCR *5*, R30-36.

Schoenenberger, C.A., Andres, A.C., Groner, B., van der Valk, M., LeMeur, M., and Gerlinger, P. (1988). Targeted c-myc gene expression in mammary glands of transgenic mice induces mammary tumours with constitutive milk protein gene transcription. The EMBO journal *7*, 169-175.

Schwertfeger, K.L., Xian, W., Kaplan, A.M., Burnett, S.H., Cohen, D.A., and Rosen, J.M. (2006). A critical role for the inflammatory response in a mouse model of preneoplastic progression. Cancer Res *66*, 5676-5685.

Shtivelman, E., and Bishop, J.M. (1989). The PVT gene frequently amplifies with MYC in tumor cells. Mol Cell Biol *9*, 1148-1154.

Shtivelman, E., Henglein, B., Groitl, P., Lipp, M., and Bishop, J.M. (1989). Identification of a human transcription unit affected by the variant chromosomal translocations 2;8 and 8;22 of Burkitt lymphoma. Proc Natl Acad Sci U S A *86*, 3257-3260.

Sircoulomb, F., Bekhouche, I., Finetti, P., Adelaide, J., Ben Hamida, A., Bonansea, J., Raynaud, S., Innocenti, C., Charafe-Jauffret, E., Tarpin, C*., et al.* (2010). Genome profiling of ERBB2-amplified breast cancers. BMC cancer *10*, 539.

Soucek, L., Whitfield, J., Martins, C.P., Finch, A.J., Murphy, D.J., Sodir, N.M., Karnezis, A.N., Swigart, L.B., Nasi, S., and Evan, G.I. (2008). Modelling Myc inhibition as a cancer therapy. Nature *455*, 679-683.

Stark, K.L., Xu, B., Bagchi, A., Lai, W.S., Liu, H., Hsu, R., Wan, X., Pavlidis, P., Mills, A.A., Karayiorgou, M*., et al.* (2008). Altered brain microRNA biogenesis contributes to phenotypic deficits in a 22q11-deletion mouse model. Nature genetics *40*, 751-760.

Stewart, T.A., Pattengale, P.K., and Leder, P. (1984). Spontaneous mammary adenocarcinomas in transgenic mice that carry and express MTV/myc fusion genes. Cell *38*, 627-637.

Storchova, Z., and Pellman, D. (2004). From polyploidy to aneuploidy, genome instability and cancer. Nature reviews Molecular cell biology *5*, 45-54.

Sugawara, W., Arai, Y., Kasai, F., Fujiwara, Y., Haruta, M., Hosaka, R., Nishida, K., Kurosumi, M., Kobayashi, Y., Akagi, K*., et al.* (2011). Association of germline or somatic TP53 missense mutation with oncogene amplification in tumors developed in patients with Li-Fraumeni or Li-Fraumeni-like syndrome. Genes Chromosomes Cancer *50*, 535-545.

Sur, I.K., Hallikas, O., Vaharautio, A., Yan, J., Turunen, M., Enge, M., Taipale, M., Karhu, A., Aaltonen, L.A., and Taipale, J. (2012). Mice lacking a Myc enhancer that includes human SNP rs6983267 are resistant to intestinal tumors. Science *338*, 1360-1363.

TCGA (2011). Integrated genomic analyses of ovarian carcinoma. Nature *474*, 609-615.

TCGA (2012a). Comprehensive molecular characterization of human colon and rectal cancer. Nature *487*, 330-337.

TCGA (2012b). Comprehensive molecular portraits of human breast tumours. Nature *490*, 61-70.

Tiede, B., and Kang, Y. (2011). From milk to malignancy: the role of mammary stem cells in development, pregnancy and breast cancer. Cell Res *21*, 245-257.

Tonon, G., Wong, K.K., Maulik, G., Brennan, C., Feng, B., Zhang, Y., Khatry, D.B., Protopopov, A., You, M.J., Aguirre, A.J.*, et al.* (2005). High-resolution genomic profiles of human lung cancer. Proceedings of the National Academy of Sciences of the United States of America *102*, 9625-9630.

Treszl, A., Adany, R., Rakosy, Z., Kardos, L., Begany, A., Gilde, K., and Balazs, M. (2004). Extra copies of c-myc are more pronounced in nodular melanomas than in superficial spreading melanomas as revealed by fluorescence in situ hybridisation. Cytometry Part B, Clinical cytometry *60*, 37-46.

Turnbull, C., Ahmed, S., Morrison, J., Pernet, D., Renwick, A., Maranian, M., Seal, S., Ghoussaini, M., Hines, S., Healey, C.S.*, et al.* (2010). Genome-wide association study identifies five new breast cancer susceptibility loci. Nature genetics *42*, 504-507.

Vafa, O., Wade, M., Kern, S., Beeche, M., Pandita, T.K., Hampton, G.M., and Wahl, G.M. (2002). c-Myc can induce DNA damage, increase reactive oxygen species, and mitigate p53 function: a mechanism for oncogene-induced genetic instability. Mol Cell *9*, 1031-1044.

van Duin, M., van Marion, R., Vissers, K.J., Hop, W.C., Dinjens, W.N., Tilanus, H.W., Siersema, P.D., and van Dekken, H. (2007). High-resolution array comparative genomic hybridization of chromosome 8q: evaluation of putative progression markers for gastroesophageal junction adenocarcinomas. Cytogenet Genome Res *118*, 130-137.

Wang, G., Zhao, Y., Liu, X., Wang, L., Wu, C., Zhang, W., Liu, W., Zhang, P., Cong, W., Zhu, Y.*, et al.* (2001). Allelic loss and gain, but not genomic instability, as the major somatic mutation in primary hepatocellular carcinoma. Genes Chromosomes Cancer *31*, 221-227.

Watson, C.J., and Khaled, W.T. (2008). Mammary development in the embryo and adult: a journey of morphogenesis and commitment. Development *135*, 995-1003.

Webb, E., Adams, J.M., and Cory, S. (1984). Variant (6 ; 15) translocation in a murine plasmacytoma occurs near an immunoglobulin kappa gene but far from the myc oncogene. Nature *312*, 777-779.

Yamada, T., Kohno, T., Navarro, J.M., Ohwada, S., Perucho, M., and Yokota, J. (2000). Frequent chromosome 8q gains in human small cell lung carcinoma detected by arbitrarily primed-PCR genomic fingerprinting. Cancer Genet Cytogenet *120*, 11-17.

Yeager, M., Orr, N., Hayes, R.B., Jacobs, K.B., Kraft, P., Wacholder, S., Minichiello, M.J., Fearnhead, P., Yu, K., Chatterjee, N.*, et al.* (2007). Genome-wide association study of prostate cancer identifies a second risk locus at 8q24. Nature genetics *39*, 645-649.

You, L., Chang, D., Du, H.Z., and Zhao, Y.P. (2011). Genome-wide screen identifies PVT1 as a regulator of Gemcitabine sensitivity in human pancreatic cancer cells. Biochem Biophys Res Commun *407*, 1-6.

Yu, Y., and Bradley, A. (2001). Engineering chromosomal rearrangements in mice. Nature reviews Genetics *2*, 780-790.

Zhang, A., Maner, S., Betz, R., Angstrom, T., Stendahl, U., Bergman, F., Zetterberg, A., and Wallin, K.L. (2002). Genetic alterations in cervical carcinomas: frequent low-level

amplifications of oncogenes are associated with human papillomavirus infection. Int J Cancer *101*, 427-433.

Zhang, X., Farrell, A.S., Daniel, C.J., Arnold, H., Scanlan, C., Laraway, B.J., Janghorban, M., Lum, L., Chen, D., Troxell, M.*, et al.* (2012). Mechanistic insight into Myc stabilization in breast cancer involving aberrant Axin1 expression. Proceedings of the National Academy of Sciences of the United States of America *109*, 2790-2795.

Zhao, X., Weir, B.A., LaFramboise, T., Lin, M., Beroukhim, R., Garraway, L., Beheshti, J., Lee, J.C., Naoki, K., Richards, W.G.*, et al.* (2005). Homozygous deletions and chromosome amplifications in human lung carcinomas revealed by single nucleotide polymorphism array analysis. Cancer research *65*, 5561-5570.

Zhu, D., Qi, C.F., Morse, H.C., 3rd, Janz, S., and Stevenson, F.K. (2005). Deregulated expression of the Myc cellular oncogene drives development of mouse "Burkitt-like" lymphomas from naive B cells. Blood *105*, 2135-2137.

Zielenska, M., Bayani, J., Pandita, A., Toledo, S., Marrano, P., Andrade, J., Petrilli, A., Thorner, P., Sorensen, P., and Squire, J.A. (2001). Comparative genomic hybridization analysis identifies gains of 1p35 approximately p36 and chromosome 19 in osteosarcoma. Cancer Genet Cytogenet *130*, 14-21.

Zitterbart, K., Filkova, H., Tomasikova, L., Necesalova, E., Zambo, I., Kantorova, D., Slamova, I., Vranova, V., Zezulkova, D., Pesakova, M.*, et al.* (2011). Low-level copy number changes of MYC genes have a prognostic impact in medulloblastoma. J Neurooncol *102*, 25-33.

Zuber, J., Shi, J., Wang, E., Rappaport, A.R., Herrmann, H., Sison, E.A., Magoon, D., Qi, J., Blatt, K., Wunderlich, M.*, et al.* (2011). RNAi screen identifies Brd4 as a therapeutic target in acute myeloid leukaemia. Nature *478*, 524-528.

Appendix A: Synteny of *MYC-GSDMC* interval between human and mouse.

The *MYCGSDMC* interval in human (a) and mouse (b) as represented in the UCSC genome browser (Feb. 2009, GRCh37/hg19 Assembly for human and Dec. 2011, GRCm38/mm10 Assembly for mouse).

a

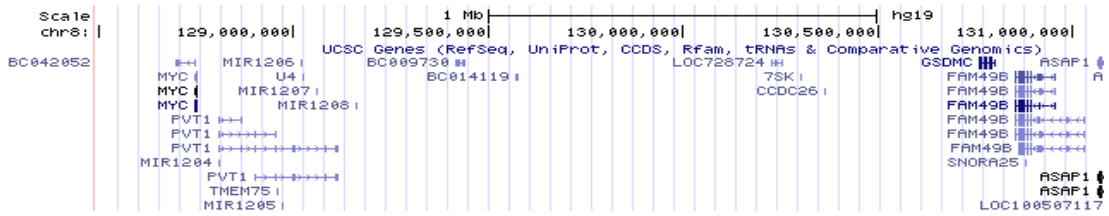

b

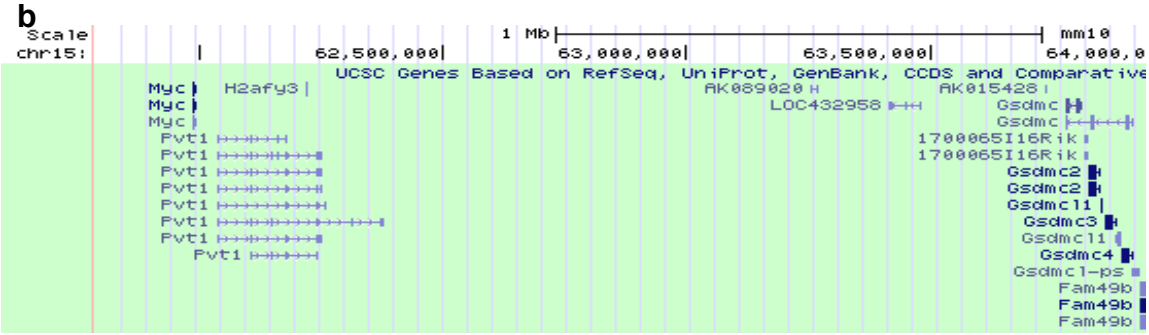

Appendix B: Reduced expression of Gsdmc transcript in mouse mammary tissue.

Semi-quantitative RT-PCR of Gsdmc transcript in mouse colon and mammary tissues. PCR was carried out using equal amount of cDNAs derived from colon and mammary tissues, for cycles as indicated. NC indicates negative control (water). PCR using primers for β-actin carried out for 20 cycles.